

**Spectral reflectance
in the Tunisian desert**

Ontvangen

30 SEP 1992

UB-CARDEX



15n 561145

BIBLIOTHEEK
LANDBOUWUNIVERSITEIT
WAGENINGEN

Promotoren:

Dr. S. B. Kroonenberg
hoogleraar in de geologie en mineralogie

Dr. Ir. M. Molenaar
hoogleraar in de landmeetkunde en teledetectie

Gerrit F. Epema

**Spectral reflectance
in the Tunisian desert**

Proefschrift

ter verkrijging van de graad van
doctor in de landbouw- en milieuwetenschappen,
op gezag van de rector magnificus,
dr. H.C. van der Plas,
in het openbaar te verdedigen
op vrijdag 16 oktober 1992
des namiddags te vier uur in de aula
van de Landbouwniversiteit te Wageningen

This thesis contains results of a research project carried out at the department of Soil Science and Geology of the Wageningen Agricultural University, The Netherlands. The project was funded by The Netherlands Remote Sensing Board (BCRS).

STELLINGEN

1. Bij veldreflectiemetingen kan men niet uitgaan van het Lambertiaanse gedrag van referentiepanelen.
Dit proefschrift.
2. De grote aandacht in de remote sensing voor atmosferische modellen gaat vaak ten koste van een zorgvuldige calibratie van de instrumenten.
Dit proefschrift
3. Landsat Thematic Mapper gegevens zijn uitermate geschikt voor het identificeren van gips, kalk en zout in droge gebieden.
Dit proefschrift.
4. Veldreflectiemetingen zijn onontbeerlijk voor een juiste interpretatie van Landsat Thematic Mapper gegevens.
Dit proefschrift
5. Vegetatie-indices zijn zinloos in gebieden met weinig vegetatiebedekking als geen rekening gehouden wordt met type vegetatie en bodem.
M. Cherlet and A. Di Gregorio, 1991, Calibration and integrated modelling of remote sensing data for desert locust habitat monitoring, FAO project ECLO/INT/004/BEL and GCP/INT/439/BEL.
6. De streef- en grenswaarden van zware metalen in de bodem dienen in de eerste plaats gebaseerd te zijn op een risico-evaluatie voor de volksgezondheid.
Milieukwaliteitsdoelstellingen bodem en water, Notitie, Tweede Kamer, vergaderjaar 1990-1991, 21 990, nr.1.
7. Interdisciplinaire onderzoeksprojecten dienen uit te gaan van een integrerende vraagstelling en niet van het zoeken van een kapstok voor diverse monodisciplinaire projecten.
8. Hoog-technologische onderzoeksprojecten in zeer arme landen dienen gevolgd te worden door toegepast onderzoek ten behoeve van het land zelf.
9. Het schatten van de infiltratie van water in een gebied aan de hand van een kartering van oppervlaktetypen met de methode van Casenave en Valentin (1989) leidt tot grote fouten.
A. Casenave et C. Valentin, 1989, Les états de surface de la zone sahélienne, influence sur l'infiltration, Editions de l'ORSTOM, Paris.

10. Niet al het water in de woestijn is luchtspiegeling.
11. Uit recent onderzoek blijkt dat de regendruppels nog net zo vallen als 50 jaar geleden.
12. Remote areas become more remote with remote sensing.
13. De aanbeveling van de nationale kruisvereniging, om een bepaald merk luiers te kopen doet afbreuk aan de geloofwaardigheid van de overige adviezen.
14. Met de verdringing van de **automobiel** door de **personal computer** als eerste gespreksonderwerp is er niets veranderd: het ego komt nog steeds voorop.

Stellingen behorende bij het proefschrift van Gerrit F. Epema: Spectral Reflectance in the Tunisian Desert.

Wageningen, 16 oktober 1992.

ABSTRACT

Epema, G. F. Spectral reflectance in the Tunisian desert. Doctoral thesis, Wageningen Agricultural University, The Netherlands. 150 pages.

Satellites provide the possibility to give a synoptical view of the earth surface at regular time intervals. Satellites operating in the optical wavelengths have however as disadvantage that monitoring of the surface characteristics becomes impossible as soon as clouds are present. Deserts and desert margins are for that reason much more appropriate for monitoring by optical satellites than temperate and wet tropical areas. Potential hazards, possibilities and often inaccessibility makes use of optical remote sensing very reasonable. Landsat Thematic Mapper (TM) satellites provide a much better spectral resolution than other satellites at reasonable spatial and temporal resolution. The presented research was hence focused on the spectral possibilities of *Landsat Thematic Mapper* for determining surface characteristics and their dynamics in desert areas. *Field measurements of reflectance* in different seasons were performed to evaluate the effect of different factors and their dynamics on reflectance. A field radiometer (MMR) with TM compatible bands was used. The study was performed in southern Tunisia in an area with large variation: footslopes, dunes and dynamical salt plains, all with few or absent vegetation cover. Dominant mineralogy is representative for many arid areas and comprises gypsum, carbonate, quartz and halite.

In order to compare results of field reflectance measurements with Landsat Thematic Mapper data, *adequate processing* of both data sets is necessary. General accepted assumptions that reference plates are ideal reflectors have to be rejected. Both wavelength and insolation angle dependant reflectance of the panel has to be determined. For large solar zenith angles also corrections have to be made for influence of diffuse irradiation (Chapter 2).

Use of calibration coefficients given for Landsat Thematic Mapper data processed in Fucino will cause large errors in calculating reflectance data. It turned out that these coefficients were not updated for deterioration of the sensors during the flight and that calculations were made based on two different definitions of bandwidth. In order to achieve adequate values of reflectance these errors were evaluated and corrected (Chapter 8).

The evaluation of factors affecting *field reflectance* can be separated in *external* and *internal* ones.

The influence of *external* factors, solar zenith angle and atmosphere was evaluated (Chapter 3-4). *Solar zenith angle dependant* reflectance turned out to be limited for this area, if measurements are performed with solar zenith angles up to 65 degrees. In spring on the footslopes reflectance values at noon were about 10% higher than those at 65 degrees. Differences on the playa were even less. Both based on accuracy and applicability of the results (observations of this area at these latitudes with Landsat TM take place with angles ranging between 28 in June and 63 degrees in December), 65 degrees can be considered as a useful limit for performing adequate measurements.

Influence of *atmosphere* on field reflectance is limited. The evaluation of the external factors leads to the conclusion that all measurements with a solar zenith angle less than 65 degrees and on clear days could be used for obtaining a field data reference set.

Field measurements showed that Landsat TM-like bands are very useful in detecting the surface characteristics (*internal factors*) in this area (Chapters 5 - 7). Gypsum has absorption bands in both middle infrared bands (comparable with TM bands 6 and 7) and carbonate in TM band 7. Since on footslopes and in dunes quartz is the other important mineral, a high reflectance in these bands points to presence of quartz. Standard field reflectance measurements showed that on footslopes gypsum, quartz and carbonate dominated areas have a different spectral signature. Differences in eolian deposits are even more clear: relations between gypsum content and indices derived from spectral reflectance could be established under field conditions.

Presence of halite on the playas could be detected by relatively high reflectance in the visible part of the spectrum, especially in the blue band. Field reflectance on plots showed that *moisture content* induces a relatively low reflectance in all bands with an extra low reflectance in the middle infrared bands. Linear relations between volumetric moisture content and reflectance in individual bands in near and middle infrared turned out to be feasible. Most *dynamical* parts of the area turned out to be the playas, where after storms moisture contents of the top layer were affected for a long time and halite efflorescences occurred shortly after the storms. Although dust slowly covering the surface, even in spring plots with higher halite content could be derived from the spectral signature. Field plots in dune parts showed a large variation in reflectance between November and May too due to changes by wind. Dynamics on footslopes were much less important than in other areas. Variation in vegetation appears to be relatively small, while also effect of storms was not visible for more than a few days after a storm.

Results of field reflectance were extrapolated to Landsat TM *satellite* data (Chapter 9). It was possible to derive directly from Landsat TM data a number of useful classes for playas, footslopes and eolian material, having variation in surface mineralogy (gypsum, carbonate, quartz, halite) and variation in surface type. Also dynamics of factors like moisture and halite could be derived using multitemporal Landsat TM data.

The presented methodology, implementing an extensive field reflectance measurement campaign, gives insight in possibilities of Landsat TM under a range of conditions. It corroborates that for operational application in arid areas Landsat TM data will be a useful source of information in addition to other types of remote sensing as for instance aerial photography.

Key words: remote sensing, arid zones, Landsat Thematic Mapper, field reflectance, gypsum, carbonate, quartz, halite, moisture content.

PREFACE

Mijn promotoren Salle Kroonenberg en Martien Molenaar wil ik bedanken voor de aangename en stimulerende begeleiding gedurende dit onderzoek. De grote vrijheid in combinatie met zinvolle suggesties stelde ik zeer op prijs.

Thanks to Axel Richter and other participants of the Free University of Berlin of our joint trip to the western desert in Egypt and the hospitality during my visits to Berlin. The discussions stimulated me largely in determining the experimental set-up for the Tunisian field campaigns described in this thesis. Professor List and others thanks for the possibility to use the Barnes radiometer.

I want to thank the Tunisian authorities for permission for this research. Mrs Koundi of the Dutch Embassy was very helpful in arranging the paperwork. Thanks also to OTC and Division des Sols in Tunis and to Direction de Forêts in Kebili for their interest and help. I had stimulating discussions in Tunisia and later on in Europe with IAO of Firenze, Reading University, NERC Reading, ORSTOM and Earthnet on our experiments in Tunisia and on the data analysis. I have to mention: Luca Ongaro, Paoli Sarfatti, Valeria Alessandro, Pam Kennedy, Kevin White, Neil Quarmby, Andrew Millington, Richard Escadafal and Pascal Gilles.

Grote dank ben ik verschuldigd aan Wout Verhoef voor het gebruiken van zijn atmosferische model en de aanpassingen van zijn model, zodat het ook met mijn gegevens kon worden gedraaid.

Ik wil hierbij alle "Wageningse" remote sensing medewerkers bedanken voor hun bijdragen. Door de grote openheid was het altijd makkelijk even binnen te lopen of veel uitgebreider op iets in te gaan. Met name wil ik bedanken: Wim Bastiaansen, Henk Buiten, Jan Clevers, Lucas Jansen, Jan Kornet, Massimo Menenti, Michel Mulders en Kees Schurer.

Iedereen van de vakgroep bodemkunde en geologie die bij dit proefschrift was betrokken bedankt. Met name wil ik noemen: Nico Konijn voor de vele discussies op Duivendaal en op de fietsweg terug, en Ab Jonker voor het tellen van de mineralen. Hoewel niet rechtstreeks bij het proefschrift betrokken wil ik toch mijn huidige hoogleraar Johan Bouma alsmede Dick Legger bedanken. Zij zorgden ervoor dat ik een mij een vaste plaats binnen de vakgroep kon verwerven en tegelijk dit proefschrift kon voltooien.

Een woord van dank is ook verschuldigd aan de verschillende studenten van de Landbouwniversiteit, de Rijksuniversiteit Utrecht en de Katholieke Universiteit Nijmegen, die deelnamen aan de veldwerken binnen het kader van een afstudeervak teledetectie en die inmiddels Ir. of Drs. voor hun naam hebben staan: Igor Staritsky, Maurits van Oostveen, Maarten van Manen, Bart Kessels, Hans de Leeuw, John van Giels, Ina Derksen, Tom Bucx, Henk Gesink en Bertine Niesten. Ook mijn dank aan Hans van Leeuwen voor analyses van gegevens terug in Nederland.

Marc Goossens was zo vriendelijk om een aantal laboratorium reflectiemetingen bij het DLR in Oberpfaffenhofen op de afdeling van Frank Lehmann uit te voeren. Soortgelijke metingen bij het laboratorium voor grond- en gewasonderzoek in Oosterbeek werden uitgevoerd door Arjen de Vries in samenwerking met Herman Vedder.

Dit onderzoek zou niet mogelijk geweest zijn zonder financiële ondersteuning van de Nederlandse Beleidscommissie Remote Sensing (BCRS). Mijn dank aan Nico Bunnik en anderen voor het gestelde vertrouwen.

Tot slot wil ik Tineke en de kinderen bedanken die mij de betrekkelijkheid van het proefschrift duidelijk maakten, maar mij wel de ruimte gaven dit te voltooien.

CONTENTS

1. General introduction	11
2. Studies of errors in field measurements of the bidirectional reflectance factor.	19
3. Diurnal trends in reflectance of bare soil surfaces in southern Tunisia.	35
4. Atmospheric condition and its influence on reflectance of bare soil surfaces in southern Tunisia.	45
5. Effect of moisture content on spectral reflectance in a playa area in southern Tunisia.	63
6. Ground reflectance of natural bare and pure surfaces as an aid in interpretation of Landsat Thematic Mapper data in southern Tunisia.	73
7. Ground spectral reflectance in a desert area in southern Tunisia.	79
8. Determination of planetary reflectance for Landsat 5 Thematic Mapper tapes processed by Earthnet (Italy).	111
9. Mapping surface characteristics and their dynamics in a desert area in southern Tunisia with Landsat Thematic Mapper.	121
10. Conclusions	143
11. Samenvatting	148

CHAPTER 1

GENERAL INTRODUCTION

GENERAL INTRODUCTION

BACKGROUND

Remote sensing instruments on board of satellites and other platforms produce data of earth surface features and their dynamics. The transformation of these data to useful information in specific research and application fields is vital for successful use of remote sensing.

In the Dutch Remote Sensing Programme (NRSP-1) different aims were formulated. Relevant for this research were "stimulating of background research" and "stimulating of research to possible applications". Background research for optical remote sensing should be directed to spectral signatures in relation to their characteristics and conditions. Applications in tropical areas should be based on phenomenological research including dynamic aspects of the phenomena. The present research fits well in these aims. Spectral signatures and their temporal variation are studied for the Landsat Thematic Mapper, an operational satellite with a high spectral resolution. As study area a desert area is chosen, where potential applications of optical remote sensing are functional considering potential hazards and difficult logistic conditions in the field. The presented study is financed in the NRSP-1 in the Background section (AO-4.2) and supervised by the Netherlands Remote sensing Board (BCRS). The future application of results of this study will be mainly related to mapping and monitoring of desert and desert margins.

Landsat Thematic Mapper is an example of a satellite scanner which records the natural electromagnetic energy reflected and emitted by the earth surface. Specific for this scanner is the spectral resolution for the reflective part of the spectrum (6 bands) in combination with reasonable spatial (30 x 30 meter) and temporal resolution (satellite overpass every 16 days) (Table 1). The thermal band was not considered in this study. Differences in spectral response and the spatial distribution of these responses are used as a means for identification of objects in a specific state. This high spectral resolution in combination with the operational status of the satellite which makes this instrument potentially useful already at this moment. Moreover studying spectral response will be a start for research of imaging spectroscopy with much higher spectral resolution, which is foreseen to be operational in satellites for the next decades.

Use of remote sensing satellites for mapping and monitoring deserts and desert margins seems very relevant if we consider potential hazards in these areas and the difficult logistic conditions. Observations with passive remote sensing are possible since the cloud coverage is generally low. Potential hazards in these areas are both natural and man-induced and comprise: strong decrease of vegetation induced by overgrazing or natural causes, salinization of oases and surroundings, erosion, threatening of villages by dunes and others. At the other hand potentials of the areas may not be used optimally: agriculture is possible if artesian water is available and used properly on the most suitable soils and presence of minerals may have been overlooked. Remote sensing is the only means to study for large areas processes like dune movements, dust transport, redistribution of salt and sediments in depressions.

AIM OF THE RESEARCH

The aim of the research was to give a contribution to an evaluation of possibilities of Landsat Thematic Mapper for determining surface characteristics and their dynamics in a desert area. For this aim the following questions have to be answered:

- 1) which factors influence reflectance under field conditions and how important are these?
- 2) is it possible to derive surface characteristics and their changes from TM-like signals?

The objects of study are sparsely vegetated footslopes, sand-dunes and playas. The research on footslopes and sand-dunes is focused on spectral possibilities of TM bands for determination of the natural variation in dominant minerals: quartz, carbonate and gypsum. For the playas the study is focused on both spatial and temporal variation in surface type, mineralogy and moisture content.

If it is possible to extrapolate the field measurements to Landsat TM and show that it is possible to derive these objects and object characteristics from TM, it may be concluded that in arid areas Landsat TM will be an useful additional source of remote sensing information. Ideally results of this study may then be used as an aid in solving problems in desert areas.

RESEARCH STRATEGY

For this research two relatively well accessible areas located in the desert of southern Tunisia, with variation in surface characteristics in space and time, were selected. These areas comprise footslopes at the foot of cuesta ridges, dunes and sand-sheets, and playas. The lithology is dominated by quartz, gypsum and carbonate on the footslopes, by quartz and gypsum in the dunes. The playas show in addition a large variation in halite content, moisture content and surface type. Despite the low annual rainfall (about 100 millimetres, falling mainly between November and February), dynamics of halite and moisture in the playa is considerable. In the whole study area wind plays a role. Outside the oases vegetation coverage exceeds 5% of the surface only in exceptional cases.

Field research and TM data acquisition was performed in both wet and dry season to establish the temporal variation. In order to determine important factors which influence reflectance much emphasis was given to field reflectance measurements with a TM compatible instrument. The field instrument, a Barnes MMR, has bandpasses comparable with Landsat TM (table 1). Results of field reflectance measurements in combination with other field observations were used for predicting and explaining Landsat TM signals.

Table 1 *Bandpasses (-3dB) of Barnes MMR field radiometer (50% power bandpass limits) and Landsat Thematic Mapper (full-width at half-maximum method) of reflectance part of the spectrum.*

	Barnes MMR		Landsat TM	
	nr. of band	wavelength limits	nr. of band	wavelength limits
Blue	1	0.458-0.525	1	0.4524-0.5178
Green	2	0.519-0.601	2	0.5280-0.6093
Red	3	0.637-0.687	3	0.6264-0.6923
Near IR	4	0.739-0.898	4	0.7764-0.9045
	5	1.174-1.334		
MIR 1	6	1.574-1.803	5	1.5675-1.7842
MIR 2	7	2.083-2.371	7	2.0972-2.3490

Including those field reflectance measurements has major advantages above purely satellite-borne campaigns with field check in specific areas:

- (1) the effect of external factors like solar zenith angle and atmosphere on reflectance can be established for a range of conditions. Landsat TM produces only data for a specific solar zenith angle and a specific atmosphere.
- (2) a direct relation between a TM-like signal and natural surface characteristics can be studied. The influence of atmosphere on field reflectance is probably limited.
- (3) reflectance of the different components present in the TM ground resolution elements can be determined. Within a Landsat TM pixel almost always a certain variation is present.
- (4) the effect of changes of the surface on reflectance as a function of for instance artificial or natural moistening can be measured directly. Landsat TM produces only data for every location on earth every 16 days at the same solar time.

To use the field data for predicting and explaining TM signals an adequate processing of both field and satellite data is a prerequisite. This is evaluated extensively in chapter 2 and 8. In addition the effect of external factors like atmosphere and solar zenith angle on the signals has been investigated (chapter 3 and 4). With the aid of field measurements relations were found between reflectance and surface characteristics and their dynamics (chapter 5-7). Possibilities to derive information from Landsat TM, using relations found in the field, was described in chapter 9.

OUTLINE OF THIS THESIS

In chapter 2 different sources of error in determination of the bidirectional reflectance factor are evaluated. The evaluation is focused on measurements and equipment used the field campaigns in southern Tunisia.

In chapter 3 diurnal variation of field reflectance is described. It was examined to which extent this variation was caused by roughness and by moisture. Reflectance was studied for a range of solar zenith angles and for both footslopes and playa parts.

In chapter 4 atmospheric condition and its influence on field reflectance is evaluated. For this aim field reflectance and atmospheric conditions (diffuse to total irradiances) were determined. The measured ratios were also used in the atmospheric model of Verhoef to predict ground reflectance derived for satellite overpasses at realistic atmospheric conditions.

In chapter 5 the effect of natural and artificial variation in moisture content on field reflectance is examined. Natural daily, seasonal and inter-seasonal variation in moisture and reflectance was studied. Field experiments were used to test linear relations between moisture content and reflectance.

In chapter 6 results of field reflectance measurements on artificial plots of pure samples of gypsum, quartz and carbonate were discussed. Three variables have been considered: different mineralogy of comparable grainsizes, different types of gypsum and difference in iron content. Spectral variation in MMR bands is explained with laboratory spectra with higher spectral resolution. Reflectance of pure plots will be used as an aid for explaining spectral variation on natural plots.

In chapter 7 field reflectance of natural plots is analyzed. Knowing influence of atmosphere and solar zenith angle spectral variation can be explained with surface characteristics. Spectral reflectance will be interpreted with factors as roughness, gypsum, calcite, quartz, halite and moisture content. The field reflectance data set is meant as a base for explaining differences in the TM data set.

In chapter 8 the derivation of reliable planetary reflectance data from Landsat - 5 Thematic Mapper data, processed by Earthnet is described. Use was made of EOSAT experiments to correct the standard gains and apply the actual bandwidth to the Earthnet tapes.

In chapter 9 mapping of surface characteristics with Landsat TM data is discussed. The averages of clusters formed with unsupervised classification are transformed with the aid of the Verhoef model to ground reflectance values. The data set from chapter 7 was used to construct maps on surface characteristics and their dynamics with Landsat TM data.

In chapter 10 general conclusions are given.

PUBLICATIONS

The chapters 2 through 9 were or will be published as separate papers, with some modifications. References are given below.

Chapter 2

Epema, G.F., 1991. Studies of errors in field measurements of the bidirectional reflectance factor. *Remote Sensing of Environment* 35: 37-49.

Chapter 3

Epema, G.F., 1990. Diurnal trends in reflectance of bare soil surfaces in southern Tunisia. *Geocarto International* Vol.5, No.4: 33-39.

Chapter 4

Epema, G.F., 1992. Atmospheric condition and its influence on reflectance of bare soil surfaces in southern Tunisia, *International Journal of Remote sensing* Vol.13, No.5: 853-868.

Chapter 5

Epema, G.F., 1990. Effect of moisture content on spectral reflectance in a playa area in southern Tunisia. *Proceedings international symposium, Remote Sensing and Water Resources, Enschede, August 20-24 1990: 301-308.*

Chapter 6

Epema, G.F. and S.B. Kroonenberg, 1992. Ground reflectance of natural bare and pure surfaces as an aid in interpretation of Landsat Thematic Mapper data in southern Tunisia. *Advanced Space Research* Vol.12, No.7: (7)39-(7)42.

Chapter 7

Epema, G.F. Ground spectral reflectance in a desert area in southern Tunisia. Submitted to *International Journal of Remote Sensing*.

Chapter 8

Epema, G.F., 1990. Determination of planetary reflectance for Landsat 5 Thematic Mapper tapes processed by Earthnet (Italy). *ESA Journal*, Vol. 14: 101-108.

Chapter 9

Epema, G.F. Mapping surface characteristics and their dynamics in a desert area in southern Tunisia with Landsat Thematic Mapper. Submitted to *Remote Sensing of Environment*.

CHAPTER 2

STUDIES OF ERRORS IN FIELD MEASUREMENTS OF THE BIDIRECTIONAL REFLECTANCE FACTOR.

Remote Sensing of Environment 35: 37-49.

Studies of Errors in Field Measurements of the Bidirectional Reflectance Factor

G. F. Epema

Agricultural University of Wageningen, Department of Soil Science and Geology, Wageningen, The Netherlands

Errors in the determination of the bidirectional reflectance factor (BRF) were studied in a measuring campaign in the desert using one radiometer, a sprayed barium sulfate panel as reference and solarimeters. The following sources of error were evaluated: (1) specific characteristics of instruments, (2) interpolations due to non-simultaneous measurement of panel and object, (3) optical properties of the panel and (4) dependence of panel reflectance on atmosphere. The most significant errors occurred if the solar zenith angle dependent reflectance of the panel was ignored. Moreover, the assumption that all irradiance is direct, was discovered to be an important source of error, in particular pertaining to panel reflectance at large solar zenith angles, at short wavelengths and non-ambertian panels. The use of simultaneous solarimeter readings when object measurements were taken under nonideal atmospheric conditions may be partly of help.

from the background in the upwelling reflected radiance field. Reflectance usually quantified using the bidirectional reflectance factor (BRF) is defined as the ratio of radiance measured over a target to that measured over a horizontal reference panel. The panel in this definition is specified to be perfectly diffuse, completely reflecting, and viewed under the same irradiation conditions and in the same geometry as the target (Milton, 1987). For comparisons with imagery from near-nadir looking satellites such as Landsat, the BRF in the field must also be measured from nadir. Milton (1987), after Robinson and Biehl (1979) and Jackson et al. (1980), presented an overview of the principles of field spectroscopy. For adequate reflectance data, however, the measurements have to be corrected in the proper manner. For practical reasons not all corrections are actually applied in field surveys. The aim of this study is to establish the effect of different types of corrections for determining the BRF for nadir observation.

INTRODUCTION

Objects may be characterized by their reflectance. This enables certain features to be discriminated

Results of a measuring campaign in April 1988 in southern Tunisia using one Barnes Modular Multiband Radiometer (MMR) and one reference panel are provided. The measuring campaign is part of a project to ascertain the importance of Landsat Thematic Mapper (TM) data for the characterization of bare soil surfaces. The measurements reported were confined to relatively good to excellent circumstances, i.e., with almost cloudless

Address correspondence to G. F. Epema, Agric. Univ. of Wageningen, Dept. of Soil Sci. & Geology, P. O. Box 37, 6700 AA Wageningen, The Netherlands.

Received 28 July 1989; revised 6 November 1990.

skies. Useful Landsat Thematic Mapper data can only be gathered without much cloud. Although the results presented here are specific to these areas and this type of instrument, they also give an indication for measurement conducted under other circumstances.

The extent of the importance of the following corrections to the raw measured voltages of the instruments for the determination of BRF has been tested:

1. Corrections for specific characteristics of the instruments.
2. Corrections for nonsimultaneous measurement of object and reference panel, occurring in a setup with one instrument necessitating correction for temporal change.
3. Corrections for optical properties of the reference reflectance panel.
4. Corrections for the dependence upon the atmosphere of a nonlambertian panel upon atmosphere. The significance of the angular distribution of the diffuse irradiance and of the ratio of diffuse to total irradiance was investigated.

EXPERIMENTAL METHODS AND CONDITIONS

Measurements were made with a Barnes Modular Multiband Radiometer (MMR) (Robinson et al., 1979) equipped with a 15° field of view (FOV) aperture. In field surveys a 15° FOV is normally used to average over surface irregularities of the target (Biggar et al., 1988). The MMR was mounted on a tripod with the viewing direction vertical and the height above the surface 1.5 m. Reflected radiation was measured over the different objects every hour. Reference radiance readings from the standard reflector painted with barium sulphate were taken at the start and finish of each measurement sequence. The BRF in a given MMR bandpass was determined by dividing the radiance reflected from an object by that from the standard reflector in the same nominal bandpass. To compare the curves of spectral response functions for the MMR with the one used, I refer to Jackson and Slater (1986).

Table 1. Bandpasses (-3 dB) of Barnes MMR Field Radiometer (50% Power Bandpass Limits) and Landsat Thematic Mapper (Full-Width at Half-Maximum Method)

Barnes MMR		Landsat TM	
Band No.	Wavelength Limits	Band No.	Wavelength Limits
1	0.458-0.525	1	0.4524-0.5178
2	0.519-0.601	2	0.5280-0.6093
3	0.637-0.687	3	0.6264-0.6923
4	0.739-0.898	4	0.7764-0.9045
5	1.174-1.334		
6	1.574-1.803	5	1.5675-1.7842
7	2.083-2.371	7	2.0972-2.3490

Table 1 shows the comparison of the bandpasses provided by the manufacturer with those obtained from Landsat Thematic Mapper (TM) data of Landsat-4 and -5 by Markham and Barker (1986). Reflectance data obtained with the MMR cannot be compared exactly with Landsat TM due to the difference in spectral response in each bandpass between the instruments (Duggin and Philipson, 1985). The MMR can be used to measure thermal radiation (not used in this study) and also temperatures inside the equipment. The output signals of the MMR bands have a range of 0.0-+5.0 V and the instrument is provided with gain switches for an adequate dynamic range. In our experiments values above 3.0 V were always measured with a gain switch on 0.5, while values below 0.1 V were measured with a larger gain setting on the multimeter. Errors between readings made at different range settings were negligible.

The effect on reflectance has been evaluated for the following factors.

Specific Characteristics of the Instruments

The following factors were studied in detail:

- a. The dark voltage in the MMR and recording system. The dark voltage is the sensor signal with all light blocked from detectors.
- b. Errors due to incorrect gain factors of the MMR.
- c. The temperature sensitivity of PbS detectors of the MMR Bands 5, 6, and 7, and the temperature sensitivity of the recording multimeter. A lower output was measured with increasing temperatures. All values were recalculated for a reference temperature of 25°. Unlike the procedure of Jackson and Robinson

(1985), the relation between temperature of instrument and voltage for this instrument was determined in the laboratory and not in the field.

Interpolations to Correct Reflected Radiance Values from the Panel for Temporal Variation during Sample Measurement

Two types of interpolations were evaluated:

- a. Linear interpolation based on time for stable atmospheric conditions.
- b. Interpolation based on solarimeter values for unstable light conditions.

When measuring the objects, in order to detect unpredictable differences between measurements due to clouds or haze, a solarimeter (type Kipp CM 11) was installed and read simultaneously as recommended by Milton (1987). Furthermore, the relationship between solarimeter readings and reflected panel values of individual bands were determined. In this way it was possible to ascertain whether solarimeter values, measuring over a broad range of the spectrum (0.3–2.8 μm), could be used to estimate the incoming radiation in the specific MMR bands.

Reflectance of the Panel for Different Solar Zenith Angles

The reflectance of the panel under diffuse illumination was determined in the laboratory with a set-up (not to scale) as given in Figure 1. The panel or standard were diffusely illuminated and sampled from nadir and the reflected radiance was recorded by the detectors, after passing a monochromator. Si or PbS detectors were used depending on wavelength, the signal for the PbS detectors being chopped to minimize errors due to drift. This setup was selected since all panel measurements in the field campaigns were made from nadir. Reflectance was calculated by the ratio of the signal from the panel to that from the standard BaSO_4 multiplied by the reflectance of the standard (DIN 5033) BaSO_4 . The sampling intervals of 15 nm were integrated over the response function of the bandpasses of the MMR as given by the manufacturer.

The solar zenith angle dependence of the reflectance of the panel viewed from nadir was

tested in the field and in the laboratory; the field method was described by Jackson et al. (1987). Since the zenith angle dependence of the panel could constitute a significant source of error and the accuracy of a field method could be unreliable, the angular dependence was determined once again in the laboratory. A setup was chosen consisting of three parts: 1) source, a halogen lamp of 400 W and a chopper and diaphragms, 2) the panel, and 3) a detector unit, including lenses, diaphragms, and filters, which provided a 1° FOV. These three parts were able to move independently of each other. For view and illumination zenith angles of 2–90°, the signal was recorded.

Atmospheric Conditions

The measured reflectance of a nonideal panel is not only determined by the total global irradiance, but also by the ratio of diffuse to direct irradiance. Consequently, the diffuse component for each panel reading was determined by shading the panel. Errors in the determination of the diffuse irradiance caused by the interruption of part of the diffuse (sky) radiance from around the solar disk were evaluated. Realistic atmospheric models (Verhoef, 1985) were used to accurately calculate the diffuse reflectance for the reference reflectance panel.

RESULTS AND INTERPRETATION

The effects on reflectance of the different types of corrections may be estimated from the voltages measured over the panel and the range of surface reflectances after the necessary corrections have been made as presented in Figures 2–4.

In Figures 2 and 3 measured voltages of the unshaded and shaded panel are provided for Bands 1 and 7. These values were used to calculate total and diffuse radiation. Values of uncorrected voltage for Bands 2–4 were about 10–15% lower than those measured simultaneously for Band 1. The maximum values of Band 7 occurred before solar noon because no temperature correction had as yet been applied to these values. During the measurement campaign, the internal temperature of the instrument was between 15°C and 33°C. Uncorrected Band 5 and 6 values differ less than 5%

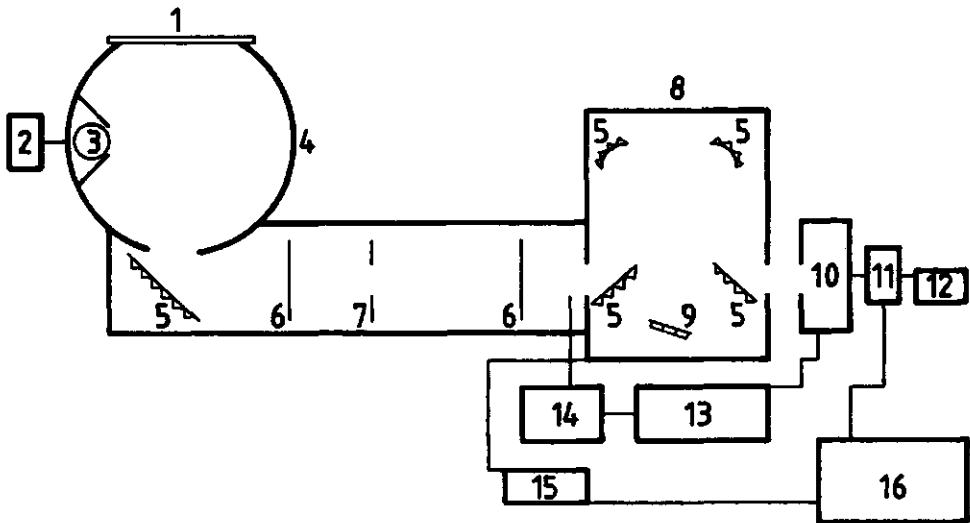


Figure 1. Experimental setup to determine panel reflectance under diffuse illumination.

Key:

- | | |
|---|--------------------------------------|
| 1 standard reflector or BaSo ₄ /Zeiss standard | 10 filterwheel |
| 2 power supply | 11 detectors |
| 3 lamp | 12 power supply |
| 4 integrating sphere (Zeiss RA3) | 13 lockin amplifier (Stanford SR530) |
| 5 mirror | 14 chopper |
| 6 lenses | 15 steering |
| 7 diaphragm | 16 computer |
| 8 monochromator (Jolin Yvon HR320) | |
| 9 grating | |

Notes:

- BaSo₄ standard according to DIN 5033 and Zeiss standard 20075
- Sampling interval: 15 nm
- Detectors: Si, PbS and photomultiplier
- Chopper: used for PbS
- Lamp: 60 W Halogen

from the Band 7 values of the unshaded panel. Uncorrected diffuse values of Bands 2-6 are between values of Bands 1 and 7.

In Figure 4 two extreme BRFs measured from nadir are given for bare soils observed in southern Tunisia as determined using our setup. For bare soils in this area most values (98%) are in between these examples.

Instruments Corrections

The dark level measurements performed under a range of temperature conditions both in the field and in the laboratory only revealed small differences. The mean dark level values for two gain factors of the multimeter provided in Table 2 show

standard deviations to be less than 0.001 units. Gain settings of the Barnes MMR also appear to have little influence on the dark level. As a result, dark voltage values are so low that they could be ignored, except for objects with a low reflectance and with very low irradiance readings.

To measure voltages above 3 V the gain switch of the MMR is set from 1.0 to 0.5. Voltages above 3 V, however, cannot be calculated directly by doubling the measured values (Table 3). For instance, Band 1 voltages measured with the gain switch on 0.5 have to be multiplied by 1.965 instead of by 2.000 to achieve an accurate value. Failure to use this multiplier will result in an error of nearly 2%. In Table 4 intercept and slopes are given for the relation between temperature and

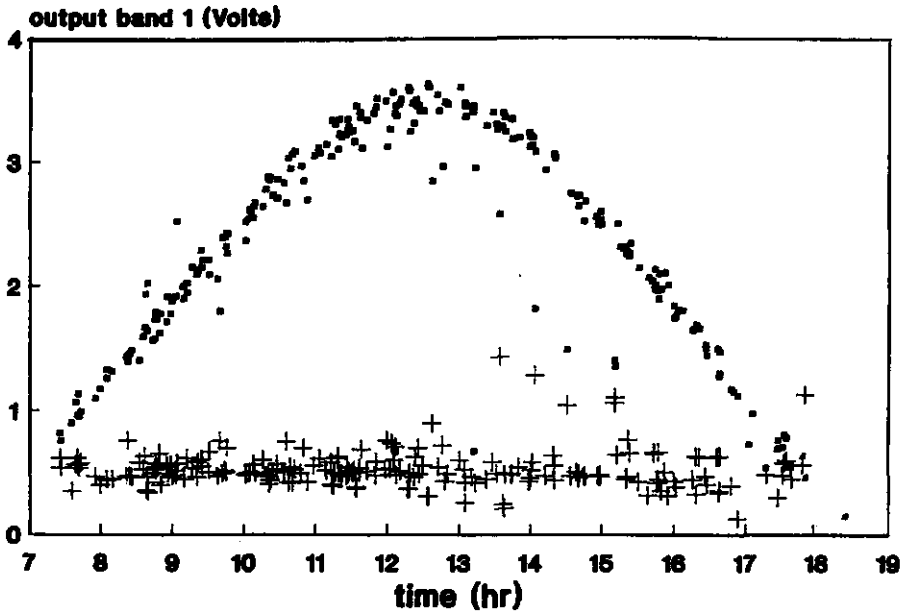
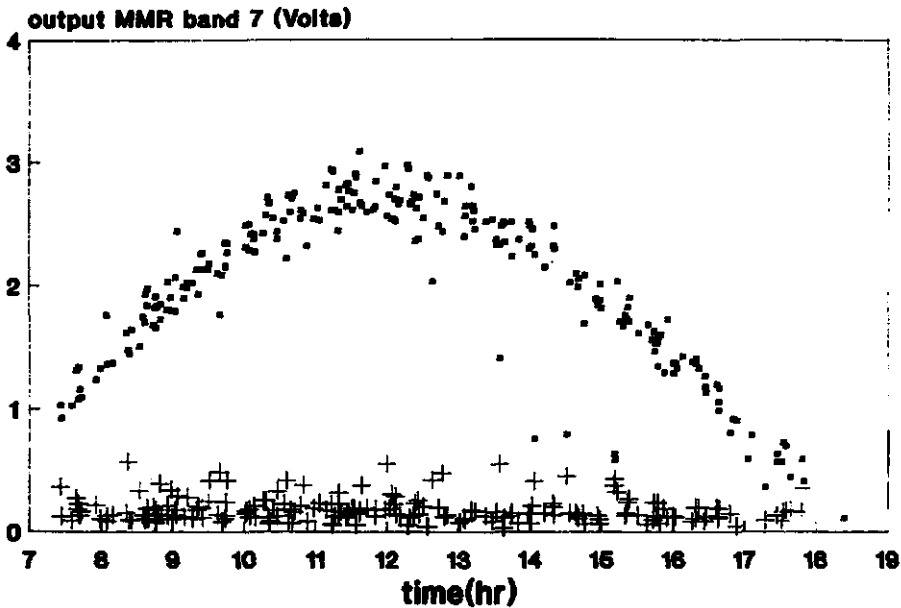


Figure 2. Uncorrected output voltages of MMR Band 1 as a function of time for April 1988 field campaign: (■) unshaded panel; (+) shaded panel.

Figure 3. Uncorrected output voltages of MMR Band 7 as a function of time for April 1988 field campaign: (■) unshaded panel; (+) shaded panel.



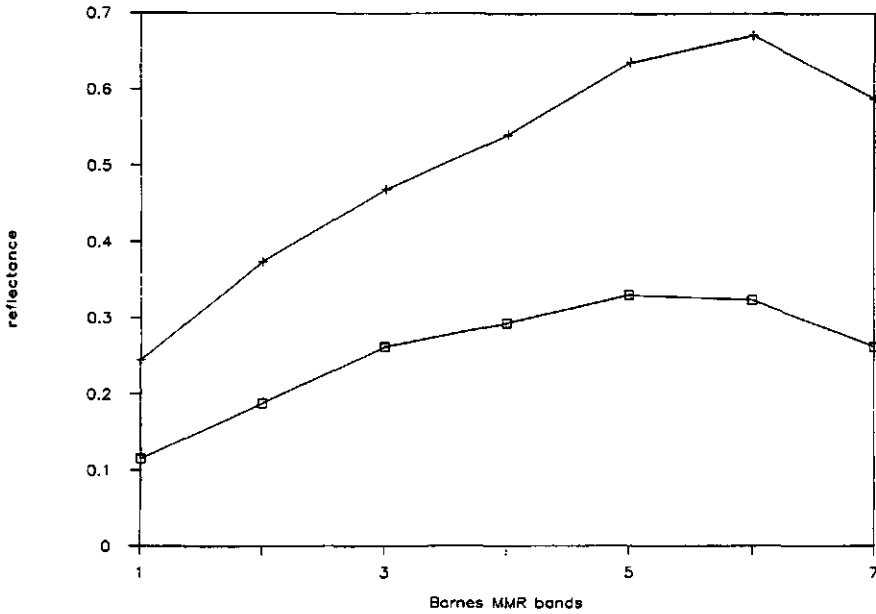


Figure 4. Bidirectional reflectance factor of two bare soil surfaces in southern Tunisia with a very low and a very high reflectance for the MMR bands.

Table 2. Dark Level Values of MMR and Multimeter for Two Multimeter Settings

	1	2	3	4	5	6	7
0-0.3 V	.0060	.0030	.0058	.0054	.0051	.0045	.0012
0-3 V	.007	.004	.007	.006	.006	.006	.002

Table 3. Multiplication Factors for Voltages Measured with Gain Setting of 0.5 to Standard Gain of 1 for the MMR Bands

MMR Band	1	2	3	4	5	6	7
Multiplier	1.965	1.985	1.985	1.989	1.989	1.992	1.987

voltage output of the sensors. The PbS sensors are very sensitive to temperature variations. The intercept/slope (a/b) ratios of the sensor are in accordance with the findings of Jackson and Robinson (1985) for Band 7, the a/b ratios of Bands 5 and 6 are higher. Note that even if voltages are not adjusted for this temperature effect, the calculated reflectance values would hardly deviate from the correct values. Both the voltage corresponding to radiance reflected by the object and the interpolated value of the reflectance of the

Table 4. Relation between Output Voltages of MMR and Sensor Temperature

MMR Bands	1	2	3	4	5	6	7
Intercept (a)	.0708.1004	.1825.3100	1.2444	1.4960	2.0462		
Slope (b)	.0001.0002	-.0001.0009	-.0169	-.0194	-.0318		
a/b	701	408	-1520	341	-73.5	-76.9	-64.3
a/b (J&R) ^b					-65.4	-64.2	-64.6

^aVoltage MMR at 25°: measured voltage at temperature T times $(a/b + 25)/(a/b + T)$.

^bJackson and Robinson (1985).

panel have to be multiplied by almost the same factor. The temperature changes of the instrument were observed to be very regular and the temperature increase seldom exceeded 2° in one of the measurement series.

The figures of both Tables 3 and 4 are probably instrument-dependent and could therefore differ for each MMR. In the laboratory, the response of the multimeter to different temperatures tested against a calibrated instrument showed deviations of less than 0.5%. Linear response of the MMR instrument was not tested. The manufacturers specification of 2% was adopted due to lack of alternative information.

Impact of Interpolations Needed Should the Reflectance Panel Not Be Measured Simultaneously with the Object

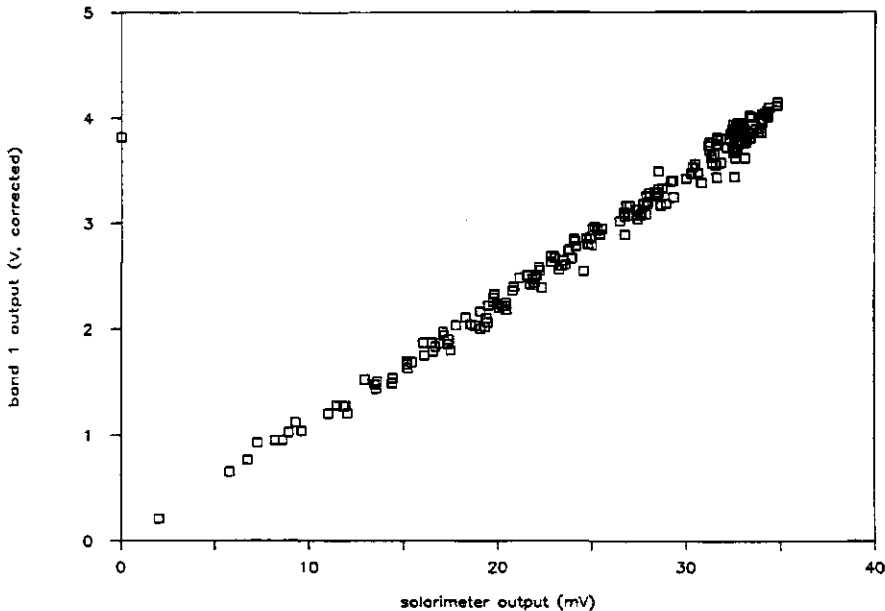
Duggin and Cunia (1983) statistically demonstrated that simultaneous, as compared to sequential, measurement of irradiance and radiance reflected from the target is the most reliable technique. Therefore, in principle, the reflectance of the reference panel or the irradiance measurement with an uplooking radiometer (Duggin, 1980) has to be determined at the same time as the object measurement. If, however, only one MMR instrument is available, another solution has to be found. In this study simultaneous solarimeter readings at the moment of measurement of the object were taken.

Under stable conditions a linear interpolation of reference panel values in 1 h provides a negligible error in reflectance. Solarimeters were only used to check the stability of the atmospheric conditions. In the period before 11:00 and after 13:30 (lowest solar zenith angle at 12:15), interpolated panel reference values in a period of 1 h are only 0.5% lower than the actual value. If in an

extreme situation, in the period 0.5 h before to 0.5 h after the highest zenith angle, the interpolated panel reflectance is determined, it would amount to 98.5% of the real value. In our campaign, measurement sequences of a series of plots and panel generally took less than 15 min.

Linear interpolations are inadequate under variable atmospheric conditions. Significant linear relations at $\alpha = 0.05$ of individual Bands 1-4 with solarimeter readings for the measurement days were detected (Fig. 5). This is remarkable since response times between MMR and solarimeter are different and since solarimeters measure a broader spectral range than the MMR. Nevertheless, on the worst day on which reliable measurements were made, deviations of up to 10% from the regression line between solarimeter readings and individual bands are feasible. In Bands 5, 6, and 7, those including only a small percentage of the total reflected solar irradiance, it is even more risky to make estimates from solarimeter values for hazy conditions. This is especially true if small thin clouds exist. The error results from a combination of the longer time constant of the solarimeter and a high frequency variation in irradiance. In

Figure 5. Relation between solarimeter output and corrected MMR Band 1 for different days.



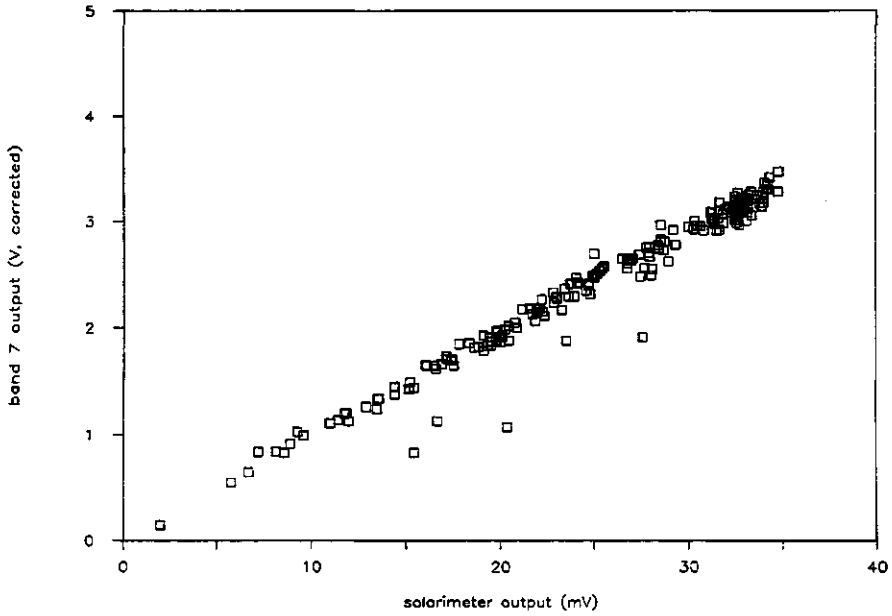


Figure 6. Relation between solarimeter output and corrected MMR Band 7 for different days.

Figure 6 showing the relationship between the output from Band 7 and the solarimeter output, the points distant to the line are the result of the variability in atmospheric transmission and of the varying ratio of direct solar to diffuse sky irradiance, averaged out by the solarimeter. If rapid changes of solar and sky irradiance occur, the use of solarimeters is inaccurate due to differences in response time between the MMR and the solarimeter. Under these conditions no reliable measurements could be determined within the scope of the setup.

Reflectance of the Panel

Reflectance values of the standard reference reflector for the MMR bands are provided in Table 5. They are significantly less than 1.00, as has generally been reported (e.g., Duggin, 1980).

Another source of error in the determination of the BRf will occur if the reflectance of the panel measured from nadir is strongly solar zenith angle dependent. Figure 7 shows panel reflectances from Bands 1 and 7 determined in the laboratory for a range of illumination zenith angles. The vertical axis is the ratio of the reflectance measured at each incident radiance zenith angle to that mea-

sured with irradiance at only 2° zenith angle. Laboratory measurements were integrated over the 15° FOV of the Barnes. This results in a smoothing of the curve and a lowering of the value at large incidence angles also stated by Biggar et al. (1988). The field experiment showed similar trends. Deviations were less than 2% for the Si detectors and up to 10% for the PbS detectors. Hence deviations for Si detectors were somewhat higher than those described by Biggar et al. (1988) (maximum 2% as compared to 1.35%). The band-passes with Si detectors show greater zenith angle dependence of the standard reflector than the longer wavelength PbS bands, as also found by Jackson et al. (1987). Although most new standard reflector panels deviate less than 30% from lambertian behavior for solar zenith angles less than 70° as our panel, the panel used was comparable with the worst panel described by Jackson et al. (1987). It is clear that under dominantly direct irradiance conditions (little or no cloud) large er-

Table 5. Reflectance of Reference Panel under Diffuse Illumination Conditions

MMR Bands	1	2	3	4	5	6	7
Reflectance	0.806	0.868	0.911	0.931	0.929	0.898	0.841

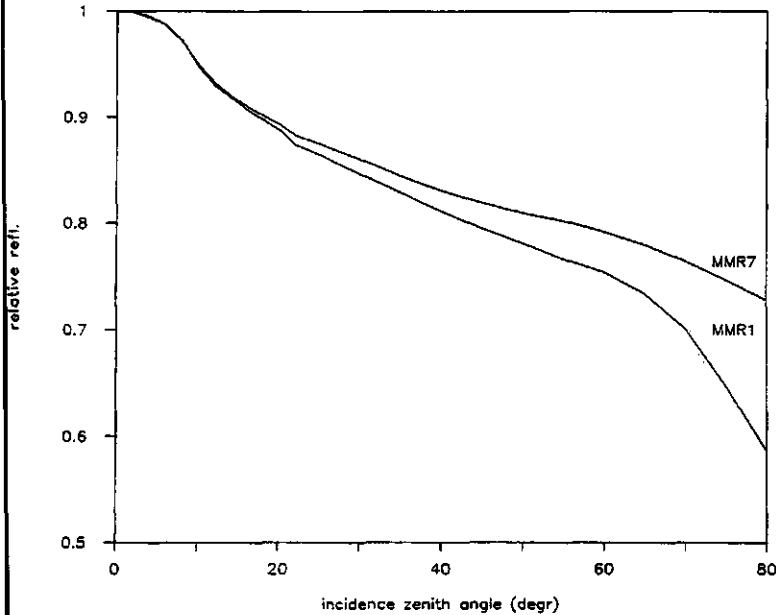


Figure 7. Relative reflectance of MMR bands for different view zenith angles in comparison with an illumination zenith angle of 2° .

rors occur if one assumes the panel to be lambertian.

The Influence of Atmospheric Conditions to Panel Reflectance

There is a difference between reflectance of a nonideal panel under diffuse and that under direct illumination. Both types of irradiance exist under all natural circumstances, the relative contribution depending on solar zenith angle, haze and cloud conditions. To obtain the adequate panel reflectance, a weighted average of direct and diffuse reflectance requires to be calculated. The reflectance of the panel has already been described for the direct component. The reflectance for natural diffuse irradiance of the panel and errors in determination the diffuse component will be described now.

A primary complication in determining the diffuse component is the nonuniform angular distribution of natural diffuse radiation; hence the laboratory values in Table 5 cannot be used directly. The nonlambertian character of the panel must be taken into account. Moreover, the angular distribution of hazy and clear sky diffuse irradiance differs (Kimes and Kirchner, 1982). In a hazy sky, the diffuse component is more concentrated

around the angle of incidence of direct radiation and does not increase at the horizons as it does in the case of a clear sky. To calculate the reflected output of our panel, taking into account the non-lambertian behavior for different types of diffuse irradiance, an atmospheric model of Verhoef with a Mie scattering by aerosol haze representing desert conditions [principles of the entire model are described by Verhoef (1985)] was used. The ratio of the output of the panel under natural diffuse conditions to the diffuse reflectance values in the laboratory for MMR Bands 1-4 is provided in Figure 8. Here results of four conditions of this type of atmosphere ranging from hazy with a horizontal visibility of 5 km to very clear with a visibility of 40 km are presented. Conclusively, errors due to diffuse radiation for these four conditions are less than 2% up to a solar zenith angle of 60° . Hence a computed mean curve corrected in this way produces not only a systematic and slight deviation from the real values of diffuse irradiance but also a negligible deviation of the total reflectance of the panel. Kimes and Kirchner (1982) made similar determinations for another panel for red and near infrared reflectance and for two types of atmosphere [adopted from Dave (1978) type #3 and #4]. Their results are in good agreement with those presented above.

The diffuse component of the irradiance may be obtained by shading the panel with an occulting disk. A drawback of this method is, however, that apart from intercepting the direct radiation a portion of the diffuse radiation is also intercepted. Therefore, the shown results in Figure 8 need to be corrected for the intercepted portion. Che et al. (1985) have suggested that measurements be performed with the shading of the occulting disk next to the reference panel. The difference between this measurement of the panel and panel reflectance without any obstructions gives a measure of the intercepted radiation. According to Che et al. (1985), better estimates of the direct and, hence, also of the diffuse component should be achieved with this method. However, on examining the atmospheric distributions of sky irradiance in Verhoef's models, it is obvious that the accuracy of this method is unreliable especially with the occulting disk at a distance of less than 3 m as we have done for practical reasons. Therefore, applying the atmospheric models of Verhoef, ratios were calculated for our panel for two distances between occulting disk and panel (2 m and 1.35 m) in the form

$$(E_T - E_S)/E_T,$$

where E_T is the hypothetical total diffuse sky irradiance on our panel (corrected, using a model) and E_S is the portion of diffuse sky irradiance intercepted by the occulting disk. In Figure 9 these ratios are given for MMR Bands 1-4, two conditions of the atmosphere, and two distances between occulting disk and panel.

It is well known that diffuse/total ratios are greater with an increasing solar zenith angle and decreasing wavelength (Iqbal, 1983). Therefore, assuming only direct irradiance, the occurrence of errors is dependent on wavelength and solar zenith angle. For example, on an average day, panel irradiances under the assumption of only direct irradiance produce a value 2% higher with a solar zenith angle of 60°, and a value 2% lower with 25° in Band 1. With increasing wavelength the deviations decrease and for Band 7 values are always within 1% up to 60°. In the case of higher zenith angles, assuming only direct irradiance, errors increase for all bands dramatically: For example, with 70° for Bands 1 and 7, reflectance values 15% and 5%, respectively, too high for our panel will

be obtained. Jackson et al. (1988) based their calculations on Kimes and Kirchner (1982) and calculated a percent error in irradiance estimation for a range of reference panels. Their panels showed less dependence on atmosphere due to being closer to lambertian behavior.

Field Techniques

Apart from the processing errors described above, errors may also occur due to inadequate measurements. I adopted most suggestions for good measurements given by Milton (1987). The sensor was placed more than 1 m above the ground, not the ideal 2 m but at 1.5 m for practical reasons. The standard panel filled the view for all bands. The operators wore dark clothes and knelt as far as possible (a distance of about 1 m), and no vehicles or other obstacles were close to the target. It was also observed that wind influenced the vegetation reflectance but, due to the specific type of vegetation, far less than the values reported by Lord et al. (1985). Furthermore, vegetation comprised only a small part of the surface and the measurements were, as much as possible, executed during periods of low wind velocity. Solarimeters were positioned centrally in the field and readings were taken simultaneously together with the target and panel measurements. It is shown above, however, that in poor sky conditions only rough estimates could be obtained from panel reflectance. For our measurements we mounted the MMR on a tripod with the sensor support directed to the sun, necessitating the repositioning of the tripod for each measurement. Although this was accomplished with care, errors with each new positioning are bound to occur.

CONCLUSIONS

It is evident that the most significant errors when calculating the BRDF may be because the reflectance of the BaSO₄ panel is assumed to be 100% or by ignoring the solar zenith angle dependence of it. This last factor could be determined in the field using the method described by Jackson et al. (1987) only if atmospheric conditions are stable; otherwise a laboratory determination is required.

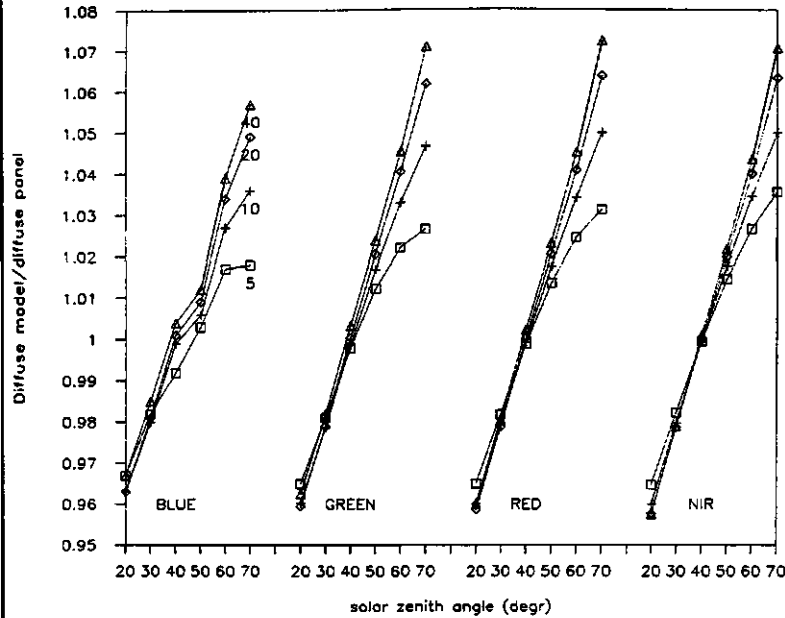


Figure 8. Relative error of diffuse irradiances as a function of solar zenith angle for four types of sky in (from left to right) blue, green, red, and near infrared MMR band-passes for visibility of 5 km, 10 km, 20 km, and 40 km.

The reflectance of a nonideal panel under natural conditions is not solely a function of the solar zenith angle; apart from direct radiation diffuse radiation also exists. The diffuse sky radiance as a function of solar zenith angle was determined using one of Verhoef's atmospheric models. In this

way, I was able to obtain correction factors for the panel and also for a specific distance between occulting disk and panel. Corrections for atmosphere are especially necessary if a large part of the irradiance is diffuse as is the case for large solar zenith angles (more than about 60–70°) and

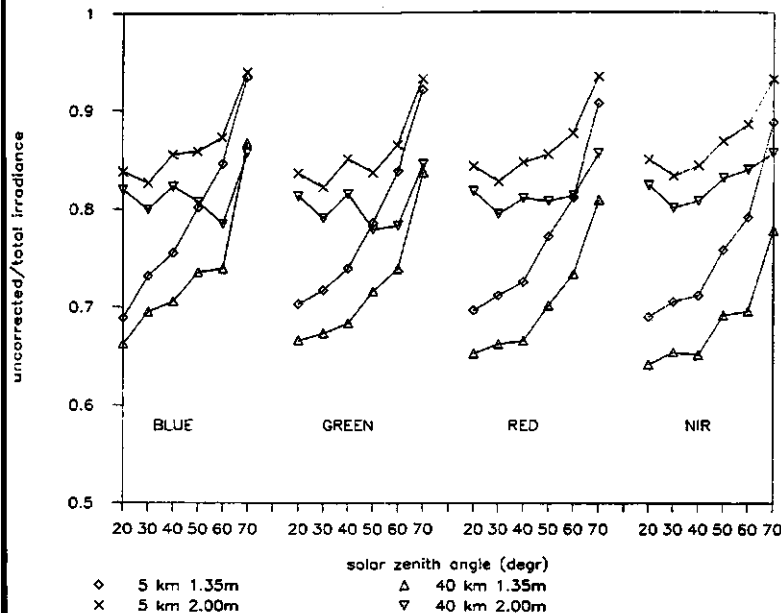


Figure 9. Relative error in diffuse radiation due to intercepting too much diffuse irradiance by the occulting disk for distances of 1.35 m and 2.00 m, respectively, with a very clear and a hazy atmosphere (calculations with the Verhoef model).

at short wavelengths. In order to avoid calculations for distance, a distance of at least 3 m between occulting disk and reference panel, although often impractical, is recommended.

Other corrections, although less important in our study, have been applied to the data set: effects of dark level, gain, and temperature sensitivity. For some instruments it may also be necessary to evaluate the linearity of the radiometer and the reliability of the multimeter or data logger. It has been shown that, for stable conditions, linear interpolations of measurements of panel reflectance bracketing sample readings cause only small errors in derived sample reflectance if measurements are recorded with a 10-s time interval accuracy. If atmospheric conditions are unstable, although solarimeters may be of help in selecting conditions where linear interpolation is feasible, the possibility of relatively large errors remain.

Adequate field techniques, such as those described by Milton (1987), are vital for appropriate BRDF determinations. It is better, however, to incorporate the determination of the amount of diffuse radiation by intercepting sunlight in a proper way in the field survey. Apart from using it to determine the total irradiance satisfactorily, the ratio diffuse/total irradiance is a good measure for the particular type of atmosphere at that moment. The ratio is much more sensitive than the total irradiance and is therefore used in atmospheric models relating satellite data to ground reflectance, as, for example, that of Verhoef (1985).

If data are treated in the manner described above, a consistent field BRDF under the specific atmospheric conditions is determined. If campaigns are to be conducted far from base laboratories, a minimum program includes:

- calibration of the reflectance standard panel in a base laboratory before the field campaign;
- determination of solar zenith angle dependence of the standard reflector in the field at start and finish of campaign;
- simultaneous solarimeter readings taken during reflectance measurements in order to avoid large errors due to changing conditions by eliminating measurements during very variable irradiance conditions, and allowing for measurements to be made under less ideal conditions.

This research is part of a project funded by the Netherlands remote sensing board (BCRS, AO 4.2). I wish to thank Professor Dr. F. K. List and Dr. A. Richter (FU Berlin) for use of the Barnes MMR and additional data on temperature sensitivity, W. Verhoef (NLR) for data on atmospheric models, Dr. K. Schurer and J. Kornet (TFDL) for the laboratory measurements and discussions, Professor Dr. S. B. Kroonenberg (AUW), Professor Dr. Ir. M. Molenaar (AUW), and Dr. Ir. M. Menenti (SC) for their critical comments to this paper, and Ninette de Zylva for checking the English.

REFERENCES

- Biggar, S. F., Labeled, J., Santer, R. P., Slater, P. N., Jackson, R. D., and Moran, M. S. (1988), Laboratory calibration of field reflectance panels, in *Recent Advances in Sensors, Radiometry, and Data Processing for Remote Sensing*, SPIE Vol. 924, pp. 232–240, Bellingham, WA.
- Che, N., Jackson, R. D., Philips, A. L., and Slater, P. N. (1985), The use of field radiometers in reflectance factor and atmospheric measurements, *Soc. Phot-Opt. Instrum. Eng.* 499:24–33.
- Dave, J. V. (1978), Extensive datasets of the diffuse radiation in realistic atmospheric models with aerosols and common absorbing gases, *Sol. Energy* 21:361–369.
- Duggin, M. J. (1980), The field measurement of reflectance factors, *Photogramm. Eng. Remote Sens.* 46(5):643–647.
- Duggin, M. J., and Cunia, T. (1983), Ground reflectance measurement techniques: a comparison, *Appl. Opt.* 23:3771–3777.
- Duggin, M. J., and Philipson, W. R. (1985), Relating ground, aircraft and satellite radiance measurements: spectral and spatial considerations, *Int. J. Remote Sens.* 6:1665–1670.
- Iqbal, I. (1983), *An Introduction to Solar Radiation*, Academic, New York.
- Jackson, R. D., and Robinson, B.F. (1985), Field evaluation of temperature stability of a multispectral radiometer, *Remote Sens. Environ.* 17:103–108.
- Jackson, R. D., and Slater, P. N. (1986), Absolute calibration of field reflectance radiometers, *Photogramm. Eng. Remote Sens.* 52(2):189–196.
- Jackson, R. D., Pinter, P. J., Reginato, R. J., and Idso, S. D. (1980), Hand-held radiometry, U. S. Department of Agriculture Publication ARM-W-19, Washington, DC.
- Jackson, R. D., Moran, M. S., Slater, P. N., and Biggar, S. F. (1987), Field calibration of reference reflectance panels, *Remote Sens. Environ.* 22:145–158.
- Jackson, R. D., Slater, P. N., and Moran, M. S. (1988), Accounting for diffuse irradiance on reference reflectance panels, in *Recent Advances in Sensors, Radiometry, and Data Processing for Remote Sensing* SPIE Vol. 924, pp. 241–248, Bellingham, WA.
- Kimes, D. S., and Kirchner, J. A. (1982), Irradiance measurement errors due to the assumption of a lambertian reference panel, *Remote Sens. Environ.* 12:141–149.

- Lord, D., Desjardins, R. L., and Dube, P. A. (1985), Influence of wind on crop canopy reflectance measurements, *Remote Sens. Environ.* 18:113-123.
- Markham, B. L., and Barker, J. L. (1986), Landsat MSS and TM post-calibration dynamic ranges, exoatmospheric reflectances and at-satellite temperatures, EOSAT Landsat Technical Notes, No. 1., EOSAT, 4300 Forbes Blvd., Lanham, MD 20706.
- Milton, E. J. (1987), Principles of field spectroscopy, *Int. J. Remote Sens.* 8(12):1807-1827.
- Robinson, B. F., and Biehl, L. L. (1979), Calibration procedures for measurement of reflectance factor in remote sensing research, *J. Soc. Photo-Opt. Instrum. Eng.* 196:16-26.
- Robinson, B. F., Bauer, M. E., DeWitt, D. P., Silva, L. F., and Vanderbilt, V. C. (1979), Multiband radiometer for field research. *J. Soc. Photo-Opt. Instrum. Eng.* 196:8-15.
- Verhoef, W. (1985), A scene radiation model based on four-stream radiative transfer theory, in *Proceedings of the 3rd International Colloquium on Spectral Signatures of Objects in Remote Sensing*, Les Arcs, France, 16-20 December 1985, ESA SP 247, pp. 143-150, Noordwijk.

CHAPTER 3

**DIURNAL TRENDS IN REFLECTANCE OF BARE SOIL SURFACES
IN SOUTHERN TUNISIA.**

Geocarto International Vol.5, No.4: 33-39.

Diurnal Trends in Reflectance of Bare Soil Surfaces in Southern Tunisia

J. Epema

Agricultural University of Wageningen

Department of Soil Science and Geology

Box 37

6700 AA Wageningen

Netherlands

Abstract

In an area in southern Tunisia diurnal trends of bare soil surfaces have been investigated. The study area comprises two main parts: the footslopes and the playas.

The diurnal variation of the bidirectional reflectance factor (BRF) in nadir direction on the footslopes is dominated by the effect of roughness. Maximum BRF is found with small solar zenith angles due to decrease in shadow related to surface roughness. For Landsat overpass it implies that the normal ground reflectance for a bare surface on the footslopes at identical surface conditions is up to 10% lower in December (solar zenith angle 63 degrees) than in June (28 degrees). Band ratios on footslopes hardly change with variation of zenith angle.

The diurnal variation in the playas is dominated by moisture. Asymmetric daily curves, with the highest reflectance in the morning have been found. Four phenomena are reported which can be held responsible for this effect. This daily effect of moisture is weather dependent and may obscure long term changes of TM signal. In band ratios even with TM band 7 the diurnal moisture change can hardly be detected.

Introduction

In an area in Southern Tunisia research has been carried out to investigate the relations between Landsat Thematic Mapper (TM) signals and ground surface characteristics and its dynamics. Landsat TM observes the earth every 16 days at the same time. Differences in signal are not only caused by changes of the surface, but also by differences in solar zenith angle and atmosphere. Ground reflectance measurements in combination with ground observations were used as an aid in understanding the observed TM signal. It is clear that also ground reflectance at a specific location is not constant. It may vary as a function of atmospheric condition, solar zenith angle and roughness of the surface. This report aims to assess the effect of diurnal variation of ground reflectance of characteristic surfaces and conditions for days with good atmospheric conditions. This gives insight to what extent observations deviate from a Lambertian behaviour. It is therefore an aid in comparing reflectance of objects observed at different times of the day. The influence of atmosphere has been reported elsewhere (Epema in preparation).

Fig. 1 the location of the study areas is given. Extensive descriptions of the area on various aspects is given by Coque (1962), Coque and Jauzein (1967), Meckelein (1977), Mitchell (1983), Millington *et al* (1987) and Ongaro (1988). The study area is situated at the margin of the Saharan Platform

and the folded Atlas ranges. A large part of the zone of subsidence is occupied by playas (locally known as chotts). The Chott el Djerid is the largest of them and has an elongated northeastern arm (Chott Fedjaj), which has been formed by faulting in the top of an anticlinal uplift (Coque 1962; Jones and Millington 1986). The cuesta ridge of the Djebel Tebaga is located in the southern part of this uplift. It is surrounded by footslopes. Locally dunes of various sizes cover parts of playa margins and footslopes. The rainfall in this area is less than 100 mm per year. Apart from some oases, vegetation cover exceeds 5% of the surface only in exceptional cases. The inner parts of the playas have no vegetation cover at all.

The study areas comprise parts of the playas and the footslope areas. The western area is located in the Chott Djerid, while the eastern area is located at the margin of Chott Fedjaj and the footslopes of the Djebel Tebaga.

(1) Playa: The appearance of the playa varies in space and time. They are underlain essentially by gypsiferous sediments. Extensive descriptions are given by Mitchell (1983) and Millington *et al* (1986). In the winter wet season, but also after individual storms, large parts exhibit standing water and upon drying relatively clean salt crusts develop. Part of the water (with sediments) is derived from the surrounding mountains and spatial distribution is a function of small relief differences and location of storms. Locally just below the surface black layers alternating with

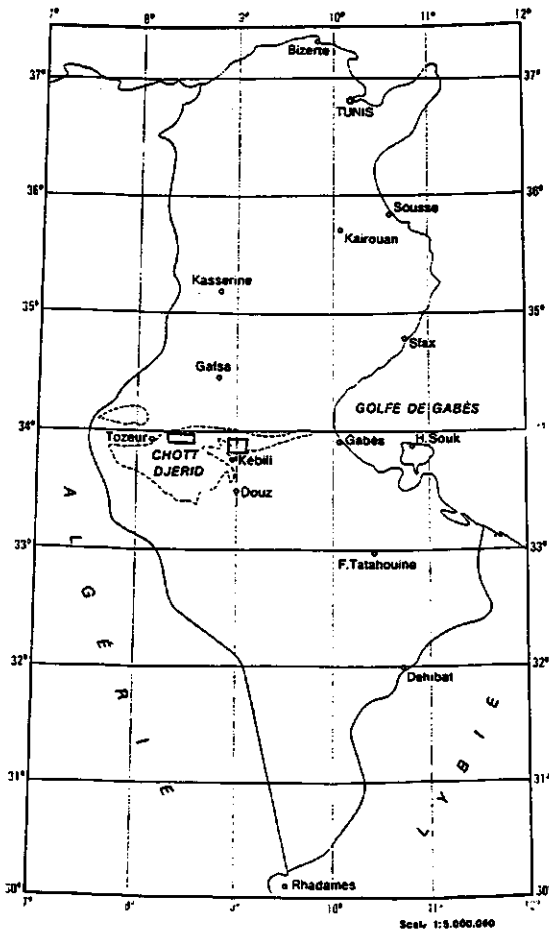


Fig 1. Location of the study areas in Southern Tunisia.

heavy layers exist. As described by Coque (1962), Mecklein (1977) and Ongaro (1988), the black layers are formed by algae. Especially in spring and summer silty and sandy

material is blown in. Spatial variation of surface type is important: thick crusts especially in the centre, polygenic structures of various sizes and changing in time and space. Large areas almost devoid of salt are present. Within the last area also relatively rough parts exist.

(2) Footslopes in the area are mainly erosional features. They show variation in presence of gypsum crusts, gypsum type and amount, incisions by gullies and cover and soil stones. As opposed to the area around Chott el Gujerat (described by Jones *et al* 1986) only small parts are alluvial fans. Vegetation is mostly limited to hummock spring vegetation is much greener and if it rains in winter period even outside these hummocks some vegetation exist.

Based on the variation in the area plots were selected for description and field reflectance measurements. In different types of diurnal curves were found. Examples of these curves will be presented, differences explained and implications for satellites given.

Experimental Methods and Conditions

Measurements were made with a Barnes Multiband Radiometer (MMR) (Robinson *et al* 1987) equipped with a 15° field of view aperture. The spectral characteristics in comparison with the Landsat Thematic Mapper (TM) deployed on Landsat-4 and -5 are given in Table 1. The MMR was mounted on a tripod (height 1.5 m) and the look direction was vertical. Hence a circular surface area with a diameter of 39.5 cm was observed.

Reflected radiance was measured over the different targets every hour. Panel data were achieved at the beginning and finish of each measurement sequence. The Bidirectional Reflectance Factor (BRF) was determined by dividing the radiance measured over a surface to the polarized and corrected radiances of the panel.

Reflectance data were gathered in accordance with the suggestions given by Milton (1987) and the data were treated as described by Epema (in preparation) measuring diffuse and total radiation not only the BRF

Table 1. Bandpasses of Barnes MMR field radiometer (50% power bandpass limits) and Landsat Thematic Mapper (full-width at half-maximum method).

Barnes MMR		Landsat TM	
nr. of band	wavelength	nr. of band	wavelength
1	0.458-0.525	1	0.4525-0.5178
2	0.519-0.601	2	0.5280-0.6093
3	0.637-0.687	3	0.6264-0.6923
4	0.739-0.898	4	0.7764-0.9045
5	1.174-1.334	5	1.5675-1.7842
6	1.574-1.803	7	2.0972-2.3490
7	2.083-2.371		

the variation in atmospheric condition between the and within the days could be determined. The ted measurements are restricted to relatively good to lent weather conditions, since only then useful sat Thematic Mapper data can be gathered.

Results and Interpretation

Variation solar zenith angle and time

Diurnal trends have been presented by showing BRF as a function of time. For conversion purposes solar zenith angle as a function of time is shown in Fig 2. The presented curves are for the first and last day of both testing campaigns. Other days of the field campaign lie in between those extremes.

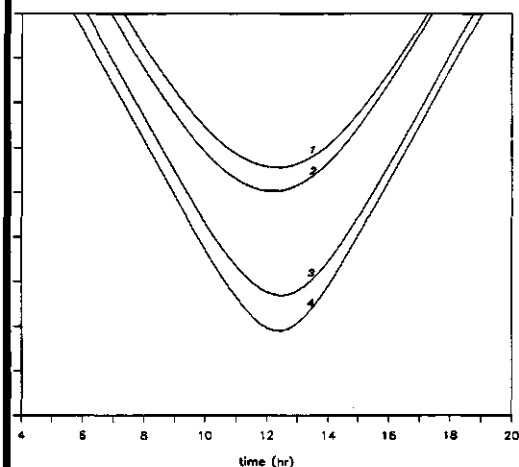


Fig 2. Solar zenith angle as a function of time in Southern Tunisia on different days. (1 = 2 December; 2 = 7 November; 3 = 8 April; 4 = 30 April)

Influence of corrections and errors

Diurnal trends of BRF may be highly affected by correction procedures. This is especially valid if panels have a non-Lambertian behaviour (Epema in preparation). In Fig 3 the variation of BRF during the day of one plot and wavelength is shown. One curve is with incomplete corrections and the other with complete corrections. The latter curve is corrected for the dark level of the system and on 100% reflectance of the reference panel by diffuse illumination. The last curve is also corrected for solar zenith angle dependent reflectance of the panel, both for direct and diffuse part of the irradiance. Several authors present diurnal trends without explaining and applying corrections, so that they may contain large errors. If panels deviate significantly from a Lambertian

surface. Only in exceptional cases the diffuse part is taken into account (Jackson *et al* 1988). This error is however limited for clean panels and for solar zenith angles up to 70 degrees. Also for the presented curves errors are not completely negligible (Epema in preparation.). Curves of the same day or of days with comparable atmospheric conditions always show similar trends.

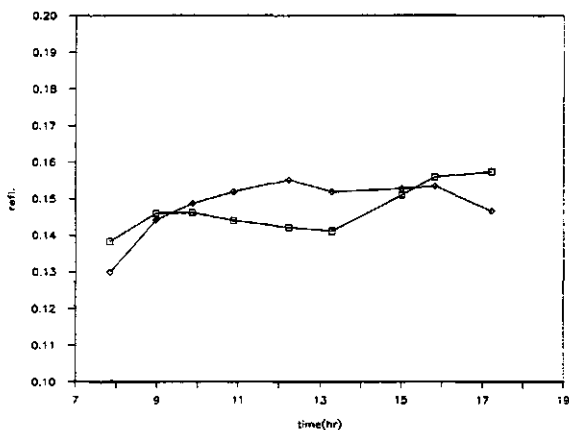


Fig 3. Variation of BRF in normal direction with incomplete (\square) and complete (\diamond) corrections.

Main type of diurnal curves

In Fig 4^a to 4^c BRF as a function of time is given for 4 different surfaces and for 3 typical MMR bands 1, 4 and 7. In band 1 the ratio diffuse/total irradiance on the surface is largest, in band 7 smallest. The BRF of the surfaces was determined on 4 different good days.

Curve 1 is representative for the bare parts of the footslopes of the area. Roughness of the surface can be described as medium according to the terminology of Walthall *et al* (1985): variations in height are in general between 1 and 2 centimeters. The BRF is highest around noon. This is most probably caused by shadow which is at its minimum with low solar zenith angles. The small asymmetry can be ascribed to the higher diffuse/total ratios in the afternoon of this day in comparison with the morning. Other parts of the footslopes, not shown here, demonstrate an even larger difference in BRF as function of zenith angle than this example. These parts had a higher coverage of stones and hence a higher roughness than the example.

Curve 2 is representative for large parts of the playa. It is an example from a smooth surface (difference in height less than 0.5 cm) with a very thin salt cover. In all bands an increase in BRF has been observed before noon, while in the afternoon in band 1 and 4 a stabilization occurs and in band 7 even an increase of reflectance. The asymmetry of

the diurnal BRF curve is due to a decrease in moisture content in the top layer. In this area four phenomena influence moisture content of the playa surface:

- (1) dew
- (2) ground water
- (3) sabakh
- (4) algae layers

(1) An evaluation of meteorological data, wet and dry bulb temperature and temperature near the surface, showed that dew was formed on several days. Visually dew has been observed on various surfaces just after sunrise. This dew disappeared however from the footslopes within an hour. Hence only in exceptional cases a small influence is possible on reflectance. In the playa zone however wet surfaces were observed for a longer period. Therefore other phenomena in addition to dew will be responsible for this fact.

(2) The ground water table in the playa (50 to 100 cm below the surface) is much higher than in the footslope area. During the night a redistribution of water is possible in the mulch layer due to the temperature gradient. This may cause a wet top layer (Philip and De Vries 1957).

(3) Moisture will remain for a longer period at the surface if Mg salts and other hygroscopic salts are present. Although NaCl dominates in the total profile also Mg chlorides are present. This phenomenon has been described by Buringh (1979) and is called sabakh.

(4) Apart from dew, sabakh and redistribution of water locally a fourth phenomenon occurs. In the lowest parts of the playa just below the surface black organic-rich layers formed by algae occur, alternating with relatively heavy clay layers exist (Meckelein 1977). The moisture content of these layers is relatively high due to the position and high clay content. These are the last sites to dry out.

As described above, in the playa area apart from the above mentioned effects of moisture content also a spatial and temporal variation in roughness and mineralogy of the top soil occurs. This is not the place for a detailed treatment, but as a general rule rougher parts show a larger amplitude in BRF than other parts. Roughness as caused by polygon forming is difficult to study in our set up since the polygons are larger than the ground observation area of the MMR. It is likely that shadow effects cause low reflectance at large solar zenith angles.

Curve 3 shows for all bands an increase in reflectance during the day. It is an example of a measurement from the second half of November period on the playa. Therefore at first sight this curve seems a variant of curve type 2. However superimposed upon the above described daily trends an overall drying out of the surface layers occurs. On the 15th of November a rain storm occurred and the surface is still drying, accompanied by an increase in salt deposition. In the winter period curves like these are likely to occur and last for relatively long times after a storm. On the footslopes it was observed that the influence of the storm only lasted for a day.

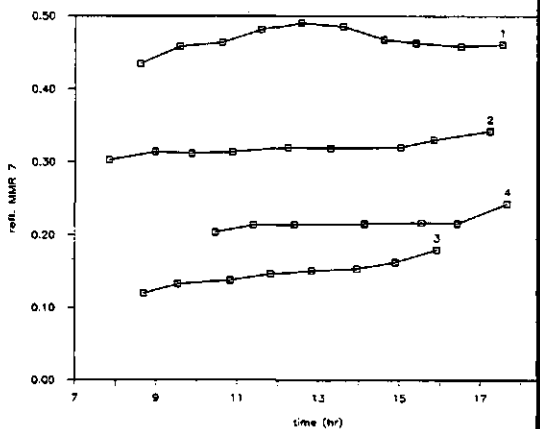
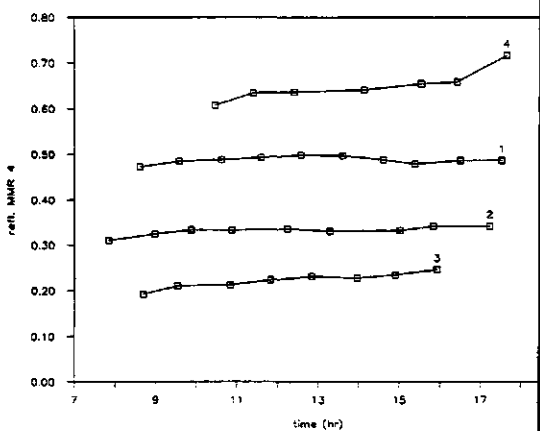
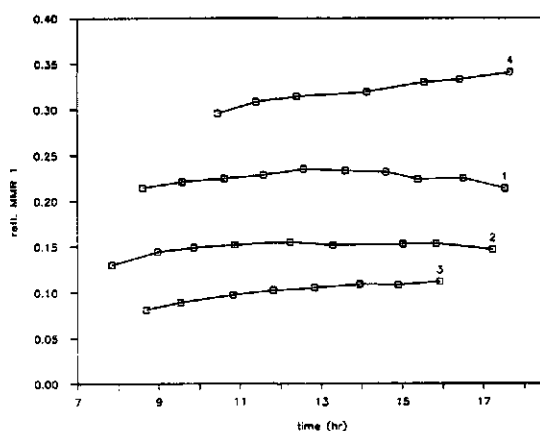


Fig. 4. Variation of BRF in normal direction 4 types of surf for band 1 (Fig 4a), band 4 (Fig 4b) and band 7 (Fig 4c).

curve 4 is an example of a BRF on a sloping surface. It near that variation on these surfaces can be explained large part if azimuthal and sloping area of surface and zenith angle and azimuth are taken into account. This example is given for the sake of completeness. Since in this area only a small part show slopes above 2%, no further study is concentrated to these type of surfaces.

Influence on Ratios

In addition to the intensity of different bands, band ratios are often an important means to discriminate surface phenomena. A well known example is the $(4-3)/(1+4+7)$ ratio used in vegetation studies with Thematic Mapper data. For TM studies of bare gypsiferous surfaces ratios have been proposed by Epema (1986) and Escadafal (1991). Mulder (1988) showed that a band divided by the sum of other bands is a good way to express the spectral characteristics. It is not the aim of this study to develop indicative ratios or discuss the soundness of the individual ratios. Only a selection of ratios is tested: $1/(1+4+7)$; $4/(1+4+7)$; $7/(1+4+7)$; $(4-1)/(4+1)$; $(7-1)/(7+1)$; $(7-4)/(7+4)$. The restriction to band 1, 4 and 7 is due to (1) the aim of testing different parts of the spectral range and (2) specific properties of the bands: band 1 is most sensitive to changes in atmosphere, band 7 is valuable for determination of gypsum and moisture and band 4 is expected to be most stable.

Three aspects are important in evaluating ratios:

- 1) difference between the ratios of different surface types.
 - 2) variation of ratio for stable surfaces as function of time, zenith angle due to roughness induced shadow, atmosphere or slope. It will be very valuable if an indicative ratio is to a large extent independent of these factors.
 - 3) change of ratio as function of change of the surface.
- Again the same plots are evaluated. In Fig 5a to 5c the three ratios as a function of time are shown. The other ratios showed similar trends.

1) It is remarkable that ratios for the examples of type 1 and 2 are comparable in magnitude. These plots show contrasting reflectance and surface characteristics. The plot of type 1 is located on the footslopes, while the plot of type 2 is situated in the playa area. This indicates that reflectance intensity remains an important parameter for identification of surfaces with reflectance in broad bands as used in M and MMR. On the other hand ratios with band 7 are not useful for the detection of gypsum (Epema 1986).

2) It is useful to note that the curves (type 1 and 4), which are not affected by change in surface characteristics, show a stable ratio, which change less than the individual bands. Ratios change less than 5%.

3) The change of a ratio as a function of change of surface characteristics can be seen in type 3 where a relative increase in reflectance with band 7 occurs due to a decrease in moisture content. The decrease as function of time of moisture

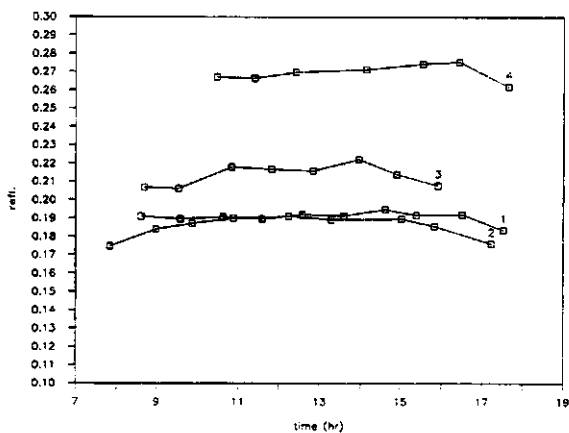


Fig. 5a

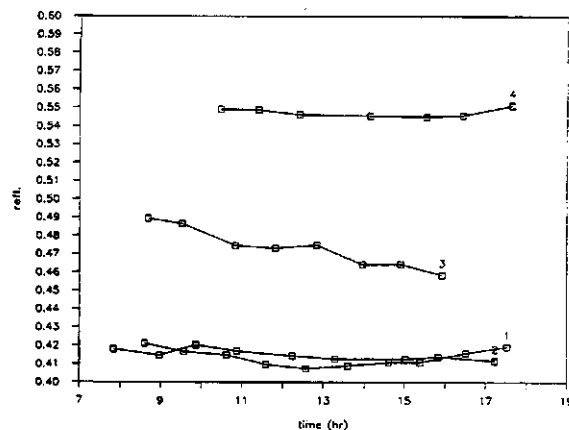


Fig. 5b

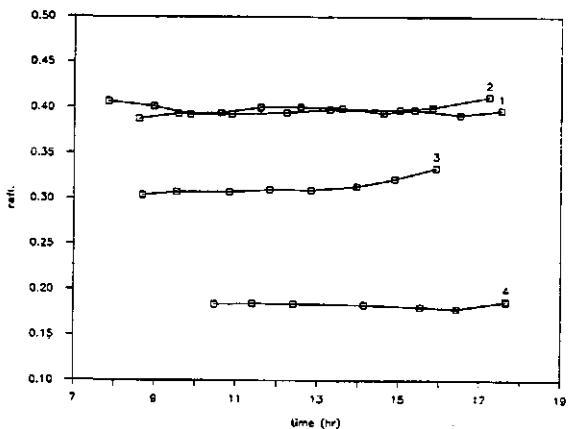


Fig. 5c

Fig. 5. Variation of BRF ratios in normal direction for 4 types of surfaces for band 1/(1+4+7) (Fig 5a), band 4/(1+4+7) (Fig 5b) and band 7/(1+4+7) (Fig 5c).

content in curve 2 cannot be detected straightforward from the ratios since not only band 7 but also the other bands are affected.

Especially for type 2 the low values in band 1 for zenith angles above 65 degrees (hence outside the range for satellite passes in this area) are remarkable. An explanation might be that the drying of the surface affects band 1 more quickly than band 7. Another possibility is that this is caused by measuring or processing errors. BRF values in band 1 with low zenith angles are most susceptible to errors due to a combination of low reflectance and small irradiances.

It can be concluded that band ratios are less susceptible to solar zenith angle than individual bands. However sometimes differences between surfaces are obscured when band ratios are used. In other cases band ratios can show differences effectively such as the presence of gypsum or they are useful for monitoring changing conditions of the surface such as the moisture content of type 3. Use of ratios will therefore depend on the specific aims of the study.

Implications for TM

Landsat Thematic Mapper passes over this part of Tunisia at 10:34. In Table 2 acquisition dates of TM and solar zenith angles, close to our measuring campaigns, are presented. It can be calculated that solar zenith angle at satellite overpass will range from 28 degrees in June to 63 degrees in December. This implies that for Landsat overpass the normal ground reflectance for a bare surface on the footslopes at identical surface conditions is up to 10% lower in December than in June, due to increased shadow related to surface roughness. Band ratios for all zenith angles are similar in the footslopes. Dew is of little influence on the TM images as it has usually disappeared before overpass. The effect of a rain storm on moisture conditions of the footslopes usually does not last longer than one day.

Table 2. Data and solar zenith angle of Landsat TM images (192/36) close to measuring campaigns.

Date	Solar zenith angle (degrees)
8 May 1987	30
18 Dec 1987	63
8 Apr 1988	37

In the smooth playa area, reflectance differences as function of solar zenith angle are small if daily variation in moisture is neglected. This can be concluded from studying the afternoon reflectance. However, for the morning hours, relevant for Landsat overpass, moist condition may cause a decrease of about 10% in reflectance. Band ratios are also affected by changes in moisture conditions of the playa surface. This superimposed effect

of moisture is different for the various measuring periods (December vs. June), as it depends on weather type time after sunrise.

It should be stressed that some problems have to be overcome before ground reflectance values can be compared directly with TM data:

- atmosphere influences both ground reflectance and relation ground reflectance and TM signal (Epema: preparation)
- plots cannot be compared directly with ground reflectance element of TM (30*30 m²). This is especially a problem on the footslopes where vegetation clumps and rills and gullies exist. Adequate description of a simple model to predict shadow are a minor prerequisite.
- the effect of drying out of the surface has to be taken into account for the playas.

Conclusions

The following conclusions may be drawn:

- (1) In this area variations during the day of BRF in normal direction for a constant atmosphere are in general less than 10%.
- (2) On the footslopes the effect of roughness dominates. Roughness causes a maximum BRF around noon due to low amount of shadow. Band ratios are almost constant for different solar zenith angles.
- (3) In the playa area moisture content is most important. It causes asymmetric daily BRF curves, with lowest reflectance in the morning. Band ratios show that band 7 is the most dependent of moisture content differences.
- (4) Band ratios are less susceptible to solar zenith angle than individual bands. However it should be stressed that differences between surfaces may be obscured when band ratios are used.

Acknowledgements

This research is part of a project funded by the Netherlands Remote Sensing Board (BCRS, AO 4.2). The authors wish to thank Prof. Dr. F.K. List and Dr. A. Richter (Berlin) for use of the Barnes MMR and Prof. Dr. Kroonenberg, Prof. Dr. M. Molenaar and Ir. N. Konijn for their critical comments to this paper.

References

- Coque, R. (1962) *La Tunisie Pre-Saharienne: Etude Geomorphologique*. Arman Colin, Paris.
- Coque, R. and Jauzein, A. (1967) The geomorphology and Quaternary geology of Tunisia. In: Martin, L. (ed.) *Guidebook of Geology and History of Tunisia*. Society of Libyan Petroleum Geologists, Handbook 3: 227-257
- Epema, G.F. (1986) Processing Thematic Mapper for mapping

- Tunisia. *ITC Journal* 1986-1:30-34
- Madafal, R. (1989) *Caractérisation de la surface des sols arides par observations de terrain et par teledetection*. Editions de l'ORSTOM, Collection Etudes et Theses, Paris
- son, R.D., Slater, P.N. and Moran, M.S. (1988) Accounting for diffuse irradiance on reference reflectance panels. *SPIE*, Vol 924 Recent advances in sensors, radiometry, and data processing for remote sensing: 241-248
- es, A.R. (1986) The use of Thematic Mapper imagery for geomorphological mapping in arid and semi-arid environments. Proceeding of Symposium on Remote Sensing for Resource Development and Environmental Management, Enschede, 273-281
- cklein, W. (1977) Zur Geomorphologie des chott Djerid. *Stuttgarter Geographische Studien*, 91: 247-301
- ington, A.C., Jones, A.R., Quarmby, N., and Townshend, J.R.G. (1986) Monitoring geomorphological processes in desert marginal environments using multitemporal satellite imagery. Proceeding of Symposium on Remote Sensing for Resource Development and Environmental Management, Enschede, 631-637
- ington, A.C., Jones, A.R., Quarmby, N., Townshend, J.R.G. (1987) Remote sensing of sediment transfer processes in playa basins. Frostick, L. & Reid, I. (eds), 1987. *Desert sediments: Ancient and Modern*, Geological Society Special Publication No. 35: pp. 369-381
- Milton, E.J. (1987) Principles of field spectroscopy. *Int. J. Remote Sensing*, vol. 8, no 12
- Mitchell, C.W. (1983) The soils of the Sahara with special reference to the Maghreb. *Maghreb Review* 8: 29-37
- Mulder, N.J. (1988) Digital image processing, computer-aided classification and mapping. A.W. Kuchler and I.S. Zonneveld (eds), *Vegetation mapping*, Kluwer, Dordrecht
- Ongaro, L. (1986) Studio integrato delle risorse naturali del Nefzaoua (Tunisia): carte delle unita di terre dell'area Kebilli-Douz. *Rivista di Agricoltura Subtropicale e Tropicale*, Trimestrale LXXX-n.2 Aprile-Giugno 1986: 165-310
- Philip, J.R. and De Vries, D.A. (1957) Moisture Movement in Porous Materials under Temperature Gradients. *Transactions of the American Geophysical Union*, Vol 38, No 2: 222-232
- Robinson, B.F., Bauer, M.E., DeWitt, D.P., Silva, L.F. and Vanderbilt, V.C. (1979) Multiband radiometer for field research. *Journal of the Society of Photo-Optical Instrumentation Engineers*, 196, 16-26

CHAPTER 4

ATMOSPHERIC CONDITION AND ITS INFLUENCE ON REFLECTANCE OF BARE SOIL SURFACES IN SOUTHERN TUNISIA.

International Journal of Remote sensing Vol.13, No.5: 853-868.

Atmospheric condition and its influence on reflectance of bare soil surfaces in southern Tunisia

G. F. EPEMA

Agricultural University of Wageningen, Department of Soil Science and Geology, P.O. Box 37, 6700 AA Wageningen, The Netherlands

(Received 28 February 1990; in final form 25 February 1991)

Abstract. The variation in the influence of the atmosphere on ground reflectance appears to be small for a stable atmosphere at different haze conditions in the study area. For a comparison of field with simulated and actual satellite data the model of Verhoef was used, which requires as input the ratio of measured diffuse to total irradiation. Relative difference in planetary reflectance of Landsat TM predicted with an atmospheric model for a specific ground reflectance and the observed range of stable atmospheric conditions turned out to be small. *In situ* measured ground reflectance and the ground reflectance derived from planetary actual TM reflectance are in good agreement.

1. Introduction

In southern Tunisia a research project has been carried out to study the potentials of Landsat Thematic Mapper (TM) data for identification of soil surfaces and their changes in time. Landsat TM observes the earth every 16 days at the same local time. Differences in signal are not only caused by changes of the surface. They are also due to differences in solar zenith angle and atmospheric condition. *In situ* ground reflectance measurements with a Barnes Modular Multiband Radiometer (MMR) in combination with observations of surface characteristics in different seasons were used as an aid in understanding the observed TM signal. The ground reflectance at a specific location is not constant either. It varies as a function of illumination conditions (i.e., atmospheric condition and solar zenith angle) and changes of the surface. This report will deal with the influence of the atmosphere. The influence of solar zenith angle to ground reflectance is reported elsewhere (Epema 1990c).

Three aspects will be discussed:

1. Variation of the atmospheric condition during the measurement campaigns. Based on the variation in the area representative plots were selected for description of surface characteristics. At these plots field reflectance measurements have been carried out. For all measurements the ratio diffuse to total irradiance was determined.
2. Influence of illumination condition on nadir *in situ* measured ground reflectance for two representative bare soils.
3. Relation between ground reflectance and TM signal for different atmospheric conditions.

With the aid of an atmospheric model of Verhoef (1985, 1990) estimates were made about possible signal differences observed by Landsat TM. The model of Verhoef

requires as input the ratio diffuse to total irradiance for two or more bands and the surfaces are assumed to be Lambertian. Different ground reflectance values and atmospheric conditions were examined. In addition an example is given for the relation between planetary reflectance, ground reflectance derived from the TM signal for a specific atmosphere and *in situ* measured ground reflectance. The planetary reflectance is the at satellite reflectance, which can be derived from the TM signal (see §3.1.).

2. Study areas

In figure 1 the location of the study areas is given. Extensive descriptions of the area on various aspects are given by Coque (1962), Coque and Jauzein (1967), Meckelein (1977), Mitchell (1983), Millington *et al.* (1987, 1989), Ongaro (1986), and Townshend *et al.* (1989). The area is situated at the margin of the Saharan Platform and the folded Atlas ranges. A large part of the zone of subsidence is occupied by playas (locally known as chotts). The Chott el Djerid is the largest of them and has

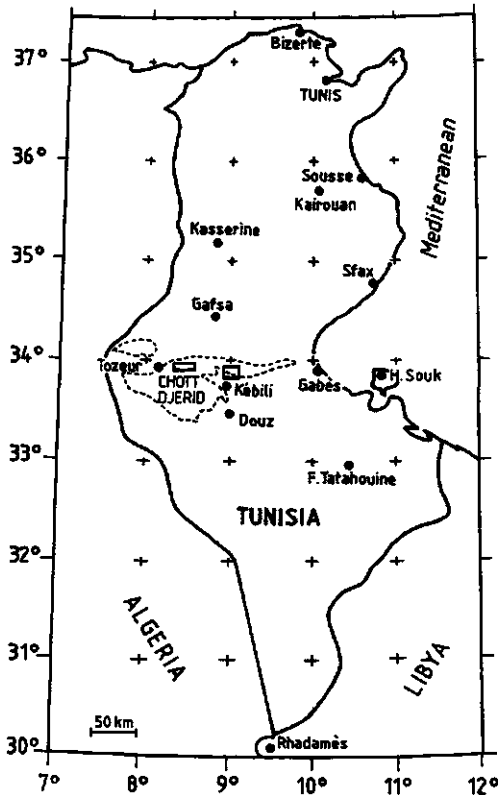


Figure 1. Location of the study areas in Southern Tunisia.

an elongated northeastern arm (Chott Fedjaj), which has been formed by faulting in the top of an anticlinal uplift (Coque 1962). The cuesta ridge of the Djebel Tebaga is located in the southern part of this uplift. It is surrounded by footslopes. Locally dunes of various sizes cover parts of playa margins and footslopes. The rainfall in this area is less than 100 mm per year. Apart from some oases, vegetation cover exceeds 5 per cent of the surface only in exceptional cases. The inner parts of the playa have no vegetation cover at all.

The study area comprises parts of the playas and the footslope areas:

1. **Playa:** The appearance of the playa varies in place and time. They are underlain essentially by gypsiferous sediments. Extensive descriptions are given by Mitchell (1983) and Millington *et al.* (1986). In the winter wet season, but also after individual storms, large parts exhibit standing water and upon drying relatively clean salt crusts develop. Part of the water (with sediments) is derived from the surrounding mountains and spatial distribution is a function of small relief differences and location of storms. Locally, black layers alternating with heavy layers exist just below the surface. As described by Coque (1962), Meckelein (1977) and Ongaro (1986), the black layers are formed by algae. Especially in spring and summer silty and sandy material is blown in. Spatial variation of surface type is important: thick crusts occur, especially in the centre; polygonal structures of various sizes and times also occur, and large areas almost devoid of salt are also present. Within this last area relatively rough parts exist also.
2. **Footslopes** in the area are mainly erosional features. They show variation in the presence of gypsum crusts, sand type and amount, incisions by gullies, and cover and size of stones. As opposed to the area around Chott el Guettar (described by Jones 1986) only small parts are real alluvial fans. Vegetation is mostly limited to hummocks. In spring vegetation is much greener and if it rains in this period even outside these hummocks some vegetation exist.

3. Theory

In this part three subjects will be treated:

1. The calculation of planetary TM reflectance.
2. The determination of the spectral extinction optical thickness. It is described how the spectral extinction optical thickness can be determined from measurements of the direct part of the reflected radiance at a certain solar zenith angle. The spectral extinction optical thickness is a good expression for the atmospheric condition, since it is in principle independent of solar zenith angle. It will be used for the description of the atmospheric condition during the measurement campaigns.
3. The most important aspects of the atmospheric model of Verhoef (1985) and the modification of the model (Verhoef 1990). This model is used to relate planetary reflectance with ground reflectance if the ratio diffuse to total irradiance is known. In areas like Tunisia, a 'darkest pixel' approach is difficult, since there are no objects with zero reflectance.

Subjects 2 and 3 are related. They will be used for different aims however, respectively for the description of the atmospheric condition during the field campaigns (§ 5.1 and 5.2), and to relate planetary reflectance with ground reflectance (§ 5.3).

3.1. Planetary reflectance

Knowing the bias and gain factors of the detectors in different wavelength bands the digital numbers from the computer compatible tapes can be converted to radiances. Values of bias and gain are given on the tapes. However for the TM tapes used here, which have been processed at ESRIN, these values are erroneously based on preflight data. Therefore values have to be used, which have been corrected for gain loss of the detectors (Epema 1990 a).

The planetary TM reflectance (ρ_p) can be calculated from the reflected radiance as received by the sensor according to:

$$\rho_p = \frac{(\pi L_\lambda d^2)}{(E_{0(\lambda)} \cos \theta_s)} \quad (1)$$

where

L_λ = spectral radiance at sensor aperture in $\text{mW cm}^{-2} \text{sr}^{-1} \mu\text{m}^{-1}$,

d = Earth-Sun distance in astronomical units,

$E_{0(\lambda)}$ = mean solar exo-atmospheric irradiances in $\text{mW cm}^{-2} \mu\text{m}^{-1}$,

θ_s = solar zenith angle in degrees.

Values of Neckel and Labs (1981) and Iqbal (1983) were adopted for the exo-atmospheric irradiance ($E_{0(\lambda)}$). Since these values have been defined for the mean Earth-surface distance they have to be adjusted to the actual distance (d). The d for a specific day can be approximated by the relation of Gurney and Hall (1983):

$$d = 1 + 0.0167 \sin \left[\frac{2\pi(D - 93.5)}{365} \right] \quad (2)$$

where D is day number of the year.

3.2. Determination of spectral extinction optical thickness

The spectral extinction optical thickness $\tau'_{\text{ext}}(\lambda)$ can be gathered from the following equation (Jackson and Slater 1986):

$$E_{\text{Sun}(\lambda)} = E_{0(\lambda)} [\exp - \tau'_{\text{ext}}(\lambda) \sec \theta_s] \quad (3)$$

where $E_{0(\lambda)}$ is the exo-atmospheric irradiance, $E_{\text{Sun}(\lambda)}$ the measured direct spectral irradiance on a surface at Earth, perpendicular to the direct solar incidence flux.

For a non-calibrated instrument this equation becomes:

$$V c'_{(\lambda)} = \frac{E_{0(\lambda)} [\exp - \tau'_{\text{ext}}(\lambda) \sec \theta_s]}{\pi} \quad (4)$$

where V is the output voltage of an instrument looking directly at the sun and $c'_{(\lambda)}$ is the calibration factor in $\text{W m}^{-2} \text{sr}^{-1} \text{V}^{-1}$. In (4) $\tau'_{\text{ext}}(\lambda)$ and $c'_{(\lambda)}$ are unknown. This equation can be solved by measuring the output voltage (V) for different solar zenith angles (θ_s) under stable atmospheric conditions. Equation (4) can also be written as:

$$\ln V = -\tau'_{\text{ext}}(\lambda) \sec \theta_s + \ln \left[\frac{E_{0(\lambda)}}{c'_{(\lambda)} \pi} \right] \quad (5)$$

Plotting $\ln(V)$ against $\sec \theta_s$ for the wavelength bands for a day with constant atmosphere gives $-\tau'_{\text{ext}}(\lambda)$ as slope and $\ln(E_{0(\lambda)}/(c'_{(\lambda)}\pi))$ as intercept (Jackson and Slater 1986). These figures are called Langley-plots. The calibration factor, $c'_{(\lambda)}$, can be calculated from the intercept since $E_{0(\lambda)}$ is known.

Direct measurement of incoming irradiation with a Barnes MMR with field of view aperture angles of 1° respectively 15° is difficult. Therefore in our set-up an alternative approach is used where the flux under direct irradiation (V_{dir}) is measured from a horizontal panel with known reflectance properties as a function of solar zenith angle. V_{dir} can be calculated by the shading method as described by Che *et al.* (1985). The V in (4) and (5) has to be replaced by:

$$V = \frac{V_{dir}}{\cos \theta_s R_{(\theta)}} \quad (6)$$

where $R_{(\theta)}$ is the reflectance of the panel under solar zenith angle θ .

Combining the different equations the calibration factor $c_{(\lambda)}$ of the Barnes in $\text{Wm}^{-2} \text{sr}^{-1} \text{V}^{-1}$ was calculated with the equation given by Jackson and Slater (1986) according to

$$c_{(\lambda)} = \frac{E_{0(\lambda)}}{d^2 e^A \pi} \quad (7)$$

where A is the intercept of the Langley plot ($\ln(E_{0(\lambda)})/(c_{(\lambda)}\pi)$).

The $c_{(\lambda)}$ -value based on days with stable atmospheric conditions may be used also for non-ideal conditions to estimate $\tau'_{ext}(\lambda)$ from the V_{dir} . In that case $c_{(\lambda)}$ is known so that the following equation based on (5) and (6) can be solved directly:

$$\tau'_{ext}(\lambda) = -\cos \theta_s \ln \left[\frac{V_{dir} c_{(\lambda)} \pi}{E_{0(\lambda)} \cos \theta_s R_{(\theta)}} \right] \quad (8)$$

The spectral extinction optical thickness ($\tau'_{ext}(\lambda)$) will be used as a characterization of the type of atmosphere, independent of the solar zenith angle.

3.3. Atmospheric model of Verhoef

The atmospheric model used here is a part of a scene radiation model described by Verhoef (1985). For the description of atmosphere the Verhoef model uses (1) Elterman's data (1970) on atmospheric optical depth, which gives the relation between aerosol optical thickness, wavelength and visibility and (2) Deirmendjian's (1969) phase functions for atmospheric haze (Mie scattering). Verhoef (1990) modified the model so that the ratio diffuse to total irradiance in different bands can be used as input. In our set-up we used these ratios for 4 or 6 TM compatible bands of the Barnes MMR (see experimental set-up) to estimate α (wavelength exponent) and β (Ångstrom's turbidity coefficient) of the Ångstrom's turbidity equation with an inversion procedure. The haze type M atmosphere of Deirmendjian (1969) was used. Some default values are used in the model: (1) water vapour content of atmosphere is 0 in all bands; this presents no problems for the scattering, since it is included in Ångstrom's concept of aerosols, but it is a problem for the parts of the spectrum where water absorption occurs; (2) single scattering albedo, and (3) ratio forward/backward scattering calculated with Deirmendjian's phase functions are independent from solar zenith angle.

Assuming the background albedo equal to the target albedo, Verhoef (1990) developed a simplified equation relating planetary reflectance ($\rho_{p(\lambda)}$) to ground reflectance ($\rho_{0(\lambda)}$):

$$\rho_{p(\lambda)} = R_{so(\lambda)} + \frac{T_{1(\lambda)} T_{2(\lambda)}}{(1 - R_{ad(\lambda)} \rho_{0(\lambda)})} \rho_{0(\lambda)} \quad (9)$$

where

$R_{so(\lambda)}$ = atmospheric reflectance,
 $T_{1(\lambda)}, T_{2(\lambda)}$ = two way transmittance,
 $R_{dd(\lambda)}$ = spherical albedo of the atmosphere.

In the Verhoef model the atmospheric factors in (9) are derived from the measured ratio diffuse to total irradiance in the different bands.

4. Experimental methods and conditions

Field measurements were made with a Barnes Modular Multiband Radiometer (MMR) (Robinson *et al.* 1979) in two field periods: November 1987 and April 1988. Results will be compared with simulated and actual Landsat Thematic Mapper data. Landsat TM tapes of two good days were used: 18 December 1987 and 8 April 1988. For the first campaign no reliable data during the campaign were available due to the weather conditions at satellite overpass.

The aim of the field measurements was to determine spectral reflectance of objects and atmospheric conditions during the measurements of reflectance. Reflectance data were gathered according to suggestions given by Milton (1987) and the data were processed according to Epema (1991).

The MMR was mounted on a tripod and the look direction was vertical downward. The instrument was equipped with a 15° field of view aperture. The spectral characteristics in comparison with the Landsat Thematic Mapper (TM) deployed on Landsat-4 and -5 are given in table 1. The selection of plots was based on the variation in the study areas. Reflected signal was measured over the different plots approximately every hour. The readings were in volts, but, if required, they can be converted to radiance by multiplying with the calibration factors. For about 15 locations 5 to 15 different plots were examined in the field campaigns. In this report the reflectance in nadir direction of two representative locations are presented as a function of atmosphere in § 5.2. Panel data were achieved at the start and finish of each measurement sequence. The reflectance for the different bands was determined by dividing the signal reflected by a surface in nadir direction to the interpolated and corrected signal of the panel according to

$$\rho'_{o(\lambda)} = \frac{V_{o(\lambda), t_1}}{V_{p(\lambda), t_0}^* + (t_1 - t_0)/(t_2 - t_0)(V_{p(\lambda), t_2}^* - V_{p(\lambda), t_0}^*)} \quad (10)$$

Table 1. Bandpasses of Barnes MMR field radiometer (50 per cent power bandpass limits) and Landsat Thematic Mapper (full-width at half-maximum method).

Barnes MMR		Landsat TM	
Number of band	(λ)	Number of band	(λ)
1	0.458-0.525	1	0.4524-0.5178
2	0.519-0.601	2	0.5280-0.6093
3	0.637-0.687	3	0.6264-0.6923
4	0.739-0.898	4	0.7764-0.9045
5	1.174-1.334		
6	1.574-1.803	5	1.5675-1.7842
7	2.083-2.371	7	2.0972-2.3490

Atmospheric effects on bare soil reflectance data in Tunisia

where ρ'_o = reflectance of an object, measured *in situ*, $V_{\theta(\lambda), t_1}$ = reflected signal on time t_1 , above object, $V_{p(\lambda), t_0}^*$ = corrected reflected signal on time t_0 , above panel, $V_{p(\lambda), t_2}^*$ = corrected reflected signal on time t_2 , above panel; $t_0 < t_1 < t_2$.

The panel readings $V_{p(\lambda)}^*$ are corrected for the panel reflectance $R_{(\theta, (\lambda))}$ under the solar zenith angle θ .

As an alternative, especially for non-stable conditions, solarimeter readings of incoming irradiance were used as an aid in the determination of reflectance. Relations between the corrected signal of the panel in the different bands and solarimeter readings were established on days with stable atmospheric conditions. These relations were used on non-stable days to derive panel reflectance from solarimeter readings.

The panel data were also used to determine the variation of the atmospheric condition between the days and within the days. Both total and diffuse irradiation have been measured. The diffuse irradiation was determined by shadowing the reference panel with a plate. After corrections for the part of diffuse irradiation blocked by the plate under specific solar zenith angles (Epema (1991), calculation of the voltage of the direct irradiation has been performed. Both the ratio diffuse to total irradiation and the amount of direct and diffuse irradiation for a specific solar zenith angle (θ_s) are useful to express the atmospheric condition. A more direct way to express this is the spectral extinction optical thickness $\tau'_{ext}(\lambda)$ which is a constant value for a specific atmosphere. A description of this calculation is given in the foregoing theory and the results will be presented in § 5.1.

5. Results

5.1. Atmospheric condition

From the measuring campaign of April 1988 six (half) days gave Langley plots, which were linear. This is a necessary, but not sufficient condition for stable atmospheric conditions. Reagan *et al.* (1984) showed that also a linear relation may occur, when the spectral extinction optical thickness varies temporally. It was assumed that these days were clear and stable enough to use for the determination of the calibration factor $c_{(\lambda)}$. Values of $c_{(\lambda)}$ were calculated according to (7).

In table 2 the mean $c_{(\lambda)}$ values with the standard deviations are given. The standard deviations are comparable with the results of Jackson and Slater (1986). The $c_{(\lambda)}$ values differ. This can be easily explained by the fact that the internal gain

Table 2. Mean and standard deviations of c and τ'_{ext} of six days with constant atmospheric conditions in the April 1988 period.

	c (in $\text{W m}^{-2} \text{sr}^{-1} \text{V}^{-1}$)		τ'_{ext}	
	mean	s.d.	mean	s.d.
MMR1	7.83	0.46	0.31	0.07
MMR2	11.70	0.23	0.27	0.05
MMR3	6.28	0.41	0.21	0.07
MMR4	12.95	0.35	0.17	0.05
MMR5	6.72	0.44	0.15	0.06
MMR6	4.68	0.26	0.10	0.06
MMR7	1.83	0.10	0.12	0.06

was changed from the factory setting (Richter, personal communication). From the Langley plots the spectral extinction optical depth ($t'_{\text{ext}}(\lambda)$) could be computed for these six days. To get an idea of the variation in the days used for the $c_{(\lambda)}$ determination mean and standard deviation of $t'_{\text{ext}}(\lambda)$ are given in table 2 too. It is important to know also for non-ideal days the $t'_{\text{ext}}(\lambda)$ at the different moments of the day. From (8) it can be concluded that this is possible if V_{dir} is measured. In figure 2 $t'_{\text{ext}}(\lambda)$ values for relatively good to excellent days are presented respectively for band 7 against band 4 and band 1.

5.2. Influence of atmosphere on ground reflectance

Stable representative surfaces have to be investigated under different atmospheric conditions in order to show the effect of atmosphere as representative examples of natural bare soil surfaces plots on the footslopes and on the playas are selected. Four different problems arise:

1. *Characteristics of plots may vary in time.*

This is very obvious for plots in the playa (Epema 1990 b). Moisture changes on diurnal and seasonal time scales. But also variation on footslopes may occur due to for instance sealing of the surface. The changes of the surface can be observed partly by direct observations in the field.

2. *Reflectance may change as a function of the solar zenith angle.*

For stable atmospheric conditions, the field reflectance for surfaces without change on the footslopes was observed to be at its maximum 10 per cent more for a solar zenith angle of 20° than for an angle of 65° (Epema 1990 c). This effect was more prominent with increasing roughness of the surface and could be ascribed to shadow. Therefore the figures will present reflectance as a function of solar zenith angle.

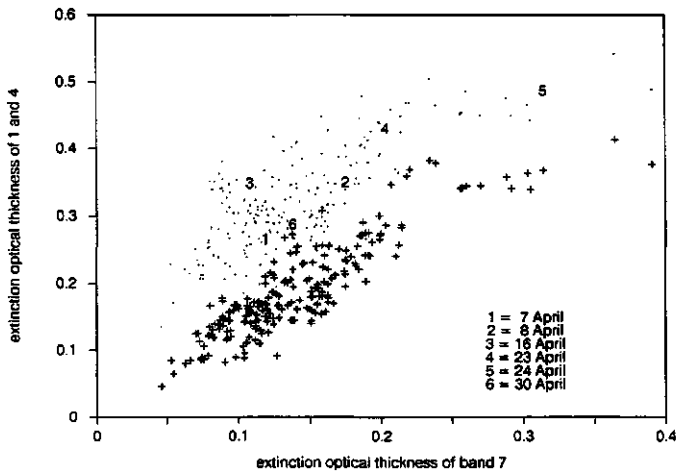


Figure 2. Relation of extinction optical thickness of MMR band 1 (●) and 4 (+) with MMR band 7 for the April 1988 campaign. (1, 2, ... mean values of relevant days of April 1988 for relation band 1 and band 7).

Atmospheric effects on bare soil reflectance data in Tunisia

3. *Problems in determining the correct incoming irradiance.*

In the experimental set-up we used there are two different ways to determine the reflectance:

- (a) the reflectance may be determined by dividing reflected radiance of the surface by the reflected radiance of a calibrated reference panel.
- (b) having the relation between reflected radiance of the panel and solarimeter readings also the solarimeter readings may be used to estimate the reflectance of an ideal reference panel. These relations are significant for all days with a stable atmospheric condition (table 3). The relation of individual bands with solarimeters differs slightly between the days. Still the general relations of table 3 were used as an estimate of the reflected radiance signal of individual bands of days with non-stable conditions. On these days it is impossible to measure under the same conditions the reflected radiance of a panel and the surface.

Both methods to determine the reflectance have a disadvantage for comparing reflectance under different atmospheric conditions. The former will fail if atmospheric conditions change. The latter may fail, since relations of incoming irradiance of individual bands with solarimeter readings vary as a function of atmosphere. Therefore the interpretation of results has to be performed with care.

4. *Errors in determination of reflectance in the field and processing of the data.* These have been discussed extensively in Epema (1991).

In figures 3 and 4 reflectance for different days are presented for three plots on the footslopes. Reflectance values in figure 3 are calculated using the panel data and in figure 4 they are based on simultaneous solarimeter readings. As an example in both figures results of band 4 are presented. Others bands show similar trends.

The scattering of points in figure 3 can be ascribed to the following factors:

1. Incorrect determinations of incoming irradiance due to changing conditions (most November data).
2. High moisture content of top layer (16 November).
3. (Small) variation in surface characteristics between the plots in the unit (7 April).
4. Inaccuracies in determination of reflectance. The higher reflectance around noon is due to the low solar zenith angle.

Table 3. Relation between reflected radiance (in volts) measured with the Barnes MMR in nadir direction and irradiance with a solarimeter (in volts). (ranges: individual bands 0 to 4 V and solarimeter 0 to 35 V).

	MMR1	MMR2	MMR3	MMR4	MMR5	MMR7
Constant	-0.171	-0.089	-0.011	-0.038	-0.075	-0.018
Std. error of Y est	0.089	0.112	0.071	0.077	0.106	0.132
X coeff	0.121	0.099	0.095	0.099	0.089	0.097
No. of observations	176	176	176	176	176	176
R squared	0.990	0.977	0.990	0.989	0.974	0.967

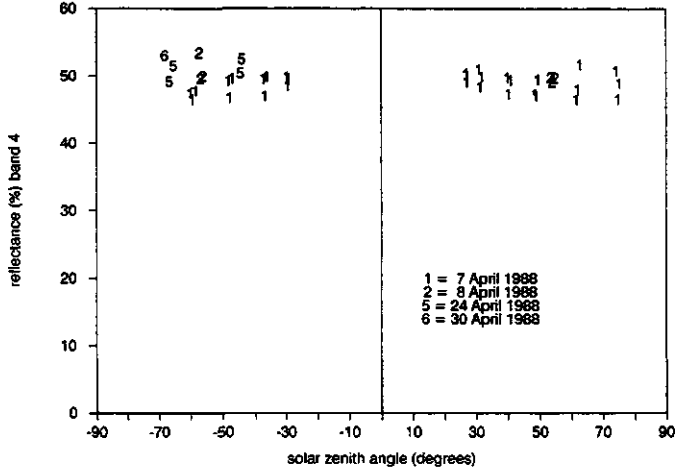


Figure 3. Reflectance (in percentage) in band 4 based on panel data as a function of solar zenith angle (angles before noon have a negative sign) for plots in the footslope area.

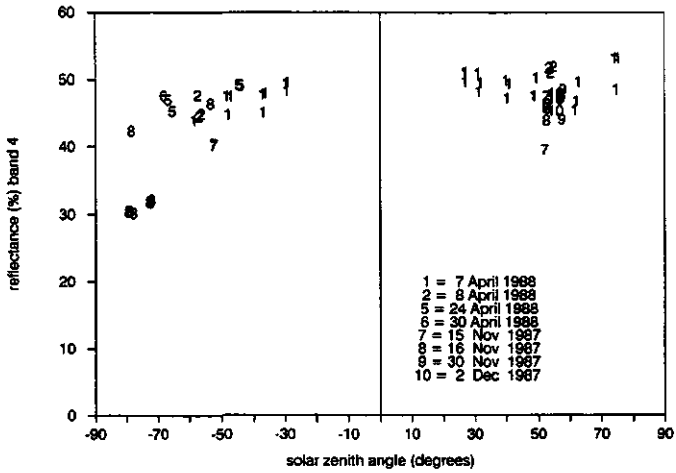


Figure 4. Reflectance (in percentage) in band 4 based on solarimeter readings as a function of solar zenith angle (angles before noon have a negative sign) for plots in the footslope area.

Atmospheric effects on bare soil reflectance data in Tunisia

In figure 4 the scattering is due mainly to variation in surface characteristics between the plots (7 April) and to the fact that the relation of individual bands with the solarimeter readings is dependent from the type of atmosphere. Hence most variation in figures 3 and 4 is not due to the atmosphere itself.

In figure 5 reflectance for two different days in April (16 and 23) for an example of the playa area is shown. Difference in optical thickness for those days was large, but both days had a rather stable atmospheric condition. The last day was more hazy, the former showed some thin clouds. Reflectance calculated from the solarimeter readings showed the same pattern and almost the same difference in reflectance. Therefore only the results based on panel data are presented. During all day surface reflectance of all bands were higher on 16 April than on 23 April. This difference can be explained partly by changes of the surface itself. On 23 April less salt was present at the surface due to the wind and the moisture content was also somewhat higher. Both effects caused a decrease in reflectance in all bands, while moisture content gave an extra decrease in band 7. This extra decrease becomes clear when ratios with band 7 to other bands are calculated and compared for these two days. However, the lower reflectance of 23 April cannot be explained completely by changes of the surface. Other factors, like measuring errors and atmosphere, play a role too.

Based on the observations on these two different bare surfaces, it is obvious that the variation in observed field reflectance in this area and during these seasons by no more than 5 per cent is caused by the atmosphere itself. Other factors are more important in causing differences in reflectance.

5.3. Influence of atmosphere on relation ground reflectance and planetary TM reflectance

The atmospheric model of Verhoef (1985, 1990) provides the possibility to relate ground and planetary reflectance if the ratio diffuse to total irradiance at a certain

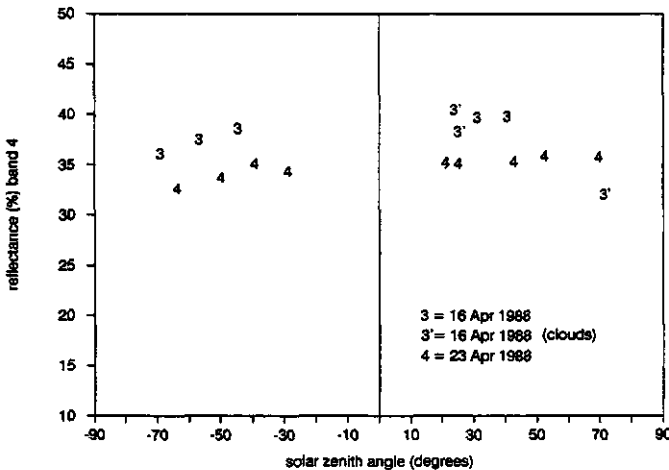


Figure 5. Reflectance (in percentage) in band 4 based on panel data as a function of solar zenith angle (angles before noon have a negative sign) for a plot in the playa area.

Table 4. Predicted planetary TM reflectance (in percentage) for satellite overpasses of 8 April 1988 and 18 December 1987 in southern Tunisia from extreme bare soil ground reflectance data (in percentage) for three different atmospheric conditions.

MMR reflectance	Predicted planetary TM reflectance						
	(Min)	37°			62°		
		(1)	(2)	(3)	(1)	(2)	(3)
MMR1, TM1	12.5	16.9	17.5	17.9	17.5	18.2	18.6
MMR1, TM2	20.0	20.7	21.1	21.3	20.1	20.7	20.9
MMR3, TM3	25.0	25.4	25.6	25.8	25.0	25.4	25.5
MMR4, TM4	30.0	30.3	30.5	30.6	30.2	30.4	30.5
MMR6, TM5	32.5	32.5	32.6	32.6	32.5	32.6	32.6
MMR7, TM7	28.0	28.0	28.1	28.1	28.0	28.1	28.1
	(Max)						
MMR1, TM1	25.0	27.6	28.0	28.3	27.2	27.9	28.2
MMR2, TM2	37.5	36.1	36.3	36.4	34.6	34.9	35.1
MMR3, TM3	47.5	46.9	47.1	47.8	45.9	46.0	46.0
MMR4, TM4	55.0	55.2	55.2	55.2	54.8	54.8	54.7
MMR6, TM5	67.5	67.5	67.5	67.5	67.5	67.7	67.3
MMR7, TM7	60.0	60.0	60.0	60.0	60.0	59.9	59.9

- (1)= atmosphere of 21 April 1988 (clear).
 (2)= atmosphere of 8 April 1988 (mod. clear).
 (3)= atmosphere of 23 April 1988 (hazy).

zenith angle is known for a given day. For the Landsat overpass of 8 April 1988 (solar zenith angle 37°) and 12 December 1987 (solar zenith angle 62°) the planetary TM reflectance is predicted from ground reflectance for three different atmospheric conditions (table 4). These conditions occurred respectively on (a) the most clear day in the April period, (b) the most hazy day without clouds and still suitable for TM imagery and (c) the day of Landsat overpass (8 April). For every band the relation between ground reflectance and planetary reflectance has been calculated for plots with a low and high ground reflectance respectively in the April period. It should be noted that in the winter period, or shortly after rainstorms, still lower reflectance values are possible. Also more hazy atmospheres may be present, especially in May and June, than those measured in April 1989. Since those conditions are not present on our satellite tapes they are not dealt with.

From table 4 it can be seen that atmospheric correction is most valuable at shorter wavelengths and in that case especially for low ground reflectance. Moreover relative difference in planetary TM reflectance for a specific ground reflectance for these atmospheres even for band 1 is always less than 10 per cent.

It is important to know how good the similarity is between *in situ* measured ground reflectance and ground reflectance predicted from planetary reflectance for a specific atmosphere. It gives insight in the reliability of the atmospheric model and the measurement and processing of the ground reflectance data.

Two important assumptions are inherent in the atmospheric model of Verhoef (1985): the surface is a Lambertian and the surroundings of the pixel have the same reflectance as the investigated spot. Both from the diurnal reflectance in nadir

Atmospheric effects on bare soil reflectance data in Tunisia

Table 5. Planetary reflectance, ground reflectance derived from TM (with atmospheric correction) and *in situ* measured ground reflectance of a homogeneous bare soil surface in the playa area (8 April 1988).

Planetary reflectance in %	Ground reflectance in % (from TM)	Ground reflectance in % (measured)
20.0	15.5	15.4
24.0	23.5	23.5
32.0	31.8	30.1
35.7	35.3	34.3
37.1	37.1	39.2
31.9	31.9	32.2

direction and from the directional reflectance measurements it is clear that the bare surfaces on the footslopes are not Lambertian. The footslopes as a whole will be even less Lambertian since within the pixel hummocks of vegetation are present. The two assumptions are more valid in large parts of the playa areas since the smooth surfaces behave almost as Lambertian reflectance and the difference in reflectance between the investigated pixel and the surroundings is often small. Therefore for a small area in the playa a comparison has been made between *in situ* measured ground reflectance and ground reflectance derived from atmospheric corrected planetary TM reflectance on 8 April 1988. The ratio diffuse to total irradiance has been determined close to satellite overpass and ground reflectance at time of overpass. The agreement between the measured ground reflectance and that based on TM using an atmospheric model is remarkable (table 5). The difference is less than 10 per cent, while many inaccuracies may exist in the procedures. The most important are:

1. Solar exo-atmospheric irradiances given by different authors vary up to 6 and 8 per cent for TM bands 5 and 7. For TM bands 1 to 4 more agreement exists.
2. Inaccuracies in the determination of the ratio diffuse to total irradiance and panel reflectance data.
3. Limitations and assumptions of atmospheric model.
4. Deviations from Lambertian reflectance.

6. Conclusions and discussion

The influence of atmosphere on reflectance in the field in out set-up was difficult to determine. A major problem was that inaccuracies in the determination of incoming irradiance at time of measurement of the plots occurred, especially for non-stable conditions. In this case the irradiance has to be estimated from solarimeter values which cause errors, since relations of incoming irradiance of individual bands with solarimeter readings vary as function of atmosphere. Other problems are changes in characteristics of natural surfaces and measuring errors. It can be concluded that for stable days differences in reflectance due to atmosphere will be less than 5 per cent in this area and during these measuring periods.

The model of Verhoef (1985, 1990) showed that, as can be expected, an atmospheric correction is most valuable at shorter wavelengths and in that case especially for low ground reflectance. However relative difference in planetary TM

reflectance for a specific ground reflectance for the observed range of stable atmospheric conditions fortunately turned out to be small. Even for band 1 differences are always less than 10 per cent.

A very good agreement has been found for an almost Lambertian surface between *in situ* measured ground reflectance data and ground reflectance values predicted from planetary reflectance applying the atmospheric condition close to the time of overpass.

The result of this study to the effect of atmosphere has some important implications for the strategy of research for the total research project. In this project the possibilities for Landsat Thematic Mapper (TM) for identification of soil surfaces and their changes in time for an area in southern Tunisia are investigated.

The most important implications for the strategy of this research project area:

1. Stable atmospheric conditions are a prerequisite for good ground reflectance measurements. Since in southern Tunisia more than 50 per cent of the days are stable enough to make reliable measurements this is no major problem. If atmospheric conditions are stable, differences in haze are of minor importance in the determination of the ground reflectance.
2. Relative differences in planetary reflectance are limited for different types of atmosphere. Therefore it is possible, if no good TM data exist from the measuring period, to use tapes close to these campaigns. If TM band 1 can be avoided by interpretation of multi-temporal data of this area, and no tapes of extreme atmospheric conditions are used, no large errors will occur by correcting those data for a mean type of atmosphere or for not correcting it at all.
3. A good fit exists between *in situ* measured ground reflectance and ground reflectance derived from atmospheric corrected TM planetary reflectance of almost ideal surfaces. Therefore it is in principle possible to understand the effect on reflectance of more complex surfaces.

It has to be stressed that the effect of atmosphere is not the only factor important in the strategy for analysing TM data. There exist other sources of error and variation in determination of ground reflectance. Sources of error are for instance incorrect positioning and dust on instruments. Also systematic errors may occur if the effect of dew is neglected or the effect of roughness on reflectance as a function of zenith angle is not taken into account (Epema 1990c).

Acknowledgments

This research is part of a project funded by the Netherlands Remote Sensing Board (BCRS, AO-4.2). The author wishes to thank Professor Dr F. K. List and Dr A. Richter (FU Berlin) for use of the Barnes MMR, W. Verhoef (NLR) for data on atmospheric models and comments to this paper, Professor Dr M. Molenaar (AUW) and Ir H. J. Buiten (AUW) for their critical comments to this paper.

References

- CHE, N., JACKSON, A. L., PHILIPS, A. L., and SLATER, P. N., 1985, The use of field radiometers in reflectance factor and atmospheric measurements. *Journal of the Society of Photo-Optical Instrumentation Engineers*, **499**, 2433.
- COQUE, R., 1962, *La Tunisie Pre-Saharienne: Etude Géomorphologique* (Paris: Armand Colin).

Atmospheric effects on bare soil reflectance data in Tunisia

- COQUE, R., and JAUZEIN, A., 1967, The geomorphology and Quaternary geology of Tunisia. In *Guidebook to the Geology and History of Tunisia*, edited by L. Martin (Society of Libyan Petroleum Geologists, Handbook 3), pp. 227-258.
- DEIRMENDJIAN, D., 1969, *Electromagnetic scattering on spherical polydispersions* (New York, American Elsevier Publication Company, Inc.).
- ELTERMAN, L., 1970, Vertical attenuation model with eight surface meteorological ranges 2 to 13 kilometres. AFRCL-70-0200, Air Force Cambridge Research Laboratories, Redford, Massachusetts.
- EPEMA, G. F., 1990 a, Determination of planetary reflectance for Landsat 5 Thematic Mapper tapes processed by Earthnet (ITALY). *ESA Journal*, 14, 101-108.
- EPEMA, G. F., 1990 b, Effect of moisture content on spectral reflectance in a playa area in southern Tunisia. *Proceedings of the International Symposium on Remote Sensing and Water Resources, Enschede, 20-24 August 1990* (Lingen: R. van Acken GmbH), pp. 301-308.
- EPEMA, G. F., 1990 c, Diurnal trends in reflectance of bare soil surfaces in southern Tunisia. *Geocarto International*, 5, 33-39.
- EPEMA, G. F., 1991, Studies of errors in field measurements of the bidirectional reflectance factor. *Remote Sensing of Environment* 35, 37-49.
- GURNEY, R. J., and HALL, D. K., 1983, Satellite-derived surface energy balance estimates in the Alaskan Sub-Arctic. *Journal Climate and Applied Meteorology*, 22, 115-125.
- IQBAL, I., 1983, *An introduction to solar radiation* (Toronto, New York, London, Paris, San Diego, São Paulo, Sydney, Tokyo: Academic Press).
- JACKSON, R. D., and SLATER, P. N., 1986, Absolute calibration of field reflectance radiometers. *Photogrammetric Engineering and Remote Sensing*, 52, 189-196.
- JONES, A. R., 1986, The use of Thematic Mapper imagery for geomorphological mapping in arid and semi-arid environments, *Proceeding of the Symposium on Remote Sensing for Resource Development and Environmental Management, 1986* (Rotterdam, Boston: A. A. Balkema), pp. 273-281.
- MECKELEIN, W., 1977, Zur Geomorphologie des chott Djerid. *Stuttgarter geographische Studien*, 91, 247-301.
- MILLINGTON, A. C., JONES, A. R., QUARMBY, N., and TOWNSHEND, J. R. G., 1986, Monitoring geomorphological processes in desert marginal environments using multitemporal satellite imagery. *Proceedings of the Symposium on Remote Sensing for Resource Development and Environmental Management, 1986* (Rotterdam, Boston: A. A. Balkema), pp. 631-637.
- MILLINGTON, A. C., JONES, A. R., QUARMBY, N., and TOWNSHEND, J. R. G., 1987, Remote sensing of sediment transfer processes in playa basins. In *Desert sediments: Ancient and Modern*, edited by L. Frostick and I. Reid. Geological Society Special Publication No. 35: pp. 369-381.
- MILLINGTON, A. C., DRAKE, N. A., TOWNSHEND, J. R. G., QUARMBY, N., SETTLE, J. J., and READING, A. J., 1989, Monitoring salt playa dynamics using Thematic Mapper data. *I.E.E.E. Transactions on Geoscience and Remote Sensing*, 27, pp. 754-761.
- MILTON, E. J., 1987, Principles of field spectroscopy. *International Journal of Remote Sensing*, 8, 1807-1827.
- MITCHELL, C. W., 1983, The soils of the Sahara with special reference to the Maghreb. *Maghreb Review*, 8, 29-37.
- NECKEL, H., and LABS, D., 1981, Improved data of solar spectral irradiance from 0.33 to 1.25 μ m. *Solar Physics*, 74, 231-249.
- ONGARO, L., 1986, Studio integrato delle risorse naturali del Nefzaoua (Tunisia): carte delle unita di terre dell'area Kebili-Douz. *Rivista di agricoltura Subtropicale e Tropicale, Trimestrale LXXX-n.2 Aprile-Giugno 1986*, 165-310.
- REAGAN, J. A., SCOTT-FLEMMING, I. C., HERMAN, B. M., and SCHOTLAND, R. M., 1984, Recovery of spectral optical depth and zero-airmass solar spectral irradiance under conditions of temporally varying optical depth. *Proceedings of IGARSS'84 Symposium, Strasbourg 27-30 August 1984*, pp. 455-459.
- ROBINSON, B. F., BAUER, M. E., DEWITT, D. P., SILVA, L. F., and VANDERBILT, V. C., 1979, Multiband radiometer for field research. *Journal of the Society of Photo-Optical Instrumentation Engineers*, 196, 16-26.

Atmospheric effects on bare soil reflectance data in Tunisia

- TOWNSHEND, J. R. G., QUARMBY, N. A., MILLINGTON, A. C., DRAKE, N. A., READING, A. J., and WHITE, K. H., 1989, Monitoring playa sediment transport systems using Thematic mapper data. *Advanced Space Research*, 9, 117-183.
- VERHOEF, W., 1985, A scene radiation model based on four-stream radiative transfer theory. *Proceedings of the 3rd International Colloquium on Spectral Signatures of Objects in Remote Sensing, Les Arcs, France, 16-20 December, 1985* ESA SP-247 (Paris: European Space Agency) pp. 143-150.
- VERHOEF, W., 1990, Informatie-extractie uit multispectrale beelden met behulp van stralings-interactiemodellen, NLR TP 90243 L, Amsterdam Nationaal lucht- en ruimtevaartlaboratorium.

CHAPTER 5

EFFECT OF MOISTURE CONTENT ON SPECTRAL REFLECTANCE IN A PLAYA AREA IN SOUTHERN TUNISIA.

Proceedings international symposium, Remote Sensing and Water Resources, Enschede, August 20-24 1990: 301-308.

EFFECT OF MOISTURE CONTENT ON SPECTRAL REFLECTANCE IN A PLAYA AREA IN SOUTHERN TUNISIA

G.F. EPEMA
Agricultural University of Wageningen
Dep. of Soil Science and Geology
P.O.Box 37
6700 AA Wageningen
The Netherlands

ABSTRACT. Field experiments and observations were performed to study the effect of moisture content on Landsat TM compatible bands. An increase in moisture content gives a decrease in reflectance in all bands. MMR band 7 showed to be most sensitive to change in moisture content. The indirect effect of wetting, disappearance of salt on part of the playa, was most prominent in MMR band 1. A preliminary procedure to estimate moisture content from TM signal is described.

1. INTRODUCTION

In the Southern Tunisian desert a research project has been carried out to study the potentials of Landsat Thematic Mapper (TM) data for identification of soil surfaces and their changes in time. In situ ground reflectance measurements with a Barnes Modular Multiband Radiometer (MMR) in combination with observations of surface characteristics in different seasons were used as an aid in understanding the observed TM signal. Field campaigns were performed in November/December 1987 and April 1988. In previous reports emphasis is laid on external influences determining the at satellite and ground reflectance, like illumination conditions (i.e. atmospheric condition and solar zenith angle). This report will deal with the influence of moisture content on reflectance. Special attention will be paid to:

- 1) field experiments with artificial wetting;
- 2) changes of reflectance due to natural rain;
- 3) implications for estimates of moisture conditions from TM images.

The studied parts of the desert area comprise playas and footslope areas (Chott Djerid and Chott Fedjaj). The vegetation cover is low to nil. Despite sparse rainfall, the groundwater table in the playa area is close to the surface (see Epema in prep. for a detailed description). Although this research is mainly concerned with the playa, the wetting experiments were also performed on the footslopes in order to exclude the influence of salt.

2. EXPERIMENTAL SET-UP

Reflectance measurements were made with a Barnes Modular Multiband Radiometer

(MMR) (Robinson et al., 1979) equipped with a 15° field of view aperture. The spectral characteristics are comparable with the Landsat Thematic Mapper (TM) deployed on Landsat-4 and -5. Band numbers are identical with the exception of MMR 6, which is comparable with TM band 5 (Epema, in prep.). Moisture condition was determined by drying the samples for 24 hours at 60 °C. The standard temperature of 105 °C cannot be applied since above 60 °C gypsum loses part of the crystal water.

In addition to the standard program, determination of reflectance throughout the day on different plots in one unit and descriptions of the surface, the following experiments and measurements were performed:

- 1) experiments with artificial wetting of some plots. The reflectance as function of time and moisture content of the top layer was determined;
- 2) repeated measurements of reflectance on moist plots on different days and seasons.

3. RESULTS AND INTERPRETATION

3.1. Wetting experiment

Despite differences on the various plots some general characteristics can be deduced from measurements of reflectance after wetting in the first hour (curves not shown here):

- 1) For all bands wetting causes a decrease in reflectance;
- 2) MMR band 6 and 7 have a very low reflectance just after wetting;
- 3) The relative reflectance of MMR 1 is in between MMR 2 to 4 and MMR 6 and 7;
- 4) Differences in reaction between MMR 2, 3 and 4 are generally small.

With the exception of one case (site F, a playa unit) reflection of artificially wetted plots was lower at the end of the day than before wetting.

In figure 1 reflectance as a function of moisture content in the upper 2 mm is given for one example, a combination of two plots on a quartz sand dune (unit S). The observation that wetting causes a decrease in reflectance is in accordance with literature, for instance: Bowers and Hanks (1965), Planet (1970), and Irons et al. (1989). This decrease is attributed to internal reflections within the film of water covering soil surfaces and particles (Planet, 1970). The anomalous behaviour of the soil surface at unit F on the day of the wetting experiment (November 18) can be attributed to an initially high moisture content due to a storm 3 days before the experiment.

The other observed general characteristic is the relatively low reflectance of MMR band 6 and 7 just after wetting. This may be caused by the prominent absorption bands centered at 1.4 and 1.9 μm , which exhibit their influence into the MMR bands. Especially at higher moisture content these absorption bands tend to broaden.

The number of points in figure 1 makes it difficult to interpret the type of relation between reflectance and moisture content. Although linear, quadratic and exponential statistical models have been proposed for this relation (Desmet et al., 1988), a more close observation of their results reveals that large parts of the relations are effectively linear. According to Menenti (1984) the relation between albedo and volumetric moisture content is linear between wet and dry albedo (α_{wet} and α_{dry}) according to:

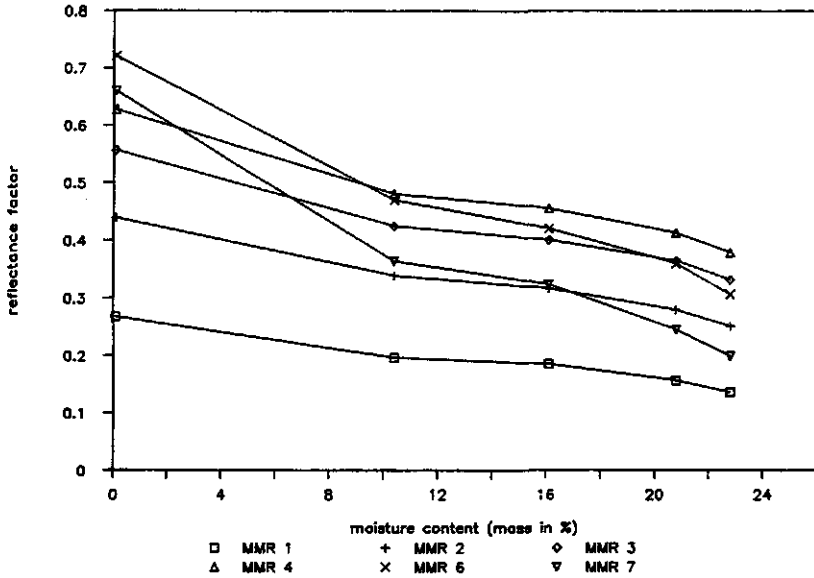


Figure 1. Relation between reflectance factor and moisture content on a quartz sand dune area (unit S).

$$\alpha = \alpha_{\text{dry}} \left(\frac{\chi - \theta}{\chi} \right) + \alpha_{\text{wet}} \frac{\theta}{\chi} \quad \text{if } \theta \leq \theta^* \quad (1)$$

where θ = volumetric moisture content
 θ^* = volumetric moisture content at saturation
 χ = porosity

It is assumed that equation 1 also holds for the individual MMR bands. In that case it depends from the wet and dry reflectance of the individual bands whether or not moisture change causes a change in spectral curves, apart from an overall decrease in reflectance. If the dry and wet reflectance are known a good estimate of changes can be calculated. In table 1 an estimate has been made based on measured wet and dry reflectance in the MMR bands for plots on unit S and F. The difference in sensitivity of the MMR bands observed can be predicted in this way.

Table 1. Dry and wet reflectance factors for unit F and S (one plot).

Unit	MMR 1	MMR 2	MMR 3	MMR 4	MMR 5	MMR 7
F dry	0.21	0.33	0.39	0.47	0.48	0.52
F wet	0.08	0.14	0.19	0.22	0.22	0.10
S dry	0.27	0.44	0.56	0.63	0.72	0.52
S wet	0.13	0.24	0.31	0.35	0.24	0.12

Apart from an increase in moisture content, on the playa unit a change in mineralogy of the top layer may occur. Salt will disappear upon wetting as has occurred on unit F. It explains the fact that upon drying not all bands reach a relative reflectance of 1 at the same time. Also at other playa sites a high susceptibility to wetting of MMR 1 has been observed, in comparison with the footslopes. This may also be attributed to the disappearance of salt upon wetting.

Salt has a relatively high reflectance in band 1 in comparison with soil material. Most soil particles have a very low reflectance at the shorter wavelengths. Goetz (1989) ascribes this to charge transfer transitions between iron and oxygen. In this area it is clear that in the wavelength range up to 1 micrometer the presence of salt is the most important modifying factor in controlling spectral characteristics after wetting.

The wetting experiments make clear that moisture may influence reflectance both in a direct and in an indirect way.

3.2 Daily change

Two factors were observed to control reflectance changes throughout the day: roughness and moisture content (Epema, in prep.). Roughness causes the highest reflectance in nadir direction to be around noon. Moisture content gives asymmetric curves with the lowest reflectance in the morning. Four phenomena have been described to be important for the high moisture content of the playa top layer in the morning. These are: (1) occurrence of dew, (2) day night cycle of redistribution of water in relation with a.o. depth of ground water, (3) presence of hygroscopic salts, and (4) presence of algae layers. In the period after rainstorms an overall drying out of the surface occurs superimposed on these effects. In figure 2 the daily asymmetry on a flat part of unit F can be detected from curves on April 16 and 23 (curves 8 and 9). The results of an overall drying out can be observed on November 18 (curve 2).

If one considers the moisture content of the top layer the maximum decrease throughout the day is only 2 %, with the exception of the first three days after the storm of November 15. On November 18 the decrease in moisture content of the plots was as high as 3.5%. Even on the wetted plots the decrease in moisture content in the late afternoon of that day was still 2.5% less than before the extra wetting.

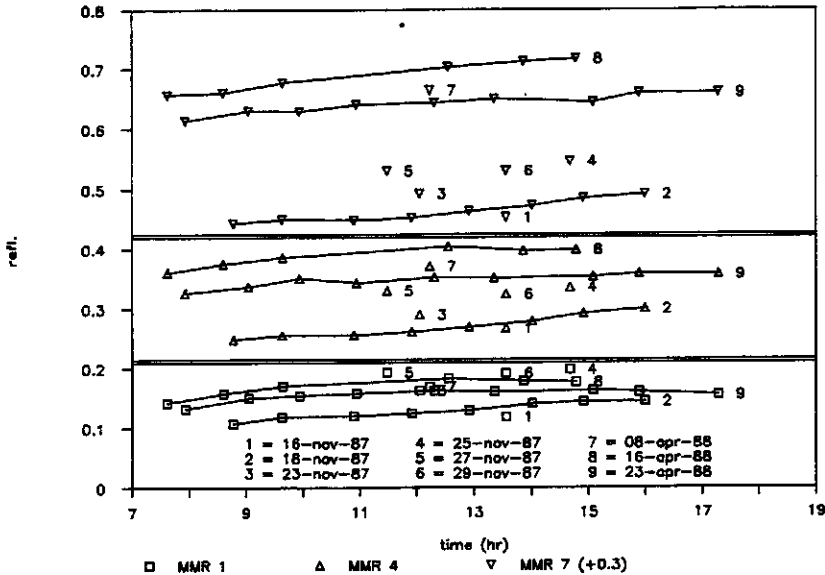


Figure 2. Reflectance factors of a flat part of unit F in both measuring campaigns (MMR 7 reflectance factor +0.3). One data point refers to one measurement. On days 2, 8 and 9 throughout-the-day measurements have been made, for the other days only single measurements are available.

3.3 Comparison between November and April measurements

On November 15 in the first measuring period a rain storm occurred. Most experiments in the November/December period in the playa were therefore performed with high moisture contents in the top layer. The April measurements were carried out after a period of prolonged drought. In Table 2 gravimetric moisture contents are given for the top 2 mm of some units in both periods (unit A and D are located in the playa). Differences in moisture content between the 2 periods up to 20% were observed. For the April period also moisture contents at 1 cm depth were determined. The difference between the moisture contents at 2 mm and at 1 cm is considerable. This demonstrates the problem of applying reflectance data to estimate moisture content deeper in the soil.

Table 2. Moisture content of top layer (0 - 2 mm).

Unit, plot	Mean value per day		between() moisture 5 to 10 mm		
	Date	Moisture content	Date	Moisture content	difference Nov.-April
A3	26Nov87	25	19Apr88	5 (19)	20
A6	26Nov87	21	19Apr88	5 (18)	16
A9	26Nov87	11	19Apr88	3 (3)	8
A10	26Nov87	18	19Apr88	5 (18)	13
D1	14Nov87	14	25Apr88	10 (20)	4
F1	18Nov87	32	16Apr88	17 (26)	15
F7	18Nov87	25	16Apr88	11 (17)	14
F7	29Nov87	19	16Apr88	11 (17)	8

In figure 2 reflectance factors of unit F for three MMR bands in different parts of the spectrum are given. Again it is obvious that band 7 shows the highest susceptibility to drying. It is also clear that spectral changes occur due to salt.

In table 3 regression coefficients are given for the relation between moisture content and reflectance for unit F. Highest correlation coefficients are found for large wavelengths. If also other units and experiments are taking into account correlation coefficients decrease.

Table 3. Results of regression analysis between reflectance and moisture content.

Regr. coeff.	Fnat Fall all			Fnat Fall all			Fnat Fall all		
	MMR 1			MMR 2			MMR 3		
Const	23.9	24.0	21.4	34.7	34.7	35.5	43.9	43.3	43.8
Slope	-.43	-.49	-.35	-.61	-.68	-.64	-.79	-.82	-.74
R square	.737	.676	.591	.895	.772	.553	.975	.884	.566
No. of obs.	5	10	22	5	10	22	5	10	22
	MMR 4			MMR 6			MMR 7		
Const	48.5	47.8	49.1	57.5	56.2	56.8	52.6	50.9	49.9
Slope	-.85	-.87	-.83	-1.2	-1.2	-1.2	-1.4	-1.4	-1.3
R square	.989	.889	.570	.967	.889	.774	.943	.867	.794
No. of obs.	5	10	22	5	10	22	5	10	22

3.4 Implications for Landsat Thematic Mapper

Wetting experiments and field observations show that moisture content plays an important role in determination of reflectance. Although within a unit significant relations were found between reflectance, (especially at higher wavelengths, MMR 4 to 7) and moisture content, it is not possible to extrapolate the relations directly to other units. Even if the relation between wet and dry reflectance is linear, the wet and dry reflectance factors differ as a function of surface types.

Based on the considerations above and other research in this area a first attempt for a procedure to map moisture content with Landsat TM data can be made:

- 1) discriminate the playa area and footslope area. Field measurements showed that the sharpest boundary is found in MMR 4 (reflectance factor of 0.45). Use of this specific value for TM band 4 (after calibration and atmospheric correction, see Epema, 1990) is therefore recommended to identify the footslopes. An alternative to discriminate playa and footslopes would be to make a multitemporal combination of Landsat TM data and assign a specific value of change as boundary;
- 2) assign to the footslope area a moisture content of less than 2%;
- 3) make a discrimination within the playa area between areas dominated by fresh salt and other areas and mask those salt dominated areas. A $MMR4 / MMR 1$ ratio above 0.51 gives an indication of the dominance of salt. Use this ratio on TM data after calibration and taking into account the atmosphere;
- 4) make a discrimination within the other playa areas between areas dominated by gypsum and other areas and mask those gypsum dominated areas. A $MMR 7$ to $MMR 4$ ratio below 0.67 gives the gypsum dominated surfaces in this area. Use this $7/4$ ratio for calibrated and atmosphere corrected data of TM;
- 5) apply the linear relations of the type presented in table 3 for MMR 4 to 7 or a combination of them to the rest of the area. Since TM 5 has the highest dynamic range this band is used preferentially. In this way moisture content can be determined for more than 80% of the surfaces.

This approach can give a first idea about moisture differences in this area. However, the above described procedure is still too simple. Also other factors give rise to a change in reflectance or have to be taken into account, e.g. roughness, texture, small differences in mineralogy, and external influences like atmosphere. Also the problem of mixed signatures within a pixel has to be solved. Only an integrated approach, which goes beyond the purpose of the present paper, will lead to a more reliable picture. Use of the thermal TM band 6 can be considered too.

4. CONCLUSIONS

- 1) Moisture content is an important variable in the playa area to determine reflectance. On the footslopes only directly after storms moisture differences are important;
- 2) Higher moisture contents in the morning result in asymmetric reflectance curves throughout the day;
- 3) MMR band 7 is most sensitive to moisture changes;

- 4) Apart from direct influence of wetting, change in reflectance is also due to change in salt on the surface. This is especially visible in MMR band 1;
- 5) Change in spectral signature on the playa is dominated by moisture content. Therefore use of ratios does not give more information on moisture content than individual bands. The different sensitivity of MMR bands to moisture content can only be applied if studied in combination with other influences on reflectance, such as roughness, texture, mineralogy and atmospheric influences.

REFERENCES

- Bowers, S.A. & R.J. Hanks, 1965. Reflection of radiant energy from soils. *Soil Science* 100:130-138.
- Desnet A., H. Eerens & R. Gombeer, 1988. Influence of some soil factors on the reflectance of bare soils. *Pedologie*, XXXVIII-3: 227-247.
- Epema, G.F., 1990. Determination of planetary reflectance for Landsat 5 Thematic Mapper tapes processed by Earthnet (ITALY). *ESA Journal*.
- Goetz, A.F.H., 1989. Spectral Remote Sensing in Geology. In: G. Asrar, Theory and Applications of optical remote sensing. 491-526, John Wiley and sons.
- Irons, J.R., R.A. Weismiller & G.W. Petersen, 1989. Soil Reflectance. In: G. Asrar, Theory and Applications of optical remote sensing, 66-106, John Wiley and sons.
- Menenti, M., 1984. Physical aspects and determination of evaporation in deserts applying remote sensing techniques. Report 10, Institute for Land and Water Management Research (ICW), Wageningen, 202 p.
- Planet, W.G., 1970. Some comments on reflectance measurements of wet soils. *Remote Sensing of Environment*, 1: 127-129.
- Robinson, B.F. & L.L. Biehl, 1979. Calibration procedures for measurement of reflectance factor in remote sensing research. *Journal of the Society of Photo-optical Instrumentation Engineers*, 196.

CHAPTER 6

GROUND REFLECTANCE OF NATURAL BARE AND PURE SURFACES AS AN AID IN INTERPRETATION OF LANDSAT THEMATIC MAPPER DATA IN SOUTHERN TUNISIA.

Advanced Space Research Vol.12, No.7: (7)39-(7)42.

GROUND REFLECTANCE OF NATURAL BARE AND PURE SURFACES AS AN AID IN INTERPRETATION OF LANDSAT THEMATIC MAPPER DATA IN SOUTHERN TUNISIA

G. F. Epema and S. B. Kroonenberg

*Agricultural University, Department of Soil Science and Geology, P.O. Box 37,
6700 AA Wageningen, The Netherlands*

ABSTRACT

Reflectance measurements with a Thematic Mapper (TM)-compatible instrument on artificial plots of pure gypsum, quartz and carbonate in a South-Tunisian desert showed that these materials can be satisfactorily separated using TM bands 5 and 7. Gypsum types differing in grain size and habit show different reflectance characteristics. Gypsum contents of natural eolian duna surfaces can be determined from satellite data provided dune areas have been delineated previously by physiographic interpretation.

INTRODUCTION

Reflectance characteristics of bare ground surfaces on footslopes, eolian dunes and in playas in a desert area in southern Tunisia have been investigated on three different scales: (1) TM imagery (6 bands); (2) ground measurements using a Barnes radiometer (7 bands); (3) laboratory measurements (750 bands). Surface materials reported here consist predominantly of gypsum, carbonate and quartz (and minor other siliceous minerals). Gypsum occurs as (1) gypsum sand of different grain size in wind-blown sand dunes, (2) as thin surface covers of large crystals weathered out of Cretaceous and Tertiary sediments and (3) as surface or subsurface crusts formed by capillary rise and evaporation of saline ground water. Carbonates occur mainly in escarpments of (partly ferruginous) Cretaceous limestones, and as a minor component in wind-blown surface sands. Quartz occurs mainly as wind-blown surface deposits from siliceous sources.

In order to be able to distinguish surface deposits of uniform mineralogy on account of their reflectance characteristics, artificial horizontal field plots of pure surface materials have been investigated. In this way the influence of other surface factors such as roughness, texture, organic matter content, moisture content, exposition, slope and illumination conditions is minimized. The resulting data were compared with reflectance data from natural plots.

Three variables have been considered:

1. different mineralogy: gypsiferous, quartz and calcareous sand of comparable grain sizes
2. different types of gypsum
3. different iron content

The reflectance of these plots is determined under comparable illumination conditions and with the same instrument as the natural surfaces. The instrument is a Barnes Modular Multiband Radiometer (MMR) /1/ equipped with a 15° field of view aperture. The instrument is mounted on a tripod, and the measuring height is 1.5 meter. The spectral characteristics are comparable with the Landsat Thematic Mapper (TM) deployed on Landsat-4 and -5. Band numbers are identical with the exception of MMR 6, which is comparable with TM band 5. For some samples laboratory spectra with high spectral resolution were determined with an IRIS Mark IV spectroradiometer.

REFLECTANCE OF PLOTS OF PURE GROUND SURFACE MATERIALS

Reflectance spectra of pure samples taken at two consecutive days with comparable atmospheric conditions at similar solar zenith angle (55°-56°) are shown in Figure 1. It is obvious that there is a large variety of reflectance factors. All curves show an increase in reflectance from MMR 1 to MMR 4, but nevertheless conspicuous differences occur between the various plots. Reflectance factors in MMR 7 and 6 have a low correlation with MMR bands 1 to 4.

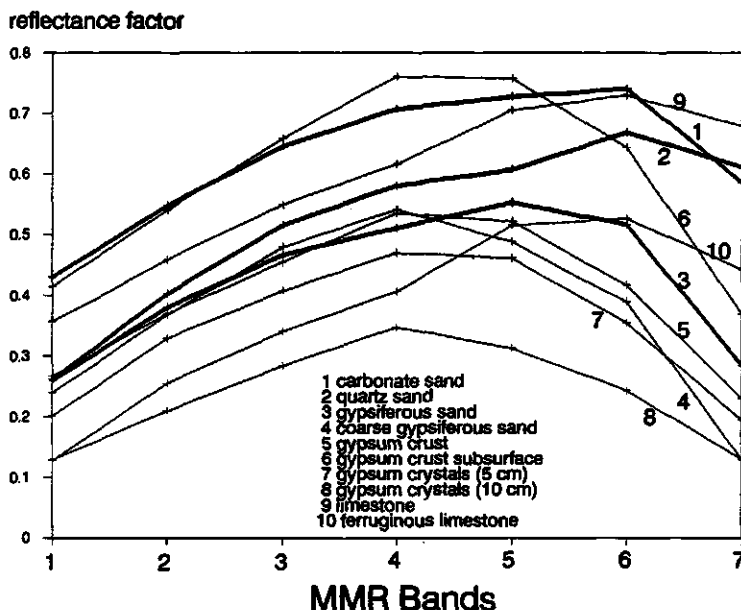


Fig.1 Reflectance factors of pure surface materials on artificial horizontal field plots.

Influence of Mineralogy

The calcareous sand has a higher reflectance than the other two. This might be due to the overall higher refractive index of carbonate grains. The gypsiferous sand shows a large decrease in reflectance in bands 6 and 7, in comparison with band 4. The calcareous sand shows a moderately strong decrease only in band 7, while quartz exhibits only a small decrease in this band. This difference in behaviour between the samples is due to absorption features. A large range of diagnostic vibrational overtone features important to geologic mapping exist in the region between 1.6 and $2.5 \mu\text{m}$ [2]. Especially diagnostic features such as position and depth of absorption features for minerals containing OH and CO_3 ions are indicative. Depending on depth and width of the dips, these phenomena can be observed in bands 6 and 7.

In Figure 2 some laboratory spectra are presented, which show the relevant dips. The features for gypsum (sample 4 and 5) are the result of OH and H_2O overtones and combinations. Apart from low reflectance in the water absorption bands positioned between MMR 5 and 6 and MMR 6 and 7 with some influence on the adjacent bands, also a band around $1.75 \mu\text{m}$, a strong band at $2.2 \mu\text{m}$ and a band $1.19 \mu\text{m}$ are present. The effect is that all samples with gypsum have a low MMR 6 and 7 reflectance.

Curves with a low gypsum content yet have a lower MMR 7 than MMR 6 value (Figure 1). This is due to the abundance of minerals having OH or CO_3 , of which only small amounts can give rise to a decrease in reflectance. The relatively strong decrease in the calcareous sand may be due to CaCO_3 absorption. A dip at $2.34 \mu\text{m}$ is highly indicative for CaCO_3 [2], see also Figure 2, sample 1).

Different Types of Gypsum

Three types of gypsum were examined: gypsiferous sand of three different grain sizes, gypsum crystals of two different grain size, and gypsum crusts. The difference in overall reflectance is due to a combination of transparency and grain size. Highest reflectance is found for the non-transparent gypsum crust below the surface. The lowest overall reflectance is shown by the coarse gypsum crystals. The difference between medium fine and coarse gypsiferous sand is not due to gypsum content (both 75%), but probably to particle size, as contrasts due to absorption features are known to increase with increasing particle size [3]. The effect of the dip at $1.19 \mu\text{m}$ on band 5 reflectance can be observed in the coarse sample but not in the fine one. However, quantitatively unimportant impurities such as inclusions of soil material within the large gypsum crystals or algae on the gypsum crust may greatly influence reflectance.

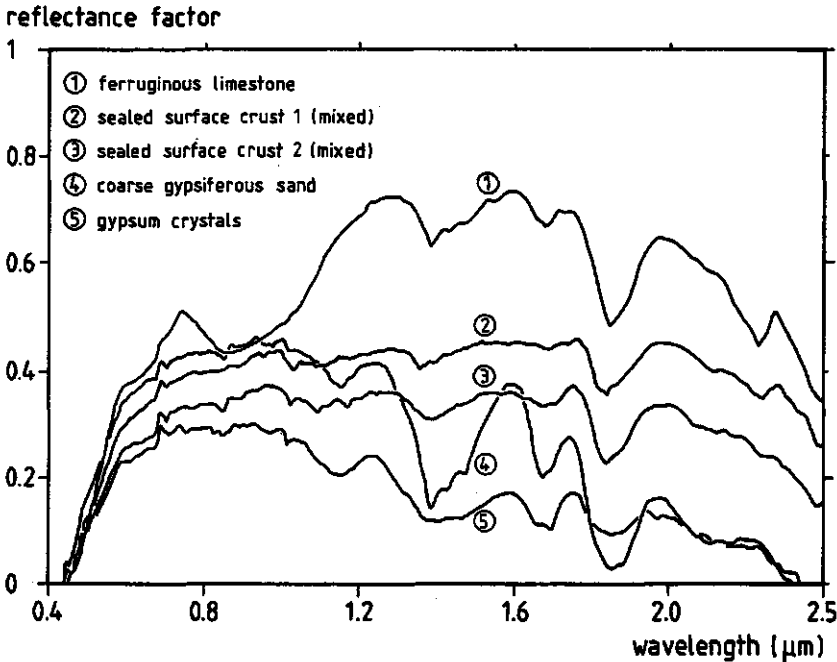


Fig. 2. Reflectance spectra of some surfaces measured in the laboratory (no absolute values due to calibration problems).

Effect of Iron

Goetz /2/ ascribes the low reflectance at shorter wavelengths for most soil samples to charge transfer transitions between iron and oxygen. This results in a strong absorption in the UV, with a wing extending into the visible part of the spectrum. Apart from this effect, different absorption bands exist up to $1\mu\text{m}$ /4/. The general effect is that iron gives a decrease in reflectance up to the near infrared. The laboratory spectrum of ferruginous limestone (Figure 2) shows two characteristic broad Fe absorption bands centered at $0.65\mu\text{m}$ and $0.875\mu\text{m}$. The relatively low reflectance in the visible part of the spectrum can be seen in Figure 1. The high reflectance of limestone, carbonate sand and subsurface gypsum crust is largely due to absence of iron.

COMPARISON OF PURE AND NATURAL BARE SOIL PLOTS

In order to compare the signatures of pure ground surface materials with natural conditions, reflectance measurements have been made on three kinds of natural ground surfaces: eolian dunes and sand sheets, gypsum crusts on footslopes and sealed soil surfaces on footslopes.

In eolian dunes and sand sheets a range of grain size and gypsum contents exists. Figure 3 shows that the signature both in natural and pure plots can be satisfactorily related to gypsum content alone. The slight scatter along the curve may be ascribed to the effect of grain size and minor amounts of carbonate.

The natural plot covered with 50% gypsum crust and 50% of gypsiferous sands had a higher $7/4$ ratio than both the pure gypsum crust and the pure gypsiferous sand. This might be ascribed to a higher percentage of carbonate (9%) in the natural crust than in the samples used for determining the reflection of pure crusts (3%).

Most parts of the footslopes have a sealed surface. The $7/4$ ratio is comparable with that of pure quartz. Therefore a high quartz component would be expected. For two units mineral counting in grain mounts have been performed using a polarization microscope. Type 1 sealed surface soil has a quartz content of 60 to 70%, while the rest consists of gypsum. Type 2 has 60% gypsum and 20% of quartz and 20% of CaCO_3 . In both cases the $7/4$ ratio is higher than would be expected on account of the gypsum content. This might be due to a higher carbonate and quartz content in the sealing crust, but as the seal was too thin to sample this could not be verified by mineralogical analysis.

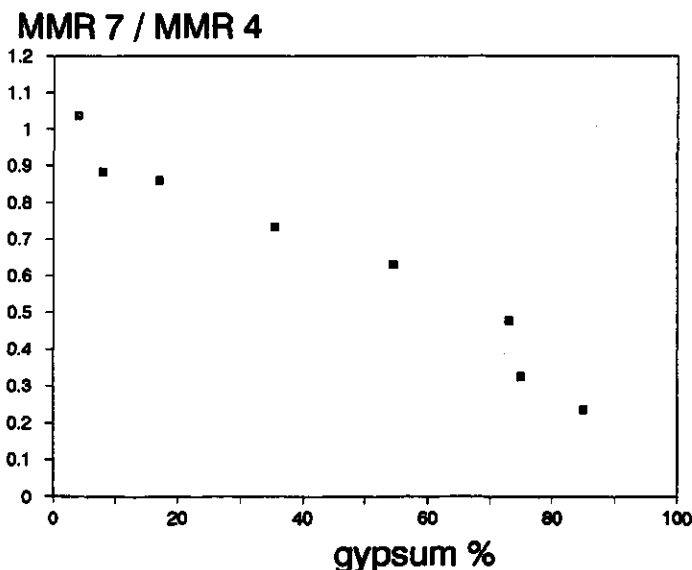


Fig. 3. Ratio MMR 7 to MMR 4 as a function of gypsum content for natural and pure eolian samples.

CONCLUSIONS AND IMPLICATIONS FOR LANDSAT TM

From this study it appears that eolian sand deposits consisting of gypsum, carbonate and quartz sand can be separated using TM band 5 and 7 signatures. Moreover, if grain size is known, gypsum content can be roughly estimated. This of course presupposes delineation of eolian deposits from the surrounding footslopes by combining physiographic interpretation and spectral analysis. On natural surfaces with crusts small differences in mineralogy and the presence of extremely thin surface seals may greatly modify 7/4 ratios, and interpretation of such surfaces from satellite imagery will therefore remain difficult.

This illustrates that only an integrated approach taking into account not only mineralogy, but also roughness, texture, vegetation cover, atmosphere, and the probable presence of mixed signatures within a pixel, will lead to adequate interpretation of Thematic Mapper data.

ACKNOWLEDGEMENTS

This research is part of a project funded by the Netherlands Remote Sensing Board (BCRS, AO-4.2). We wish to thank Prof. Dr. F.K. List and Dr. A. Richter (FU Berlin) for use of the Barnes MMR, F. Lehmann (DLR Oberpfaffenhofen) for the possibility of making laboratory spectra and A.T.J. Jonker for the mineral countings.

REFERENCES

1. B.F. Robinson, M.E. Bauer, D.P. DeWitt, L.F. Silva and V.C. Vanderbilt, Multiband radiometer for field research. *Journal of the Society of Photo-Optical Instrumentation Engineers*, 196, 16-26 (1979).
2. A.F.H. Goetz, Spectral Remote Sensing in Geology. Chapter 12 in G. Asrar, *Theory and Applications of Optical Remote Sensing*, John Wiley and sons, 1989, 491-526.
3. J.R. Irons, R.A. Weismiller and G.W. Petersen, Soil Reflectance. Chapter 3 in G. Asrar G (ed.) *Theory and Applications of Optical Remote Sensing*, John Wiley and Sons, 1989, 66-106.
4. M.A. Mulders, *Remote sensing in soil science*, Developments in soil science 15, Elsevier, Amsterdam-Oxford-New York-Tokyo, 1987.

CHAPTER 7

GROUND SPECTRAL REFLECTANCE IN A DESERT AREA IN SOUTHERN TUNISIA.

Submitted to International Journal of Remote Sensing.

GROUND SPECTRAL REFLECTANCE IN A DESERT AREA IN SOUTHERN TUNISIA

G.F.Epema

*Wageningen Agricultural University, Department of soil science and geology, P.O.Box 37
6700 AA Wageningen, The Netherlands*

ABSTRACT

Spectral reflectance of a desert area in Southern Tunisia, consisting of playas and footslopes with or without sand cover, has been investigated with a TM compatible field radiometer. Reflectance could be explained with a range of surface characteristics, varying in importance for the different units. The derivation of surface characteristics from the signal, was mainly possible for factors affecting only specific bands. It appears possible to (1) discriminate plots on footslopes dominated by gypsum, carbonate and quartz, (2) determine gypsum content of eolian sand, (3) determine moisture and salt differences on the playas, (4) discriminate different surface types in the playa. Multitemporal observation are useful for a further discrimination in surface types in the playa area. Based on these field experiments one may conclude that it is possible to derive from Landsat TM a range of very important characteristics in this and other arid areas.

INTRODUCTION

In Southern Tunisia several research projects are carried out to study the potentials of Landsat Thematic Mapper (TM) data for identification of soil surfaces and their changes in time (Townshend *et al.* 1989, Epema 1990a) and for vegetation identification and dynamics (Ongaro 1986). Promising results have been obtained so far but some major questions have still to be solved. This holds both for the processes at a regional scale and for the relation between Landsat TM data and surface characteristics. This study aims to tackle the latter problem. Since vegetation cover is scarce emphasis will be laid on bare soils. Although the main factors affecting bare soil reflectance are known (Stoner and Baumgardner 1981, Mulders 1987, Goetz 1989 and Irons *et al.* 1989), their effect under natural conditions is not well studied.

In this study in situ ground reflectance measurements with a TM compatible instrument (a Barnes Modular Multiband Radiometer; MMR) in combination with observations of surface characteristics in different seasons have been carried out for two aims: (1) to determine the effect of different factors on reflectance, and (2) to examine the possibilities of TM like bands for identification of surface characteristics under natural conditions.

Including field reflectance measurements has major advantages above purely satellite-borne campaigns: (1) A direct relation between a TM-like signal and surface characteristics at the same time can be studied; (2) reflectance of the different components present in the TM ground resolution elements can be determined; and (3) the effect of changes of the surface on reflectance as a function of for instance artificial or natural moistening can be measured directly.

The application of field reflectance measurements requires adequate processing and an evaluation on the influence of external factors such as atmosphere and solar zenith angle. This has been discussed in previous papers (Epema 1990b, 1991, 1992).

After description of experimental set up, study area and factors affecting ground reflectance, results of laboratory reflectance measurements with higher spectral resolution of natural samples will be treated. These data give a prediction for reflectance in TM-like bands. Spectral differences of field reflectance data are examined by simple statistical methods first for the total data set and subdivided in playa and non-playa area. Hereafter a refining of the subgroups is made. For these subgroups the major causes for reflectance differences are investigated with the aid of field observations and laboratory data. In addition it is tested if a multitemporal approach gives additional information for explanation of reflectance differences with surface characteristics.

EXPERIMENTAL METHODS AND CONDITIONS

Plots were selected for field reflectance measurements, description of surface characteristics and sampling. The selection was based on a general knowledge of the main factors affecting reflectance and the variation in the area, observed on satellite images and in the field. Measurements were performed in two periods: November/December 1987 and April 1988.

Determination of reflectance was done with a Barnes Modular Multiband Radiometer (MMR) (Robinson *et al.* 1979) equipped with a 15° field of view (FOV) aperture. In field surveys a 15° FOV is normally used to average over surface irregularities of the target (Biggar *et al.* 1988). The MMR was mounted on a tripod with the viewing direction vertical and a height above the surface of 1.5 meter. In principle, during a day, reflected radiation was measured over the different objects every hour. Reference radiance readings from the standard reflector painted with barium sulphate were taken at the start and finish of each measurement sequence. The reflectance in a given MMR band was determined by dividing the radiance reflected from an object by that from the standard reflector in the same nominal band. To compare the curves of spectral response functions for the MMR with the one used, I refer to Jackson and Slater (1986). Table 1 shows the comparison of the bandpasses provided by the manufacturer with those obtained from Landsat Thematic Mapper (TM) data of Landsat-4 and -5 by Markham and Barker (1986). For further details on the measurements of reflectance one is referred to Epema (1991). For this part of the study, measurements are used for stable atmospheric conditions and solar zenith angles less than 65° of both standard measuring days and individual measurements. Repeated measurements on different days on individual plots in order to examine moisture influence in detail are not used in the statistical analyses. The laboratory reflectance measurements have been performed with an Infra-Analyzer 500, which measures from 600 to 2500 nm.

Apart from reflectance measurements, the following surface characteristics have been determined in the field and laboratory for selected sites:

- moisture content. Gravimetric and volumetric moisture content determinations. After Vieillefon (1979) samples were dried for 24 hours at 65°C in stead of 105°C as used in the standard methods. In this way no crystal water from gypsum will be extracted, while the determination of the moisture content is not due to large errors.

- gypsum, carbonate, quartz, anhydrite, halite, free iron content and determination of some ions. Presence, type and if possible amount of the minerals has been estimated in the field. For a selection of samples the content has been determined in the laboratory by counting of grain mounts, with X-ray analysis or chemically (methods of Hesse 1971). Also, water soluble salts in a 1:2 extract and in 0.5 N HCl are determined for the cations Ca^{2+} , Mg^{2+} , Mn^{2+} , Fe^{3+} , K^+ , Na^+ and the anions Cl^- , SO_4^{2-} and CO_3^{2-} .
- organic matter content with the method of Begheijn (1976).
- roughness and texture. Stereophotographs have been taken. However roughness in this study will be used only in a qualitative way. Texture analysis has been performed with dry sieving.
- vegetation cover, type and aspect. In this article only plots with a coverage less than 1% are examined.

Table 1 Bandpasses (-3dB) of Barnes MMR field radiometer (50% power bandpass limits) and Landsat Thematic Mapper (full-width at half-maximum method) of reflectance part of the spectrum.

	Barnes MMR		Landsat TM	
	nr. of band	wavelength limits	nr. of band	wavelength limits
Blue	1	0.458-0.525	1	0.4524-0.5178
Green	2	0.519-0.601	2	0.5280-0.6093
Red	3	0.637-0.687	3	0.6264-0.6923
Near IR	4	0.739-0.898	4	0.7764-0.9045
	5	1.174-1.334		
MIR 1	6	1.574-1.803	5	1.5675-1.7842
MIR 2	7	2.083-2.371	7	2.0972-2.3490

STUDY AREA

In figure 1 the location of the study areas is given. Extensive descriptions of (parts of) the region on various aspects are given by Coque (1962), Coque and Jauzein (1967), Meckelein (1977), Mitchell (1983), Ongaro (1986), Millington *et al.* (1987), Townshend *et al.* (1989), Millington *et al.* (1989) and Epema (1990a). The areas are situated at the margin of the Saharan Platform and the folded Atlas ranges. A large part of the zone of subsidence is occupied by entirely flat playas (locally known as chotts). The Chott el Djerid is the largest of them and has an elongated northeastern arm (Chott Fedjaj), which has been formed by faulting in the top of an anticlinal uplift (Coque 1962; Jones and Millington 1986). The cuesta ridge of the Djebel Tebaga, consisting mainly of dolomitic limestones is located in the southern part of this uplift. It is surrounded by footslopes. Sandsheets and dunes of various size and mineralogy cover parts of playa margins and footslopes.

Rainfall in the study areas is less than 100 millimetres per year. Yet the ground water table in the playas is generally at less than 1 meter depth, due to artesian water inflow. Apart from some oases, vegetation cover exceeds 5% of the surface only in exceptional cases. The inner parts of the playa have no vegetation cover at all due to high salt content, except for some parts covered with small dune fields. The species are typically for this area adapted to low rainfall and high halite and gypsum content of the soil (Floret and Pontanier, 1982; Epema *et al.*, 1985; Ongaro, 1986). In spring vegetation is much greener and if it rains in this period even outside these hummocks some vegetation exist.

The study areas comprise parts of the playas and the footslope areas with or without eolian cover. One area is located in Chott Djerid in the west, while another area is located at the margin of Chott Fedjaj and footslopes of Djebel Tebaga in the east. In the playa area reflectance differences are dominated by moisture, in the footslopes, and in the sand-covered playas and footslopes other factors predominate. No large differences in morphology, mineralogy and moisture condition exist between sand sheets on the footslopes and on the playa. Therefore in the following discussion playa areas and non-playa areas are treated separately.

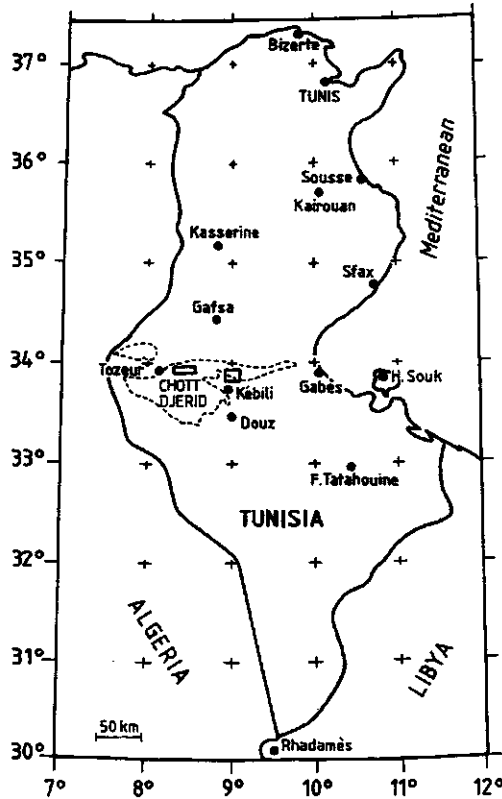


Figure 1 Location of the study areas.

FACTORS AFFECTING GROUND REFLECTANCE

Both internal and external factors determine reflectance. The most important external factors are solar zenith angle and atmosphere. For bare surfaces the dominant internal factors affecting reflectance up to the near infrared are:

- 1) surface morphology, texture, structure, roughness and stones.
- 2) mineralogy, especially in combination with iron
- 3) organic matter content
- 4) moisture content

Surface morphology

Roughness causes a decrease in reflectance in all bands. Spectral curve shape is hardly affected. Desmet *et al.* (1988) observed this independence from wavelength and found a 6% higher reflectance for smooth than for rough surfaces. Also particle size hardly influences the signature in this trajectory. We will discuss surface roughness and microrelief for both playa and non-playa areas.

Playa area

The playa shows only minor height differences. The major zones are those dominated by deposition, those with thick salt crusts and zones with seepage points (aiouns). The location of the major zones and ephemeral channels has remained constant for several years (10 at least) as can be observed from satellite images.

Within these major zones, the appearance of the playas varies considerable in space and time. In the first place capillary rise of ground water and subsequent evaporation lead to various patterns of salt deposition. In the wet winter season, but also after individual storms, large parts exhibit standing water and upon drying relatively clean halite-rich salt crusts may develop. Large parts of the playa also receive runoff water with sediments from the surrounding mountains. In addition, especially in spring and summer, silty and sandy material is blown in. Also loose surface material may be redistributed by wind within the playa or transported to outside the area. All these processes act as input, redistribution and output mechanisms in the playa (Millington *et al.* 1989), these processes cause a great variety of surface types differing in microrelief and mineralogy.

A classification was made of the dominant surface types, because it was thought that surface microrelief might be of importance for reflectance characteristics. They were classified in a relatively dry season. In the wet season or after storms, the morphology of the surface types may change considerably depending on intensity and amount of rainfall. The following surface types have been distinguished (cf. also figure 2):

- Type A :dry porous brown crusts, with friable, rough surfaces (1 to 2 cm height difference). Small gypsum crystals are present.

- Type B :very thin (0.1 cm.) light brown crusts, with or without presence of polygons, due to salt (halite) growing, with a diameter of in general 30 to 60 centimetres and of height of polygon fringe of 0.5 centimetres and a polygon fringe diameter of 3 centimetres. The polygon fringes are not connected with the rest of the profile, and are therefore less moist and less dark than the area within the polygons. The surface is often covered with a thin

transparent halite layer. Small salt cuboids with a diameter of 0.5 to 2 centimetres are scattered over the surface types A and B. Concentrations of these cuboids are sometimes so high that even on satellite images these patterns can be found.

- **Type C**: dry, thin flaky crusts. These crusts occur mainly within polygon patterns with sides of 10 to 20 meters. Loose sand with gypsum crystals are present in parts where these crusts are blown away.

- **Type D**: thick halite salt crusts generally exhibiting polygons. The diameter of the polygons is between 60 and 200 centimetres. The height of fringes increases with increasing polygon diameter and range from 5 to 30 centimetres.

- **Type E**: aiouns, characterised by quasi-circular features, with diameters from 30 meters to 1000 meters. The centre (diameter less than 3 meter) is formed by a source, and rises somewhat above the surrounding area. The groundwater table is close to the surface. Periodically water comes to the surface and spreads out over the surroundings. Therefore circular features develop around the sources. These aiouns are also described by Jones and Millington (1986), Roberts and Mitchell (1987) and Millington *et al.* (1989).

- **Type F** smooth, brown to greybrown crusts with polygonal cracks. These were observed in the Chott Djerid area only.

The very locally present black or dark green layers on the surface are not further examined. These layers, in general not on but just below the surface, are formed by algae (Coque 1962, Meckelein 1977 and Ongaro 1986).

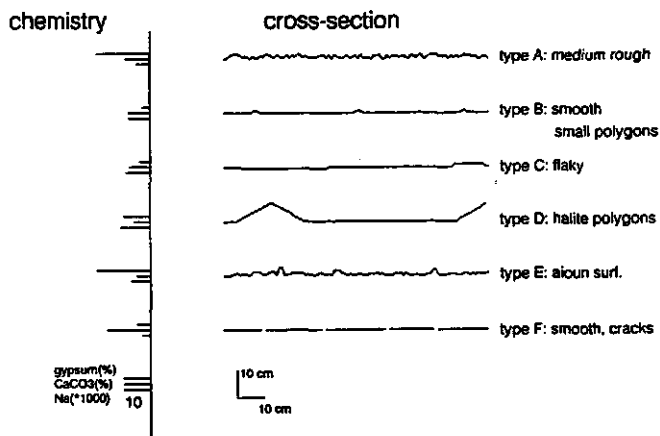


Figure 2 Simplified cross-sections of playa surface types and examples of gypsum, CaCO_3 , and Na content.

Non-playa area

Footslopes in the area are mainly erosional features. The top layers are often sealed. Close to the mountain ridge footslopes are incised by gullies. Parts of the surface are covered with gravel and stones and eolian material.

The stones of this area are from the Djebel Tebaga mountain ridge. Occasionally they are covered with iron-rich desert varnish as also been observed by White (1990). The influence on the spectrum depends on the source of the stones, coverage, presence of desert varnish and the reflectance of the soil surface itself. Within our data set on natural surfaces only minor influence of stones on spectral reflectance has been observed.

Eolian sand can be found as thin sheets on the footslopes or in the gullies, as sheets with dunes less than 1 meter, as scattered small dunes on the gypsum crusts and footslopes, and deposition behind hummocks. The appearance of the different sand types varies as a function of wind direction and also of the sealing of the surface.

Mineralogy

Soil minerals primarily affect spectra in an indirect manner. They impose their crystal structures on the energy levels of ions bound to the structures. Many of the absorption features up to 1 μm are due to iron in some form. Iron may be present as part of primary, secondary minerals and non-crystalline material. Other principal constituents like silicon, aluminium and oxygen have no absorption features in this region. Iron causes a strong absorption in the UV, due to charge transfer transitions between iron and oxygen. The wing of this absorption extends into the visible part of the spectrum. This absorption causes the increase in reflectance with increasing wavelength for most soil samples. Moreover other Fe absorption bands, caused by electronic processes, exist up to 1 μm (Mulders 1987).

Table 2a Chemistry playa types in mass fraction (%), mmol/kg water soluble (1) or mmol/kg acid soluble (2).

type	TyO ₂	CaSO ₄ (%)	CaCO ₃ (%)	Mn (2)	Fe (2)	TOO (1)	Ca (1)	Mg (1)	K (1)	Na (1)	Cl (1)	Ca (2)	Mg (2)	Mn (2)	K (2)	Si (2)	SO ₄ (1)
A	Fj	20.40	9.55	1.6	33.0	8.82	1400	309	82	3213	6381	4675	1212	5424	107	74	679
B	Fj	3.41	8.01	1.1	18.0	3.42	663	206	32	8644	10735	1818	745	8993	48	66	515
B	Dj ¹	2.32	9.64	1.1	21.0	2.83	413	340	67	9236	11979	1802	1159	10149	76	61	0
B	Dj ²	3.06	8.81	3.9	16.0	3.14	1430	160	49	6488	10401	2993	707	8887	53	58	1170
C	Fj	4.04	8.41	1.5	30.0	2.43	700	149	31	9126	11433	1910	336	9311	47	59	504
C	Fj ³	35.10	10.70	2.0	33.0	10.30	1081	238	36	2494	3022	4308	1416	2820	60	67	972
D	Dj ⁴	10.00	5.59	1.6	16.0	2.58	1275	140	49	10171	11203	2805	513	10796	52	52	1190
D	Dj	11.70	4.72	1.6	15.0	4.30	1710	309	66	11171	13890	2801	391	10636	66	44	1422
E	Dj	21.20	4.53	0.8	12.0	17.60	1807	167	47	6836	7222	3844	509	7678	53	60	1240
F	Dj	5.38	16.10	2.0	37.0	8.93	700	388	60	3156	4441	2362	2307	4326	81	99	277
cuboids 1		3.97	4.31	0.6	9.4	2.38	1285	204	26	11667	12291	1400	370	12339	36	62	987

Fj = Fedjaj
Dj = Djerid

¹ = close to F
² = close to D
³ = sub-surface
⁴ = polygon

Table 2b Results of X-ray analysis

		Halite	Gypsum	Quartz	Calcite	Anhydrite	Clay
A	Fj	++(+)	++	(+)	+	+	-
A	Fj	++(+)	++	++(+)	(+)	-	(+)
B	Fj	+++(+)	+	++	++(+)	-	(+)
B	Dj close to F	+++(+)	+	++	++	-	+
B	Dj close to D	++++	(+)	+	(+)	-	-
C	Fj	+++	+	++(+)	++(+)	-	+
C	Fj	++	++	++(+)	+	-	(+)
D	Dj polygon	+++(+)	+	+	+	-	-
E	Dj	+++	++	+	(+)	-	-
F	Dj	++	+	+++	+++(+)	-	+
cuboids1		+++	+	(+)+	+	-	(+)
cuboids2		+++	(+)	+	(+)	-	(+)
cuboids3		+++(+)	+	(+)	(+)	-	-
cuboids4		++++	-	-	-	-	-
other white		++++	-	-	-	-	-
dust on salt		+++	+	++(+)	++(+)	-	-

Legend: (+) minor; + few; ++ moderate; +++ much; ++++ dominant

Table 2c Characteristics of representative non-playa areas (% based on mineral countings)

	Gypsum %	Quartz %	Calcite %	Diameter (µm)
Footslopes				
-type 1 (Quartz dom.)	31	67	2	
-type 2 (gypsum dom.)	59	21	20	
-type 3 (Carb. dom.)	5	15	80	
Eolian sand				
-Gypiferous sand	75	25	0	300-420
-sand (sm. dunes)*	72	28	0	210-300
-sand (sheets)*	17	81	3	75-150
-quartz sand	6	92	2	75-150
Gypsum crust				
-dark	86	10	3	
-light	84	6	9	

*area consisting of small dunes and sandsheets

A large range of diagnostic absorption features important to geologic mapping exist in the shortwave infrared part (1.0 and 2.5 µm) (Goetz 1989). Most of these features are caused by overtones and combination of tones of OH⁻ and CO₃²⁻ ions, which are present in a range of minerals. Position and depth of absorption features are highly indicative for mineral type. Position, depth and width of the dips determine if these phenomena can be observed in broad bands like MMR 6-7. Most characteristic absorption bands in this area are related to gypsum and calcite.

Dominant minerals in the playa area are halite, gypsum and quartz. Halite occurs in thick crusts, in thin transparent layers and as halite salt cuboids. Directly after rainstorms halite occurs also in other forms, such as hexagonal shape, small needles and as lines on the surface. Halite content on the surface may differ strongly in time.

Secondary gypsum on the playa is found in evaporitic material in white non-transparent layers and in crystals of sizes from millimetres up to several centimetres. Apart from secondary gypsum this mineral can also be transported from outside the playa by water or wind. Locally remnants of dunes are present.

Other evaporitic salts than halite and gypsum are rare. In some parts hygroscopic salts like MgCl₂, present for instance in type D, and CaCl₂ or salts causing fluffy surfaces like Na₂SO₄ were observed. Calcite, quartz and clay minerals in the playas are mostly clastic. In table 2a and 2b the chemistry and results of X-ray analysis are given for the different surface types, surface sub-types and some particular phenomena on the surface for the dry season. In figure 2 gypsum, calcite and Na content are presented for the 6 surface types of the playa. The correlation between chemistry and surface type (roughness) is very clear: smooth surfaces with polygons if halite dominates, medium rough surfaces if gypsum dominates, and type F if carbonate dominates.

The footslopes show variation in mineralogy, presence of gypsum crusts, type and amount of sand cover, incisions by gullies and cover and size of stones. The top layers are often slightly sealed. A differentiation can be made in sealed surfaces dominated by quartz, gypsum, or calcite. In table 2c results of mineral countings of the toplayers are given. The calcite dominated areas are most rare in this area. They are old Cardium levels (Ongaro, 1986). One or more petrogypsic horizons are found on different depths in many profiles. Locally the

(degraded) crusts forms part of the surface. Two types of gypsum crusts with a difference in mineralogical composition has been observed in this area (Epema and Kroonenberg 1992). The dark coloured crusts have a lower calcite content than the lighter coloured crusts.

Eolian sand mainly consists out of mixtures of gypsum and quartz (table 2c). In areas with sand sheets covered with small gypsum dunes the mineralogy of the dunes is dominated by gypsum and the sand sheets by quartz. In general the gypsum sand is coarser than the quartz dominated sand. The top layer is often somewhat more coarse and rich of gypsum than the layer just below the surface. The eolian cover on the playa shows a comparable variation as the deposits on the footslopes.

Based on morphological differences the following surface types should be distinguished on the footslopes:

- eolian material
- footslopes with sealed crusts
- footslopes with gypsum crusts

A further subdivision of these surface types will be on mineralogical composition.

Organic matter

Organic matter content is another factor, which may affect both curve shape and intensity. Since it forms a coating on the surface of grains the effect is considerable above contents larger than 2% (Stoner and Baumgardner 1980). Soils with organic matter content below 2% (and iron oxide contents below 1 %) as often present in arid areas are considered by Stoner and Baumgardner (1980) as minimally altered soils. This implies that curve shapes will be comparable. The effect of organic matter will be in these areas mainly on total reflectance.

Moisture content

Moisture content of the top layer affects reflectance in two ways:

- due to internal reflections in the water layer covering the particles reflectance decreases in all MMR bands. This is attributed by Planet (1970) to internal reflections within the film of water covering the particles.
- specific absorption bands exists in the shortwave infrared part of the spectrum due to combination of tones and overtones of OH. The two most prominent absorption bands are centred at 1.45 μm and 1.95 μm (Goetz 1989). These bands are so broad that they affect the adjacent MMR bands 6-7 (Epema 1990a).

LABORATORY SPECTRA

In the laboratory spectra have been determined for different halite, gypsiferous, carbonate and quartz samples from the area for a range of grainsizes and mixtures. Also characteristic laboratory spectra were determined for almost pure samples of gypsum, carbonate and quartz. These have been derived from natural samples of the area, with high contents (>75%, based on mineral countings), by making use of the difference in specific gravity. We will discuss the results of the laboratory spectra with special emphasis to the pure samples, since these show the most distinct absorption features.

For this area from blue up to the near infrared only one sample showed a distinct absorption feature. As reported by Epema and Kroonenberg (1992) this feature for a specific iron-rich part of the mountain ridge is centred at 0.87 μm . All spectral curves show an increase in reflectance with increasing wavelength. This results from the strong absorption in the UV due to charge-transfer functions of iron. Halite and gypsum crusts, with a low iron content show a less strong increase in reflectance than the other samples. Besides iron the overall reflectance is determined by grain size. The spectra show a decrease in reflectance with increasing grain size for sizes above 100 μm . Reflectance factors of MMR 4 between grain size of 100 μm and 600 μm differ between 0.05 and 0.1. Gypsum crusts and crystals have a higher reflectance than gypsiferous sand up to a wavelength of 1 μm .

Above 1 μm many absorption features could be observed for the pure sand samples and the gypsum crusts derived from the area (figure 3). The sealed surface crusts of the footslopes show less prominent absorption features, but the location of the dips were however identical. Curves of playa samples show no prominent absorption features.

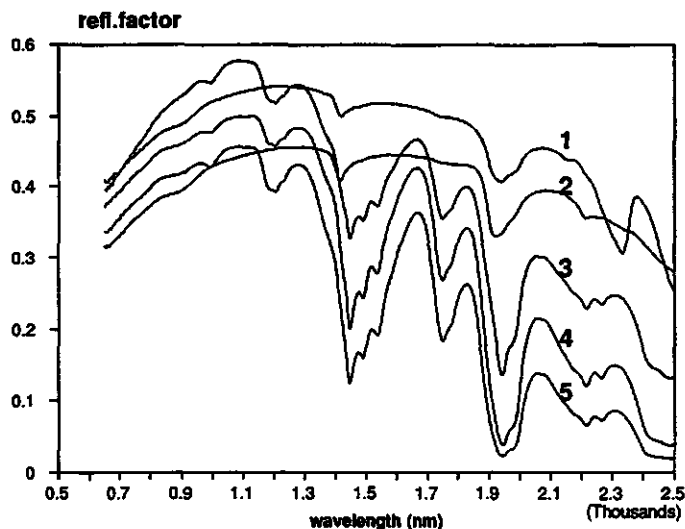


Figure 3 Spectral curves of laboratory spectra for carbonate (1), quartz (2), gypsum sand (3,4) and gypsum crust (5).

The following absorption dips bands have been found for gypsum: 0.990 μm , 1.100 μm , 1.205 μm , 1.445 μm , 1.495 μm , 1.535 μm , 1.750 μm , 1.945 μm , 2.215 μm , 2.265 μm , 2.485 μm . The features for gypsum are the result of OH and H₂O overtones and combinations of tones of the fundamental transitions of water. OH is an integral part of all gypsum minerals. From position, depth and width of the absorption features it can be predicted that all samples with gypsum will show a low MMR 6 and 7 field reflectance. The dip at 2.330 μm , highly indicative for CaCO₃, is caused by CO₃²⁻. Due to this dip it can be expected that MMR 7 field reflectance of carbonate dominated plots will be relatively low. Carbonate and quartz samples show absorption dips associated with OH, since these samples are not completely pure. Therefore it can be expected that also natural surfaces with a low gypsum or CaCO₃ content have a lower MMR 7 reflectance than MMR 6.

An attempt to relate reflectance in one specific band with the amount of quartz, carbonate or gypsum is hampered by the fact that also other effects, influence the level of reflectance. A way of minimizing the effect of other factors is the use of ratios of bands affected by the specific absorption to non-affected bands. Still the results of the ratios will not be straightforward if the denominator is affected by other specific absorption features. Also grainsize affects the depth of the absorption dips (Irons *et al.* 1989). If we resample the results of laboratory spectra to bandpasses of the MMR, band 7 as nominator and 4 as denominator are most useful. From the laboratory spectra we can predict the following representative ratios for MMR 7 / MMR 4 for quartz, carbonate and gypsum sand with a diameter of 150 μm : respectively 0.97, 0.82 and 0.34. With increasing grainsize the ratio for gypsum decreases to about 0.20 for a diameter of 600 μm . In figure 4 MMR 7 / MMR 4 ratio is given for mixtures of gypsum with quartz sand. For this example dominant grainsizes for this area have been selected: quartz sand between 75 and 150 μm and gypsum sand between 300 and 420 μm .

For crushed natural gypsum crusts the MMR 7 / MMR 4 ratio is between 0.5 and 0.4, while for the gypsum crystals this ratio is in between the sand and crusts. For gypsum crusts the absorption in MMR 6 is more pronounced than that in MMR 7. In this way gypsum crusts can be separated from gypsum/quartz or gypsum/carbonate mixtures of eolian sand. Carbonate sand has a MMR 7 / MMR 4 ratio and MMR 6 / MMR 4 ratio in between quartz and gypsiferous sand. Still carbonate sand can be discriminated from quartz-gypsum mixtures. At a given MMR 7 / MMR 4 ratio the MMR 7 / MMR 6 ratio is for carbonate somewhat higher than for the quartz and gypsum mixture, giving this MMR 7 / MMR 4 ratio.

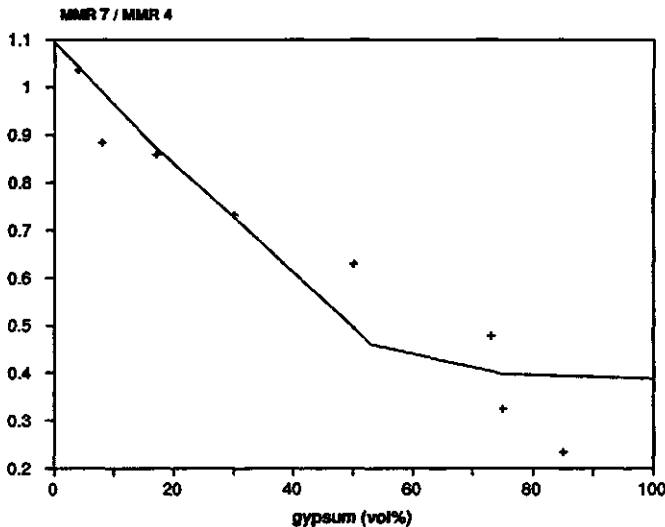


Figure 4 Ratio MMR 7/4 as a function of gypsum content for laboratory data (____), for a grainsize between 75 and 150 μm for quartz and between 300 and 420 μm for gypsum sand, in comparison with field observations (+).

MAJOR SPECTRAL DIFFERENCES IN THE FIELD

In order to examine the major spectral differences for bare soils in this area two standard statistical tests have been performed: linear regression analysis between bands and principal component analysis on the different bands. Low correlation coefficients point to differences in information content of the investigated bands. Principal component analysis shows the major direction of the variation. The first two or three factors for Landsat TM bands contain generally more than 90% of the variation present. In table 3 correlation coefficients are given for the whole data set of bare soils and subdivided in playas and non-playa areas. In table 4 results of principal component analysis are presented for the whole data set and the following subsets: (1) plots on the playa of November/December period (2) plots on the playa for the April period and (3) the non-playa plots (a combination of plots on footslopes and on sand dunes).

Table 3 *Correlation coefficients of regression analysis between MMR bands for all bare soils (n=1298), for playa units (n=811) and non-playa area (n=404).*

	1	2	3	4	5	6	7
1	-						
2	.928						
	.891						all
	.889						playa
							footslopes
3	.848	.969					
	.731	.912					
	.756	.945					
4	.801	.947	.983				
	.643	.870	.950				
	.664	.871	.956				
5	.651	.830	.894	.924			
	.369	.626	.767	.836			
	.303	.440	.506	.558			
6	.430	.607	.680	.709	.877		
	.196	.401	.527	.576	.901		
	.007	.057	.094	.119	.316		
7	.145	.245	.294	.312	.493	.786	
	.195	.392	.506	.543	.845	.962	
	.064	.027	.017	.013	.028	.573	

Table 4 Factor matrix based on principal component analysis for all observations, playa area in April, playa area in November/December and non playa area.

All							
	MMR1	MMR2	MMR3	MMR4	MMR6	MMR7	%explained variation
Factor 1	.98	.90	.79	.73	.29	.28	81.1%
Factor 2	.17	.37	.47	.51	.94	.94	15.9%
Factor 3	-.00	.19	.36	.46	.15	.09	2.2%
Factor 4	-.02	-.00	.16	-.03	.01	.02	0.4%
Factor 5	.00	-.00	-.00	.00	.10	-.09	0.3%
Factor 6	-.06	.11	.00	.01	.00	.01	0.2%

Playa April							
	MMR1	MMR2	MMR3	MMR4	MMR6	MMR7	%explained variation
Factor 1	.95	.98	.99	.96	.96	.96	94.1%
Factor 2	-.22	-.16	-.09	-.04	.25	.26	3.6%
Factor 3	.18	.03	-.10	-.21	.00	.11	1.7%
Factor 4	.06	-.08	-.01	.02	.06	-.05	0.3%
Factor 5	.02	-.06	.02	.03	-.06	.05	0.2%
Factor 6	.00	.01	-.04	.03	-.00	.00	0.1%

Playa Nov./Dec.							
	MMR1	MMR2	MMR3	MMR4	MMR6	MMR7	%explained variation
Factor 1	.90	.96	.96	.95	.55	.50	68.0%
Factor 2	-.33	-.25	-.17	-.18	.82	.85	27.3%
Factor 3	.28	.09	-.15	-.24	-.03	.09	3.0%
Factor 4	.01	.05	-.16	.10	.08	-.07	0.8%
Factor 5	-.04	.04	-.05	.06	-.11	.11	0.6%
Factor 6	.06	-.09	-.01	.04	-.01	.01	0.2%

Non-playa areas							
	MMR1	MMR2	MMR3	MMR4	MMR6	MMR7	%explained variation
Factor 1	.94	.99	.99	.97	.29	-.22	64.9%
Factor 2	-.16	-.02	.03	.07	.95	.96	31.0%
Factor 3	.32	.07	-.12	-.22	-.04	.11	3.1%
Factor 4	-.06	.07	.06	-.03	-.10	.09	0.5%
Factor 5	.03	-.04	-.04	.09	-.05	.05	0.3%
Factor 6	.02	-.06	.06	-.02	-.01	.01	0.1%

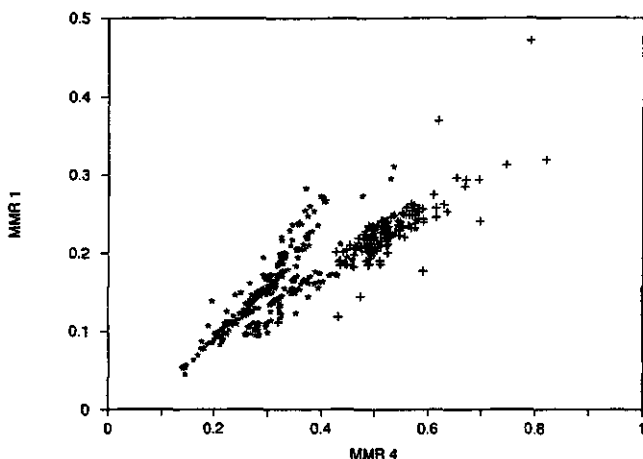


Figure 5a Scatter plot of MMR band 1 to MMR band 4 for playas(*) and non-playa areas(+)

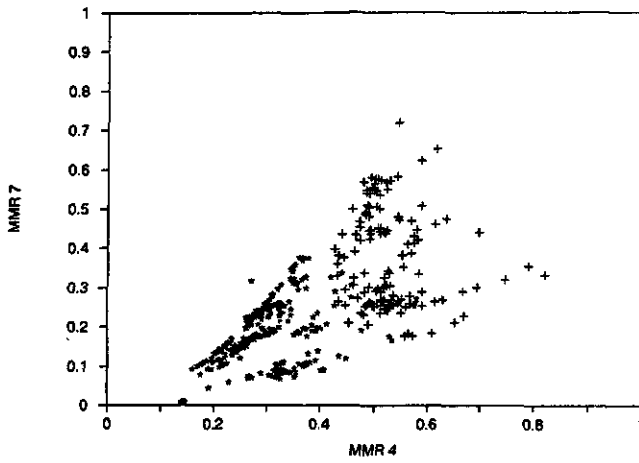


Figure 5b Scatter plot of MMR band 7 to MMR band 4 for playas(*) and non-playa areas(+)

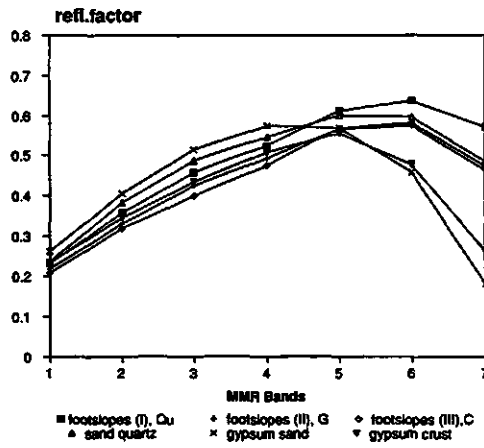


Figure 6a Representative spectral curves of non-playa areas

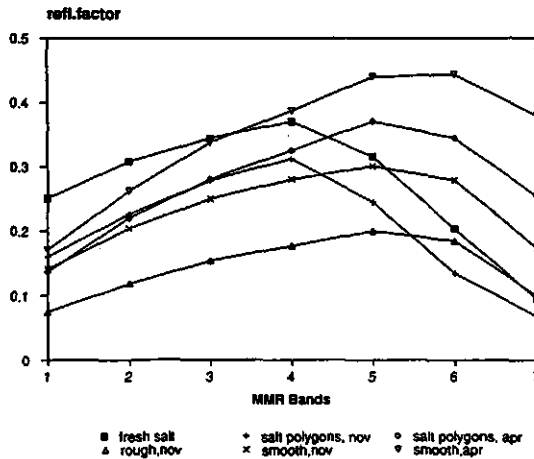


Figure 6b Representative spectral curves of playa area

In figure 5a and 5b two examples of scatter plots for band combinations with low correlation coefficients are given. In addition some examples of spectral curves are shown (figure 6a and 6b).

Three phenomena are prominent considering the first four bands:

- increase in reflectance for all curves from band 1 to 4,
- high correlations between the bands,
- deviations of specific samples from these high correlations.

The observed increase in reflectance from MMR band 1 to 4 is, as explained before, due to iron absorption in the UV (Goetz, 1989). This absorption has a wing extending into the visible part of the spectrum.

The high correlations between bands 1-4 are caused by:

- 1) external factors, like solar zenith angle and atmosphere, which affect these bands in a comparable way. For medium rough surfaces, dominant on the footslopes and sand dunes, noon reflectance in April (25°) is 10% higher than the reflectance with a solar zenith angle of 65° (the limit of our data set). The influence of solar zenith angle on smooth surfaces is even smaller (Epema 1990b). It appeared that spectral curve shape is not influenced significantly for solar zenith angles under consideration: between 25° and 65°. Epema (1992) showed that atmospheric conditions hardly influences field reflectance for these data sets.
- 2) some internal factors, which behave wavelength independent, like roughness, texture, different grain characteristics, presence of stones and even moisture content. Epema (1990a) showed that for the playa units the influence of moisture in bands 1 to 4 is very comparable. The absolute effect on reflectance is however considerable. Often a 10% lower reflectance is observed for the morning hours than in the afternoon.
- 3) other internal factors, which behave wavelength dependent, but for which factors differences in amount in this area are so small that curve shape is hardly affected. This holds for both organic matter content and iron of most soils. In this area organic matter content is generally low: between 0.4 and 1.2% on the footslopes and even less in the playas. For these low contents the influence on the spectral signature will be mainly on the intensity. Only small differences in iron content on the footslopes and playas in this area exist. Free iron ranges from almost 0 to 0.5% and Fe^{3+} up to 40 mmol/kg.

Solely plots with an iron content close to 0 deviate significantly from the regression lines between MMR bands 1-4. In this area the coverage of the surface with salt, especially halite, gives the largest deviations from the regression lines. Also gypsum crusts have a relatively high reflectance at shorter wavelength.

The reflectance above 1 μm will be determined by the same factors as described above. The low correlations of the higher bands with the first four are caused by two factors, which behave different in the two parts of the spectrum: mineralogy and moisture. Effects of roughness and external factors are comparable with MMR bands 1-4.

From the laboratory and field reflectance measurements and field observations and laboratory analyses it may be concluded that on footslopes and dunes differences in gypsum are the main cause for a low correlation between band 6 and 7 and the other bands. The effect of mineralogy is moreover dependent from the texture.

The decrease in reflectance as a function of increasing moisture content in MMR band 6 and 7 is more pronounced than in other MMR bands. The prominent absorption bands centred at 1.45 μm and 1.95 μm are so broad that they affect the adjacent MMR bands 6-7 (Epema 1990a). Lowest correlation coefficients were found in the November/December period in the playas, when moisture differences were considerable. Difference in moisture content in this region of the footslopes showed to be unimportant.

SPECTRAL DIFFERENCES IN THE PLAYA

General

The subdivision of the playa surface in 6 types, as given in figure 2, is primarily based on morphogenetic differences. These differences are visible in the morphology of the surfaces. Every type and sub-type has its specific mineralogic composition in the dry season and exhibits a specific variation in moisture and halite content in the wet season. From the above it can be concluded that moisture content and halite content are the main factors affecting spectral curve shape for the playas. Roughness variation is responsible for a variation in level of reflectance. It is unclear if the variation in gypsum and carbonate content is such that it can be derived from the signal.

In this section we will test by examining the feature space of both seasons to what extent it is possible to differentiate surface types and sub-types and if also direct relations with mineralogy exist.

The data set of the wet season consists of plots of type A, B, C and D, measured once or during a whole day. The data set of April was expanded with plots in the seepage zone (type E) and the western border zone of Chott Djerid (type F). The number of measurements on plots has no direct relation with the size of the area. They may be representative for a long period, as for the data of April, or only for one or two days as some plots in the wet period. The differentiated clusters are presented in feature space plots of 1-4 and 7-4 (figures 7a-7d)

A first examination of the feature space plots of both seasons reveal the following:

- spectral variation in the dry season is small
- reflectance in MMR 7 in the wet season was less than in the dry season
- range of values in MMR 1 of wet season is higher than for dry season
- values of MMR 1 for a specific MMR 4 value are in general higher in the wet season.

Differences between the seasons can be explained by higher halite and moisture contents in the wet season.

November/December period

In the November/December period 10 clusters were discriminated based on their reflectance spectrum (figures 7a-7b). These clusters can be explained with a combination of surface type (roughness), halite content and moisture condition (table 5a). Within the clusters the variation is determined by (small) differences in halite salt, other mineralogical differences, roughness, presence of cuboids for type A and B and moisture content.

Table 5a Explanation of clusters for the playa area for November/ December.

cluster nr.	surface halite type	moisture cont.	remarks
1	D	5	
2	B	5	
3	A	2	
4	B	5	
5	A	1	
6	D	2	polygon fringe
7	B	1	
8	D	4	
9	A,B,C	2,3	
10	A	2	

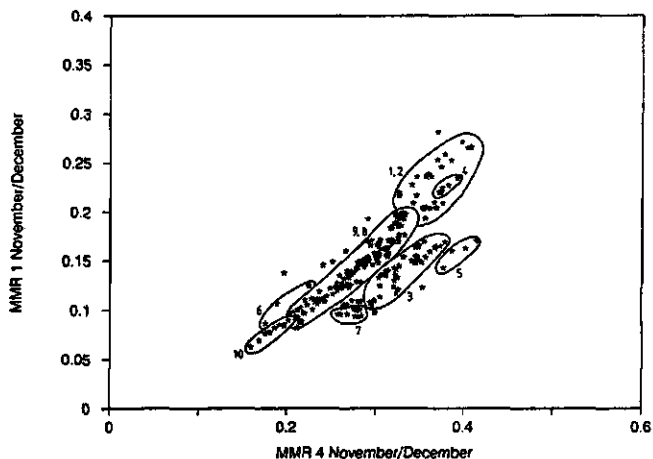


Figure 7a Scatter plot of MMR band 1 to MMR band 4 for playa area in November/December

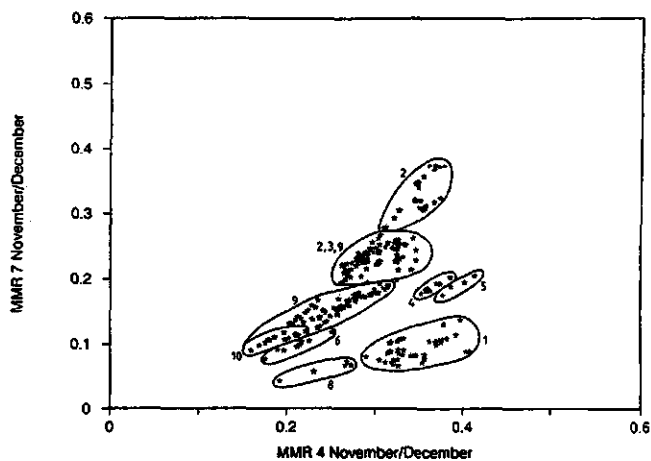


Figure 7b Scatter plot of MMR band 7 to MMR band 4 for playa area in November/December

Table 5b *Explanation of clusters for the playa area for April.*

cluster nr.	surface type	halite cont.	moisture cont.	remarks
11	E	2	2	
12	B	2	2	
13	B	1	1	most smooth part
14	C	1	1	
15	A,B,D,F	1	1	

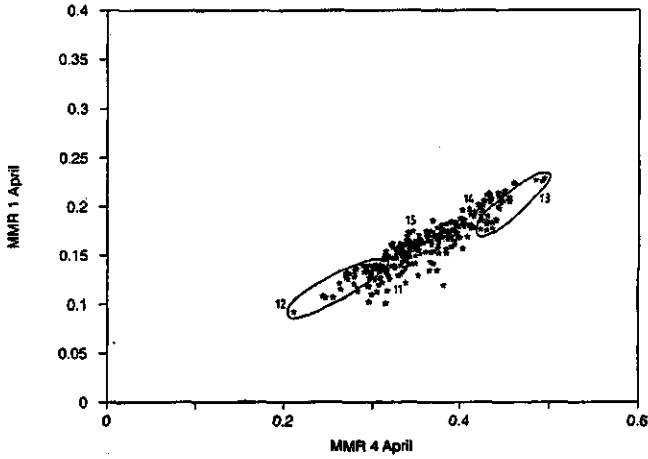


Figure 7c *Scatter plot of MMR band 4 to MMR band 1 for playa area in April*

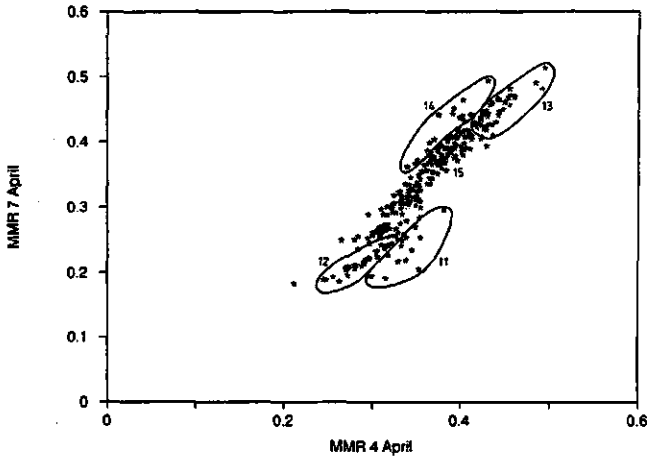


Figure 7d *Scatter plot of MMR band 4 to MMR band 1 for playa area in April*

A further clustering to types and subtypes of A, B and C seems difficult since differences between plots are gradual and measurements are made on different days. Differences in moisture content depend on the combined effect of number of days after the storm and specific behaviour of type and subtype. It is interesting to test if, when we single out one day, as for instance Landsat TM performs, surface types have a different position in the feature space. For this aim we measured in an area on Chott Fedjaj 14 plots of types A, B and C on one single day over an area of 1 by 0.1 kilometre. The gravimetric moisture content of the top layer varies over this transect for type B between 18 and 25% and for type A of cluster 3 and C between 11 and 15 %. All reflectance values fall in clusters 3, 9 and 10. The following was observed:

- Two plots of type A form part of cluster 10. The high moisture content of these rough plots can be observed by the eye already.
- Five plots of type A span the whole variation in cluster 3.
- Seven plots of type B and C, all with a thin halite salt layer, are part of cluster 9. Reflectance of type C is less than type B, despite the lower moisture content. For type B plots with polygon fringes have a somewhat lower 4 to 1 ratio and a somewhat higher 7 to 4 ratio.

Measurement on a single day provides at least for this part of Chott Fedjaj the possibility to discriminate between type B and C. It is interesting to note that roughness overrules moisture or halite differences for this area. Only from the 7/4 ratio the higher moisture content of type B can be detected.

No extensive chemical analyses have been performed during the November/December period. Halite contents are so high that chemical analyses and X-ray analysis will be inaccurate. The amount of white or almost white surfaces is a more accurate indication of halite differences. Linear combination of the estimated components halite and non-halite suffice in explaining reflectance differences within subgroups. Implicitly in these relations are moisture differences between halite and non-halite. Epema (1990a) found for specific plots in this area linear relations between moisture content and reflectance, with the largest effect in band 6 and 7. It is unlikely that other relations are found between reflectance and other factors than moisture and halite content.

April period

In the April period differences in spectral signature are limited. The variation in moisture content and halite salt efflorescence during the second measurement campaign was small for all locations. The moisture content in the playa area varies in general between 5 and 12%. Only two areas have a somewhat higher moisture content:

- the aioun zone with type E surface types, where periodically water from the subsurface origins,
- a few parts directly along the road due to occasional flooding out of the ditch along the road crossing Chott Djerid.

Apart from these 2 groups (respectively 11 and 12 in table 5b) only 2 more groups could be explained which do not belong to the major group.

Most remarkable is that type E, one of the two extra groups examined in the dry period, has a specific location in the feature space. The other new surface type F has no distinctive different spectral pattern. Within the major group a further clustering is difficult due to gradual differences between plots and the range of factors affecting reflectance. Variation

between plots are due to amount and type of halite salt cuboids, small salt crystals, moisture differences, dust on the surface, small ridges and low polygonal structures in type B, and relative quantity of type A versus type B.

If we consider again the same area on Chott Fedjaj with an extension of 1 by 0.1 kilometre and plots of types A, B and C in this season 3 distinct clusters appear. Type C plots are a part of cluster 14. Type B and A are part of cluster 15, but in this area all type B plots have a higher reflectance than type A plots. This indicates that there might be a possibility to cluster plots within the rest group 15.

The higher reflectance of type B in comparison with type A (moisture content respectively 5% instead of 3%) indicates that difference in roughness is sometimes more important than difference in moisture content.

Linear regression analysis has been performed for the April data set, consisting of all surface types, between reflectance indices and mineralogy. Reflectance values of single bands, PC factors and band ratios were tested. Most correlation coefficients were not significant ($\alpha=0.01$). Only significant ($\alpha=0.01$) relations were found with chemical analysis related to gypsum (Ca^{2+} , H_2O and SO_4^{2-}) for band 6 and 7 and ratios with 6 and 7 over band 1 to 4 and PC factors stressing difference between bands 6 and 7 and the other bands. The main cause that the spectral variation in the playa due to gypsum is less than on the footslopes, is due to the fact that gypsum contents never exceed 20%. Relations with other factors like halite are not significant for the whole data set due to the many other factors affecting reflectance.

For parts of the data set significant linear relations ($\alpha=0.01$) were found. For instance, significant linear relations ($\alpha=0.01$) have been found for type B surfaces between area covered with salt cuboids and reflectance in band 2 to 4.

Reflectance of plots consisting of different surface types, or different elements from one surface type can be calculated from a linear combination of the components.

SPECTRAL DIFFERENCES ON THE FOOTSLOPES

General

Surface materials of the footslopes and eolian deposits consist predominantly of gypsum, carbonate and quartz with minor other siliceous minerals (table 2c). Occurrence of these minerals and influence on spectral signature of the minerals varies considerably in this area (Epema and Kroonenberg 1992). It will be examined to what extent it is possible to explain the position in the feature space in relation to presence of gypsum, quartz and carbonate content and to dominant surface type. From figure 5a and 5b characteristic scattering of non-playa area can be seen. In addition a scatter plot of $\text{MMR } 7 / \text{MMR } 6$ to $\text{MMR } 7 / \text{MMR } 4$ is given (figure 8). Both ratios give a higher value with increasing quartz content. Use of the second ratio has been discussed before in 4.3.1. The first ratio will give additional information, when carbonate is present in the samples.

Field signatures will be treated in the following surface types:

- eolian material
- footslopes with sealed crusts
- footslopes with gypsum crusts

Hereafter differences between these groups will be examined.

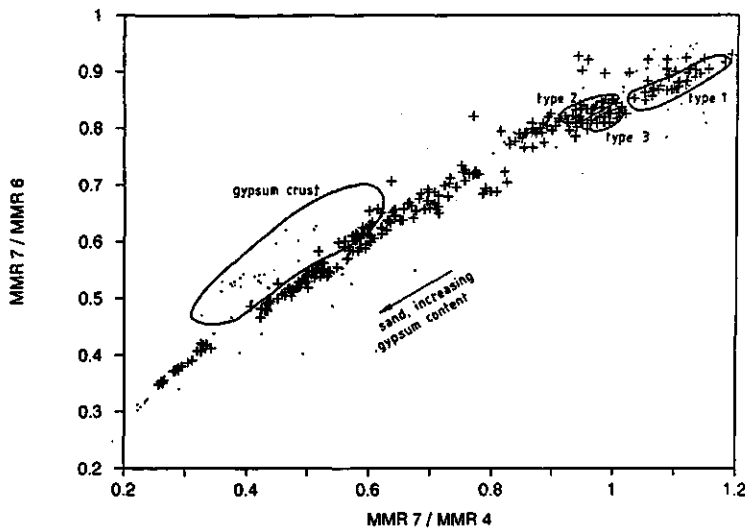


Figure 8 Scatter plot of MMR band ratio 716 to MMR band ratio 714 for non-playa area

Eolian material

Quartz and gypsum are the dominant minerals of the eolian material. Carbonate content is mostly less than 5%. Therefore an estimation of gypsum content from the signal should be based on a model for mixing quartz and gypsum. In figure 4 MMR 7 / MMR 4 values of field measurements are given as a function of gypsum content in combination with the relation I found for laboratory spectra of a mixture of quartz and gypsum sand of the dominant grainsizes in this area. The dominant grainsizes, used in the laboratory experiment, are for quartz between 75 and 150 μm and for gypsum sand between 300 and 420 μm . Scattering around the regression line of the field samples are mainly caused by deviations from these dominant grainsizes. If grainsize is not known inversion of this regression model may cause wrong estimation of gypsum content. Since carbonate content is low MMR 7 / MMR 6 values are strongly related to MMR 7 / MMR 4 values (figure 8)

Footslopes with gypsum crusts

Gypsum crusts have like gypsiferous sand a low MMR 7 / MMR 4 and MMR 6 / MMR 4 ratio. Epema and Kroonenberg (1992) reported that two types of gypsum crusts exist, with different carbonate content (9% and 3%). The former has a higher MMR 7 / MMR 4 ratio than the latter. Typically for gypsum crust is the extra low MMR 6 reflectance and the relatively low MMR 4 / MMR 1 ratio, due to low iron content. The coverage of surfaces with degraded gypsum crust occasionally exceeds 50%. In general the area in between the gypsum crusts are dominated by temporarily sealed gypsiferous sand.

Footslopes with sealed crusts

Three types of footslopes can be discriminated in this area by examining the dominant minerals quartz, gypsum and calcite. Results of countings of grain mounts of 3 typical footslope samples were presented in table 2c.

A first examination of the spectral curves reveals the remarkable high MMR 7 and MMR 6 values for this gypsum and carbonate content. Most probably this is due to the high quartz component and small grain size of the sealing crust, which is too thin to sample. Despite the minor influence of absorption, it is still possible to cluster the 3 surface types dominated by quartz (type 1), gypsum (type 2) and carbonate (type 3) (figure 8). Type 1 and 2 sealed surfaces can be discriminated, since for type 1 both MMR 7 / MMR 4 and MMR 7 / MMR 6 ratios are higher. This was valid for all selected plots (9) and for all solar zenith angles (nr. of measurements 150). The surface dominated by calcite (type 3) can be discriminated from type 2 by its slightly lower MMR 7 / MMR 6 ratio. This illustrates the presence of carbonate, which causes a larger decrease in band 7 than in band 6.

Coverage with stones occurs for all 3 surface types. Most dominant are calcite and dolomitic rich stones, which cover occasionally more than about 20% of the surface. The effect on spectral curve shape is still limited, since in general the stones are dust-covered and hence reflectance is comparable with the sealed surfaces. Due to an increase in shadow, an effect on overall reflectance exist. For stones covering type 2, for instance, negative relations are found between size and reflectance.

Discrimination between eolian sand, footslopes and gypsum crust

From figure 8 it appears that a spectral discrimination between footslopes and gypsum crusts, between gypsiferous eolian sand and footslopes and between eolian quartz sand and gypsum crusts is possible. Problems arise by separating spectrally footslopes from quartz dominated sands and gypsum crust from gypsiferous sand.

Footslope type 2 is most difficult to separate in a spectral way from quartz-rich eolian sand, since it has comparable 7/4 and 7/6 ratio. Both footslope types 1 and 3, dominated by carbonate and quartz have a relatively low 7 to 6 ratio in comparison with mixtures of sand and gypsum. For our sample set it turned out that with the aid of the MMR 4 / MMR 1 ratio footslopes of type 2 can be discriminated from eolian sand. It is unlikely however that this ratio can be used for the whole area as discriminating criteria. Spectral misclassifications between sand and footslopes will occur.

Both types of gypsum crusts can be differentiated from gypsiferous sand, having a relatively extra low MMR 6 reflectance. For a specific MMR 7 / MMR 4 ratio the MMR 7 / MMR 6 ratio is higher as can be concluded both from laboratory and field measurements. Moreover the MMR 4 / MMR 1 ratio of the crusts is lower than that of plots dominated by gypsiferous sand.

MULTITEMPORAL CHANGES

In order to compare influence of changes of the surface in time on spectral reflectance the effect of external factors, like solar zenith angle, solar azimuth and atmosphere, should be minor. The influence has been discussed in previous articles (Epema 1990b, 1991, 1992). For surfaces with a random orientation of roughness elements the effect of solar azimuth angle will be minor. So for most playa plots a multitemporal analysis can be performed by comparing field reflectance measurements of different times of the day with the same solar zenith angle. For surfaces with a specific orientation as for instance sand ripples or surfaces with changing forms as some dunes or plots on a sloping angle no direct comparison is possible. In figure 9a-9c both footslopes and playa reflectance with as much as possible the same solar zenith angles is given. In addition to the line of no change lines with a 10% deviation are given, which is about the accuracy of reflectance measurements.

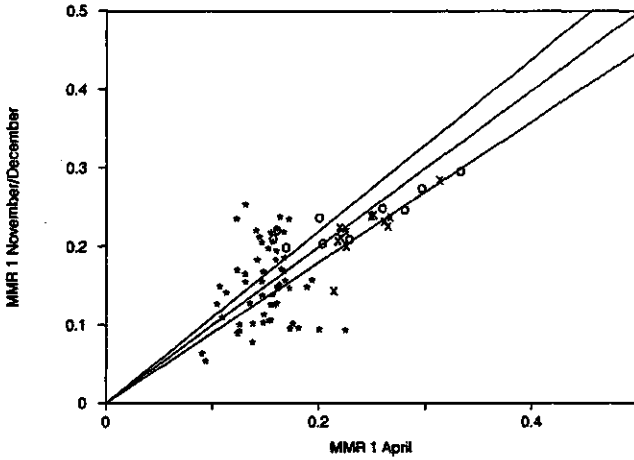


Figure 9a Comparison November/December and April reflectance in MMR 1 (lines of no change and less than 10% change)

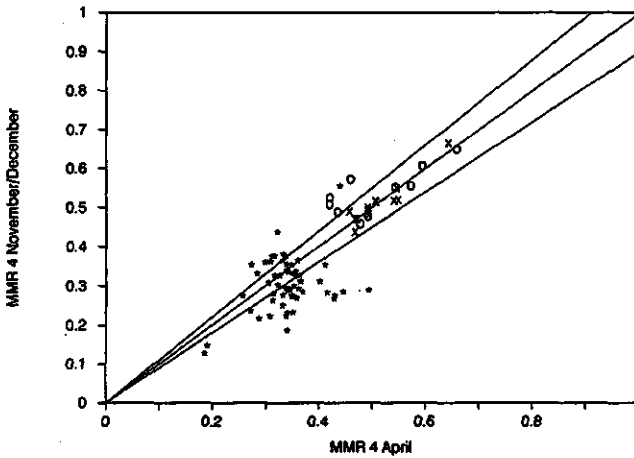


Figure 9b Comparison November/December and April reflectance in MMR 4 (lines of no change and less than 10% change)

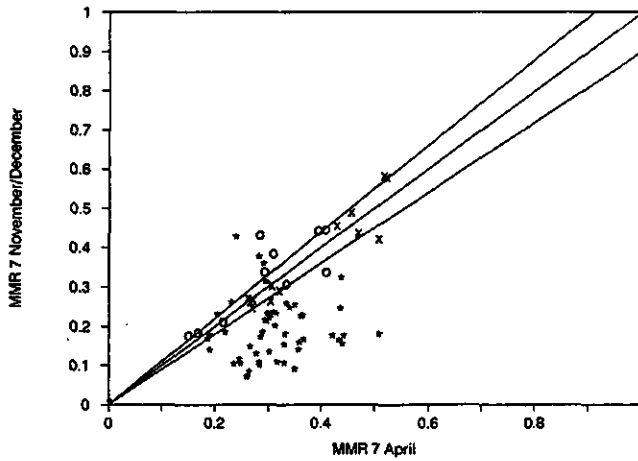


Figure 9c Comparison November/December and April reflectance in MMR 7 (lines of no change and less than 10% change).

For the non-playa units differences are small. Only for the sand dune area more than 10% difference in reflectance has been found. In these areas both orientation of ripples and shape of sand dunes may change. In one unit the reflectance in band 7 was higher for the November/December period. This is caused by the sealing of the surface in that period, which gives less absorption due to gypsum.

As expected considerable differences are found between reflectance in November/December and April for the playa plots. The influence of moisture can be detected from MMR 7 reflectance. The only plots with a higher reflectance in November/December are two type A plots in a small oval area within type B. This high reflectance is caused by an almost equal moisture content of the very top layer and less roughness in the November/December period. The influence of salt, counteracting the effect of moisture can be seen most clearly in band 1. The lowest reflectance in all bands has been found for the wet area in zone dominated by deposition directly after the storm but before salt efflorescence.

A very clear impression of the salt and moisture influence on reflectance in time is given in figure 10 (after Epema 1990a). This example presents reflectance for a smooth plot from directly after the storm over the November/December period and for April.

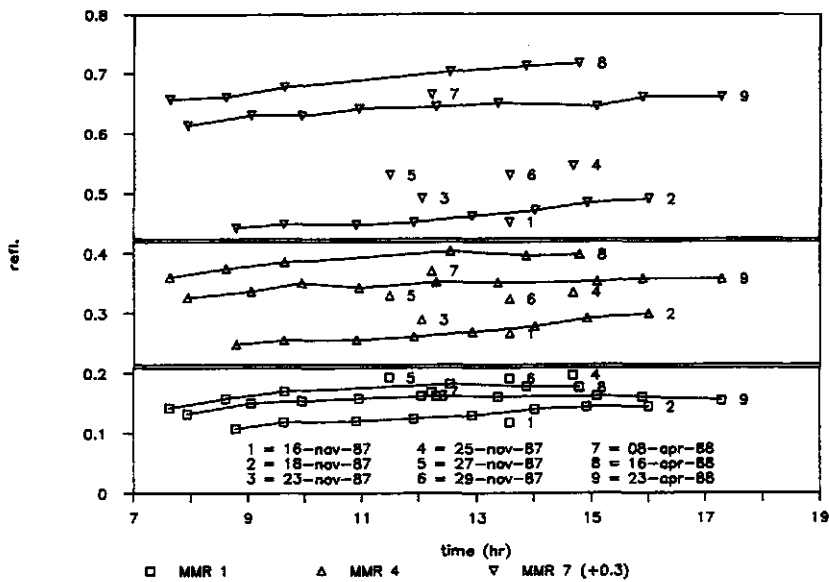


Figure 10 Reflectance factors of a smooth part of type B plot in both measuring campaigns (MMR 7 reflectance factor +0.3). One data point refers to one measurement. On days 2, 8 and 9 throughout-the-day measurements have been made, for the other days only single measurements are available.

CONCLUSIONS

Surface characteristics may affect reflectance in specific bands, in some bands more than in other bands or in all bands analogous. Evidence of all these effects were found for the MMR data:

- gypsum affects the reflectance in MMR 6 and 7, by having a range of characteristic absorption dips due to OH⁻. Carbonate decreases reflectance in MMR 7 since CO₃²⁻ has a dip at 2.33 μm. Iron affects MMR bands 1 to 4 or occasionally specific band 4 due to electronic effects.
- Moisture content affects reflectance in MMR 6 and 7 more than the other bands. In these bands absorption of OH adds to the effect of internal reflection within the water film covering the particles.
- Roughness, texture, transparency and coverage with stones have mainly an effect on all bands.

It was also found that absorption of gypsum and carbonate depends on texture of the surface material. Differences in iron content are so small that spectral curve shape in MMR bands 1-4 are in general comparable. Only in 2 cases this shape deviates significantly from the average: with coverage of halite salt and gypsum crust when iron content is close to 0.

Based on surface characteristics one could make a discrimination in 4 groups: playa areas, footslopes, sand on playas and sand on footslopes. Based on spectral characteristics it was better to discriminate playa areas without sand cover from the other groups. In the former group differences in moisture and salt content give a strong spectral variation both in space and time. The moisture content of the very top layer of footslopes and sand covered sections exceeds only for a few days 2%, while salt efflorescence of halite occurs only occasionally outside the playas without sand cover. The non playa area can be analyzed in 3 groups: (1)

colian material, (2) footslopes with sealed crusts and (3) footslopes with gypsum crusts. In the following scheme an overview is given on the best treatment of the spectral data including explanations of spectral differences. This scheme is the basis for the rest of the section.

possible explanations

playa	wet season	one day	multitemporal
	10 clusters based on moisture and halite discrimination type D and some subtypes	type C from type A and B	
	dry season	one day	more types and subtypes
	type E, type C, more moist parts	type C from type B	
non playa	collan dep.	relation with gypsum content if grainsize is known	
	sealed surfaces	3 groups:	dominated by gypsum dominated by quartz dominated by carbonate
	gypsum crusts	2 groups:	dark colour light colour

Based on our data set the best possibility for a spectral discrimination between playa area and non-playa is by using in the wet season a reflectance factor of 0.42 in MMR 4. Another approach may be by using a difference in reflectance between the wet and dry season. However in that case also some dune plots will be classified as playa.

For the field data of the wet season it is possible for the playa area to spectrally explain 10 clusters. Although differences are mainly caused by influence of halite salt and moisture, surface type D and different surface sub-types of A and B could be indicated due to their specific response to these factors and since also roughness plays a role. If measurements are restricted to one day, it is possible to discriminate spectrally type C as well. Some of the clusters have been formed since measurements have been done on different days after the storm.

In the dry season correlations between bands are much higher than for the wet season. Still it is possible to discriminate plots of the aioun zone (type E), plots of type C, and some wet variants of type B. Within the rest group differences in reflectance are due to a range of factors. Remarkable is that smooth plots of type A reflect more than rough plots of type B, despite the somewhat higher moisture content of the smooth plots. Significant linear relations ($\alpha=0.01$) have been found between reflectance and analyses related with gypsum content. Relations with other factors as halite were not significant in this period.

The surface material of the non-playa areas consists predominantly of gypsum, carbonate and quartz. Moisture content and organic matter content are generally low and hence produce no significant different curves. The same holds for iron content with the exception of surfaces with gypsum crusts which have a very low iron content and hence a somewhat lower 4/1 ratio than the other plots. It is most useful to treat field signatures in the following groups: (1) eolian material, (2) footslopes with sealed crusts (3) footslopes with gypsum crusts.

(1) Due to relatively low amount of carbonate, amounts of gypsum and quartz are important in determining reflectance for eolian material. Non-linear relations were found between MMR 7 /MMR 4 ratio and gypsum content for laboratory conditions, which can also be applied to the field data. A problem remains that the relations are grainsize dependent.

(2) For the plots on the footslopes 3 types of sealed surfaces can be discriminated based on spectral signature: those dominated by gypsum, quartz and carbonate. Remarkable are the high values in band 6 and 7 for both gypsum and quartz dominated footslopes.

(3) Gypsum crusts have low reflectance in band 6 and 7. For pure plots they can be discriminated from gypsiferous sand due to extra low reflectance in band 6.

These 3 groups could be discriminated spectrally from each other for our data set. The spectral difference between gypsum dominated footslopes and eolian quartz-rich sand with some gypsum is small.

Other factors than mineralogy play also a role in determining reflectance, like roughness, texture, stone coverage and slope. Since those factors do not specifically affect one or more bands, it is impossible to retrieve unambiguously those factors from the spectral data. For one surface type or one specific part of the area statistical significant relations can be found. I found for instance linear relations between stone coverage and reflectance for footslopes dominated by gypsum.

Reflectance of vegetation in these areas does only show occasionally the well-known high reflectance in the near infrared. Presence of many dead parts, small leaves and often occurring dust cover gives also in MMR 4 less reflectance than most bare soils. The rapid change in vegetation aspect and coverage after rainstorms cannot be neglected always.

DISCUSSION ON RETRIEVING INFORMATION FROM SPECTRAL CHARACTERISTICS

From the above it appears that reflectance spectra can be explained with a range of factors. The reverse, retrieving characteristics from the signal, will be the subject of a following paper. It can already be concluded that it is not unambiguously possible. Problems will occur for factors which affect all bands equally and especially if different factors act together or counteract each other. A subdivision in plots in groups playa, footslopes and sand covered areas, or subgroups will be a prerequisite for adequate interpretation of the signal. These subdivisions can probably be done largely based on spectral signal itself. After subdivisions it has to be tested which surface characteristics can be inferred from the signal directly or indirectly. The following characteristics can probably derived quantitatively or qualitatively: gypsum, carbonate, quartz content or presence on sand and footslopes respectively, and halite, moisture content and surface type describing roughness and dominant mineralogy on the playas. A multitemporal approach enhances both the subdivisions in playa and non-playa and the subdivisions in sub-groups and surface types and characteristics for the playa.

If we want to infer the possibilities of TM for mapping surface characteristics from the signal we cannot simply extrapolate the results of the field measurements. The following differences exist:

- 1) field reflectance data cannot be compared directly with reflectance data inferred from TM digital numbers.
- 2) ground resolution elements will consist of different surface types or surface sub-types.
- 3) data are present for the whole area on a limited numbers of days on one time of these days.

The first point is for a large part solved in former publications (Epema 1990b,c, 1991a, 1992).

Under the assumption that reflectance for a pixel is determined by a weighted average of surface elements, two approaches can be followed for the second point. A specific signal for a pixel has to be attributed to a specific cluster or an estimate can be made on the percentage belonging to specific clusters by linear mixture modelling. A complication occurs for vegetation, which is mostly present in clumps. The shadowing effect prevents a weighted average between vegetation and surface type. An extra problem arises in the case of sand surfaces, where a non linear relation was found for the field data between reflectance and percentage of gypsum. Estimates with TM with this relation will produce errors if the ground observation elements consists of a mixture of domains with different gypsum contents, as for instance in areas with sandsheets and small sand dunes.

The last point has as disadvantage that less information is present for the different surface types on response in time to drying out of the surface in comparison with the field data. An advantage however is that a simultaneous signal is achieved for all locations. Field data of the wet season showed possibilities to indicate surface types in the wet season on the playas.

ACKNOWLEDGEMENTS

This research is part of a project funded by the Netherlands remote sensing board (BCRS, AO 4.2). I wish to thank Prof.Dr. F.K.List and Dr. A. Richter (FU Berlin) for use of the Barnes MMR, and discussions, and Prof. Dr. S.B. Kroonenberg (AUW), and Prof. Dr. M.Molenaar (AUW) for their critical comments to this paper.

REFERENCES

- Begheijn, L.Th., 1976. Determination of organic and inorganic carbon in soils by potentiometry. *Analyst* 101: 710-716.
- Biggar, S.F., Labeled, J., Santer, R.P., Slater, P.N., Jackson, R.D. and Moran, M.S., 1988. Laboratory calibration of field reflectance panels. *SPIE, Vol 924 Recent advances in sensors, radiometry, and data processing for remote sensing*, 232-240.
- Coque, R., 1969. *La Tunisie Pre-Saharienne: Etude Geomorphologique*. Armand Colin, Paris.
- Coque, R. and Jauzein, A., 1967. The geomorphology and Quaternary geology of Tunisia.. In: Martin, L.(ed.) *Guidebook to the Geology and History of Tunisia*. society of Lybian Petroleum Geologists, Handbook 3, 227-257.

- Desmet A., Eerens H. and Gombeer R., 1988. Influence of some soil factors on the reflectance of bare soils. *Pedologie*, XXXVIII-3, 227-247.
- Epema, G.F., Van Dijk, H., Elzinga, E. and Van den Hoek, A.I., 1985. Soil and vegetation mapping with the aid of Landsat Thematic Mapper Images near Kebili (Tunisia), Agricultural University of Wageningen, department of Soil Science and geology.
- Epema, G.F., 1990a. Effect of moisture content on spectral reflectance in a playa area in southern Tunisia. *Proceedings international symposium, Remote Sensing and Water Resources, Enschede, August 20-24 1990: 301-308, Lingen.*
- Epema, G.F., 1990b. Diurnal trends in reflectance of bare soil surfaces in southern Tunisia. *Geocarto International Vol.5, No.4 33-39.*
- Epema, G.F., 1990c. Determination of planetary reflectance for Landsat 5 Thematic Mapper tapes processed by Earthnet (ITALY). *ESA Journal, 14, 101-108.*
- Epema, G.F., 1991. Studies of errors in field measurements of the bidirectional reflectance factor. *Remote Sensing of Environment 35, 37-49.*
- Epema, G.F., 1992. Atmospheric condition and its influence on reflectance on bare soil surfaces in Southern Tunisia. *International Journal of Remote Sensing. International Journal of Remote Sensing Vol.13, No.5: 853.*
- Epema, G.F. and Kroonenberg, S.B., 1992. Ground reflectance of natural bare and pure surfaces as an aid in interpretation of Landsat Thematic Mapper data in Southern Tunisia. *Advanced Space Research Vol.12, No.7: (7)39-(7)42.*
- Floret Ch. and Pontanier R., 1982. *l'Aridite en Tunisie Presaharienne. Travaux et documents de l'ORSTOM no. 150, Paris 544p.*
- Goetz, A.F.H., 1989. Spectral Remote Sensing in Geology. In: G. Asrar, *Theory and Applications of optical remote sensing*, John Wiley and sons, 491-526.
- Hesse, P.R., 1971. *A textbook of soil chemical analysis*, John Murray, London.
- Irons, J.R., R.A. Weismiller & G.W. Petersen, 1989. Soil Reflectance. In: G. Asrar, *Theory and Applications of optical remote sensing*, John Wiley and sons, 66-106.
- Jackson, R.D. and Slater, P.N., 1986. Absolute calibration of field reflectance radiometers. *Photogrammetric Engineering and Remote Sensing Vol. 52, No 2, 189-196.*
- Jones A.R. and Millington A., 1986. Spring mound and aioun mapping from Landsat TM Imagery in south-central Tunisia. *Symposium on Remote sensing for Resources Development and Environmental Management, Enschede, 607-613.*
- Meckelein, W., 1977. Zur Geomorphologie des chott Djerid. *Stuttgarter geographische Studien 91: 247-301.*
- Millington, A.C., Jones, A.R., Quarmby, N., Townshend, J.R.G., 1987. Remote sensing of sediment transfer processes in playa basins. In: Frostick, L. & Reid, I. (eds), 1987, *Desert sediments: Ancient and Modern*, Geological Society Special Publication No.35, 369-381.
- Mitchell, C.W., 1983. The soils of the Sahara with special reference to the Maghreb, *Maghreb Review 8: 29-37.*
- Markham, B.L. and Barker, J.L., 1986. Landsat MSS and TM post-calibration dynamic ranges, exoatmospheric reflectances and at-satellite temperatures, *EOSAT Landsat Technical Notes (EOSAT, 4300 Forbes Blvd, Lanham, MD 20706) No. 1.*
- Mulders, M.A., 1987. Remote sensing in soil science. *Developments in soil science 15, Elsevier, Amsterdam-Oxford-New York-Tokyo.*
- Ongaro, L., 1986. Studio integrato delle risorse naturali del Nefzaoua (Tunisia): carte delle unita di terre dell'area Kebili-Douz. *Rivista di agricoltura Subtropicale e Tropicale, Trimestrale LXXX-n.2 Aprile-Giugno 1986, 165-310.*

- Planet, W.G., 1970. Some comments on reflectance measurements of wet soils. *Remote Sensing of Environment*, 1: 127-129.
- Roberts, C. and Mitchell, C.W. 1987. Spring mounds in southern Tunisia in Desert sediments: Ancient and Modern, L Frohstick and J. Reid, Eds Blackwell, U.K.: geological Society London, Spec. Publication no 35, 321-336.
- Robinson, B.F., Bauer, M.E., DeWitt, D.P., Silva, L.F. and Vanderbilt, V.C., 1979. Multiband radiometer for field research. *Journal of the Society of Photo-optical Instrumentation Engineers*, 196:8-15.
- Stoner, E.R., Baumgardner, M.F., Biehl L.L., and Robinson, B.F., 1980. Atlas of Soil Reflectance Properties. Purdue University, West Lafayette, Indiana.
- Townshend, J.R.G., Quarmby, N.A., Millington, A.C., Drake, N.A., Reading A. J., White, K.H., 1989. Monitoring playa sediment transport systems using Thematic mapper data, *Advanced Space Research*: Vol. 9, No.1, (1)177-(1)183.
- Vieillefon, J. 1979. Contribution to the improvement of analysis of gypsiferous soils, *Cahiers/ORSTOM, Serie pedologie* 17: 195-223.
- White, K. H., 1990. Spectral Reflectance Characteristics of Rock Varnish in Arid Areas. School of Geography, University of Oxford, Research Paper 46.

CHAPTER 8

DETERMINATION OF PLANETARY REFLECTANCE FOR LANDSAT 5 THEMATIC MAPPER TAPES PROCESSED BY EARTHNET (ITALY).

ESA Journal, Vol. 14: 101-108.

G.F. Epema

*Agricultural University of Wageningen, Dept. of Soil Science and Geology, Wageningen,
The Netherlands*

Determination of Planetary Reflectance for Landsat-5 Thematic-Mapper Tapes Processed by Earthnet (Italy)

Abstract A method is described by which Landsat Thematic-Mapper (TM) data from tapes that have been radiometrically corrected based on pre-flight data by Earthnet (Italy) can be converted for use in the determination of planetary reflectance. It is shown that, depending on the TM band concerned, a correct gain factor gives a 1 to 20% higher estimation of planetary reflectance (at the satellite) than use of the original data on these tapes. In addition, correct use of bandwidths gives a 4 to 14% higher planetary reflectance value.

1. Introduction

Processing of Landsat Thematic-Mapper (TM) tapes by EOSAT has been extensively described in recent publications¹⁻³. These have shown both the possibilities and limitations of determining planetary reflectance with calculations using quantised radiance values (Q_{cal}) from the radiometric calibrated tapes. At ESA's Earthnet facility in Fucino, Italy, most standard tapes are calibrated based only on pre-flight data and not with the aid of the internal calibration source or ground measurements during the flight. A method is therefore described by which data from tapes processed by Earthnet can be re-processed in order to obtain reliable planetary reflectance data.

2. EOSAT tapes

EOS uses so-called 'TIPS processing' to convert uncalibrated quantised digital numbers (DNs) to calibrated quantised radiance values (Q_{cal}) according to:

$$Q_{cal} = P_B + P_G \cdot Q \quad (1)$$

where

- Q_{cal} = calibrated quantised radiance in DN's
- P_B = processing bias from TIPS in DN's*
- P_G = unitless processing gain from TIPS*
- Q = uncalibrated quantised radiance in DN's.

Based on the Q_{cal} , the spectral radiance can be determined from

$$L_w = A_{0w} + A_{1w} \cdot Q_{cal} \quad (2)$$

where

- L_w = spectral radiance, in $\text{mW cm}^{-2} \text{ster}^{-1} \mu\text{m}^{-1}$
- A_{0w} = post-calibration offset constant, in $\text{mW cm}^{-2} \text{ster}^{-1} \mu\text{m}^{-1}$
- A_{1w} = post-calibration gain constant, in $\text{mW cm}^{-2} \text{ster}^{-1} \mu\text{m}^{-1}$ per DN
- Q_{cal} = quantised calibrated radiance, in DN's.

The A_{0w} and A_{1w} are, respectively,

$$A_{0w} = L_{MINw} \quad (3a)$$

$$A_{1w} = (L_{MAXw} - L_{MINw})/255 \quad (3b)$$

where

- L_{MINw} = spectral radiance at $Q_{cal} = 0$ DN
- L_{MAXw} = spectral radiance at $Q_{cal} = 255$ DN.

$L_{MIN\lambda}$ and $L_{MAX\lambda}$ values specific to Landsat Thematic-Mapper data with TIPS processing after 15 January 1984, and hence to all Landsat-5 TM tapes, are presented in Table 1.

Knowing the spectral radiance, the unitless effective planetary reflectance at the satellite (r_p) can be calculated from

$$r_p = \frac{(\pi \cdot L_\lambda \cdot d^2)}{(E_{sun\lambda} \cdot \cos \theta_s)} \quad (4)$$

where

- L_λ = spectral radiance at sensor aperture, in $\text{mW cm}^{-2} \text{ster}^{-1} \mu\text{m}^{-1}$
- d = Earth-Sun distance in astronomical units
- $E_{sun\lambda}$ = mean solar exo-atmospheric irradiance, in $\text{mW cm}^{-2} \mu\text{m}^{-1}$
- θ_s = solar zenith angle, in degrees.

* P_B and P_G are TIPS coefficients from linear regression of observed internal calibrator (IC) peak versus reference peak.

Table 1. Spectral radiances, $L_{MIN\lambda}$ and $L_{MAX\lambda}$, in $mWcm^{-2} ster^{-1} \mu m^{-1}$, and mean solar exo-atmospheric irradiance in $mWcm^{-2} \mu m^{-1}$ for EOSAT processed imagery

Band	$L_{MIN\lambda}$	$L_{MAX\lambda}$	$E_{sun\lambda}$
TM-1	-0.15	15.21	195.7
TM-2	-0.28	29.68	182.9
TM-3	-0.12	20.43	155.7
TM-4	-0.15	20.62	104.7
TM-5	-0.037	2.719	21.93
TM-7	-0.015	1.438	7.452

Table 2. A_0 , A_1 and E_{sun} values as represented on the Earthnet tapes; E_{sun} values based on full-width half-maximum method, and bandwidths based on two methods

	A_0	A_1	$E_{sun}^{(1)}$	$E_{sun}^{(2)}$	B-W ⁽³⁾	B-W ⁽⁴⁾
TM-1	-0.06662	0.04197	137.2	129.2	70.1	66
TM-2	-0.15732	0.10345	162.6	150.0	88.9	82
TM-3	-0.11269	0.06500	119.3	104.3	76.6	67
TM-4	-0.23286	0.11705	140.6	134.0	134.3	128
TM-5	-0.08640	0.02727	49.67	47.6	226.5	217
TM-7	-0.05114	0.01692	19.99	18.8	268.8	252

¹ E_{sun} (in Wm^{-2}) based on quadratic moment method, on tape

² E_{sun} (in Wm^{-2}) based on full-width, half-maximum method; correct values to use in relation to A_0 and A_1

³ Bandwidth (nm) for quadratic-moment method

⁴ Bandwidth (nm) based on full-width, half-maximum method.

Table 3a. Examples of Landsat-5 TM detector reflective band gain data

Detector	Band					
	1	2	3	4	5	7
1	236.3227	96.0744	152.3627	85.1172	363.9618	585.6809
2	234.6015	95.7134	153.5105	84.7039	359.6590	580.2047
3	237.2970 (max)	95.6122	152.0179	84.1867	361.7650	584.8107
4	234.4515	95.6488	153.3537	83.8414	360.5733	581.5428
5	238.0773	95.7841	152.0701	84.5281	362.4290	590.7480
6	233.9485 (min)	95.3500	151.6597	84.4484	362.6152	580.6885
7						
16						

Table 3b. Examples of Landsat-5 TM detector reflective bias data

Detector	Band					
	1	2	3	4	5	7
1	2.2965 (max)	2.2691	2.4569	2.6652	3.5727	3.8241
2	1.9313	1.5379	1.9920	2.1440	3.2601	3.2194
3	1.8734	1.8693	1.9709	2.4287	3.2736	3.3549
4	1.8895	1.5357	1.7282	1.9523	3.2701	3.2758
5	1.7628	1.5069	1.8442	2.2046	3.1314	3.1052
6	1.9744	1.8161	1.7437	2.3107	3.2506	3.2558
7	1.7435	1.5605	1.8571	2.6408	3.1252	3.0121
16						

The solar exo-atmospheric spectral irradiances for the TIPS-processed EOSAT data are given in Table 1.

The solar zenith angle in the centre of the image is normally given on tape. In other cases, it can be calculated from tables⁴, if the time of the Landsat overpass is known.

The Earth—Sun distance (d) for a specific day can be read from tables, such as those presented by Iqbal⁴, or can be approximated from the Gurney & Hall⁵ relation

$$d = 1 + 0.0167 \sin \left[\frac{2\pi(D-93.5)}{365} \right] \quad (5)$$

where D is the day number.

3. Earthnet tapes

The processing of most Earthnet TM tapes is based on pre-flight calibration data. In the calculation of planetary reflectance using those data, two important errors can be introduced through:

- (i) the application of wrong bandwidths for determination of solar exo-atmospheric irradiance;
- (ii) the use of gain and bias based on pre-flight data, without considering the gain change of detectors.

3.1 Bandwidth

For tapes that are calibrated based on pre-flight data, Earthnet provides so-called A_0 and A_1 data for application in equations of type (2). There is a difference, however, in that A_0 and A_1 values have other units, since they are not per micron (μm), but rather in $\text{Wm}^{-2} \text{ster}^{-1}$ and $\text{Wm}^{-2} \text{ster}^{-1} \text{DN}^{-1}$, respectively. Therefore, the E_{sun} units are also different, namely Wm^{-2} . These data, which can be found on Earthnet tapes, are given in Table 2. However, since in the Earthnet processing the A_0 and A_1 determinations are based on the full-width half-maximum bandwidth method, the solar exo-atmospheric irradiance (E_{sun}) determination has also to be based on this method. In Table 2, therefore, E_{sun} bandwidth values determined with the full-width half-maximum method are presented in addition to E_{sun} values based on the quadratic-moment method. For Earthnet tapes, the $E_{\text{sun}}^{(2)}$ values of Table 2 have to be used.

3.2 Effect of gain change

On the tapes processed by Earthnet using the pre-flight data, the raw data (DN_r) are calculated to provide DN_p (DN after correction for pre-flight data) values according to:

$$\text{DN}_p = (\text{DN}_r - \text{bias}(d)) / \text{gain}(d) \quad (6)$$

Pre-flight gain and bias data for examples of the 16 detectors are given in Tables 3a and 3b, provided by Earthnet. To achieve a simple recalculation of planetary reflectance, average values of gain and bias (m_d) were used instead of specific detector values.

In Table 4, for the Landsat-5 Thematic Mapper, averages of gain (in $\text{DN per mWcm}^{-2} \text{ster}^{-1}$) and bias (in DN), and also the gain in $\text{DN per mWcm}^{-2} \text{ster}^{-1} \mu\text{m}^{-1}$ are given. Formulae from Barker & Wanchoo³ for calculating the gain GI_w as a function of days after launch ($=T_{\text{orb}}$) for bands 1 to 4, can be used to determine the GI_w during the flight:

$$GI_w \text{ (with IC temperature correction)} = B_0 + B_1 \cdot \exp(-B_2 \cdot T_{\text{orb}}) \quad (7)$$

Regression coefficients and inferred variables for Equation (7) are given in Table 5.

For the short-wave infrared bands (TM bands 5 and 7), gains show a periodic change according to:

$$GI_w = C_0 + C_1 \cdot \cos[(T_{\text{orb}} - C_2) / C_3] \quad (8)$$

Table 4. Characteristic Landsat-5 TM gain and bias data for pre-flight conditions

TM band numbers						
1	2	3	4	5	7	
235.64	95.85	152.28	84.54	362.92	586.19	Mean gain of detectors in DN/(mW/cm ² .sr) in Table 3a
1.83	1.69	1.88	2.24	3.29	3.21	Mean bias of detectors in DN (Table 3b)
15.55	7.86	10.20	10.82	78.76	147.72	Gain based on pre-flight data (= mean gain times spectral bandwidths = gain(m _p))

Table 5. Regression coefficients and inferred variables for Landsat-5 TM visible and near-infrared band exponential regression model (Eqn. 7) of IC gain decay with time

Regr. coeff. and inf. var.	Band-averaged values			
	Band-1	Band-2	Band-3	Band-4
B ₀ (DN per mWcm ⁻² ster ⁻¹ μm ⁻¹)	13.10 ±0.02	6.801 ±0.008	8.470 ±0.012	10.082 ±0.008
B ₁ (DN per mWcm ⁻² ster ⁻¹ μm ⁻¹)	1.073 ±0.04	0.306 ±0.035	0.654 ±0.045	0.687 ±0.035
B ₂ (day ⁻¹) × 1000	6.10 ±0.40	10.80 ±2.00	8.51 ±1.03	10.70 ±0.90
Coefficient of variation (%)	±1.30	±0.73	±1.26	±1.10

Table 6. Regression coefficients and inferred variables for TM shortwave infrared band apparent (IC) gain change with time

Regr. coeff. and inf. var.	Band average values	
	Band-1	Band-2
C ₀ (DN per mWcm ⁻² ster ⁻¹ μm ⁻¹)	78.086 ±0.028	144.144 ±0.238
C ₁ (DN per mWcm ⁻² ster ⁻¹ μm ⁻¹)	0.620 ±0.295	1.136 ±0.343
C ₂ (day)	0.688 ±6.105	4.541 ±6.427
C ₃ (day)	8.906 ±0.113	13.547 ±0.144

Table 7. Gain of Landsat-5 TM for pre-flight and 1000 days after launch and its ratio

TM band numbers						
1	2	3	4	5	7	
15.55	7.86	10.20	10.82	78.76	147.72	Gain based on pre-flight data (= mean gain times spectral bandwidths = gain(m _p))
13.11	6.80	8.47	10.08	78.02	145.28	Gain (m _p) based on formula of Barker & Wanchoo (1988) ⁷
1.19	1.16	1.20	1.07	1.01*	1.02**	gain (m _p)/gain (m _p) about 1000 days after launch

* max 1.0094 **1.0168
min 1.0076 1.0329

Regression coefficients and inferred variables for Equation (8) are given in Table 6.

A corrected DN_c can be found from

$$DN_c = [DN_p \times \text{gain}(m_d) + \text{bias}(m_d) - \text{bias}(m_c)]/\text{gain}(m_c) \quad (9)$$

Since no values of bias (m_c) are found, Equation (9) was simplified assuming bias (m_d) and bias (m_c) equal to

$$DN_c = \{(DN_p \times \text{gain}(m_d))\}/\text{gain}(m_c) \quad (10)$$

This implies that the original DN s have to be multiplied by the ratio of $\text{gain}(m_d)$ to $\text{gain}(m_c)$. Gains based on pre-flight data and for 1000 days after launch, as well as the ratios of the two types of gain factors, are presented in Table 7.

Confidence intervals in Table 6 indicate that the change in gain for bands 5 and 7 is difficult to predict for a certain T_{orb} . Maximum and minimum values of this ratio for bands 5 and 7 are therefore presented in Table 7. The ratios for the other bands remain almost constant more than 1000 days after launch.

4. Implications for Earthnet data

For an adequate determination of planetary reflectance, an equation similar to Equation (5) has to be used. The difference is that the digital numbers found on Earthnet tapes calibrated with pre-flight data have to be multiplied by $\text{gain}(m_d)/\text{gain}(m_c)$. Thereafter the values have to be multiplied by A_1 and summed with A_0 of Table 2 to get L . E_{sun} values have to be gathered from $E_{sun}^{(2)}$ and not from $E_{sun}^{(1)}$ in Table 2.

Applying the right E_{sun} and gain to the data gives a much better estimate of planetary reflectance than using the pre-flight data and E_{sun} for a wavelength interval based on the quadratic-moment method. Minor sources of error are caused by the use of average values of gain and bias instead of specific detector values, and the assumption that the mean bias remains constant.

In Table 8, an overview is given of the ratios of planetary reflectance determined as described above to values based on pre-flight data. Errors in band 3, and to a lesser extent in bands 1 and 2, are very important.

New A_0 , A_1 and E_{sun} values for practical applications are presented in Table 9. These data can be used to derive planetary reflectances from DN s on Earthnet tapes that are corrected based on pre-flight data. The values in Table 9 are representative for 1000 days after launch. However, they can be applied without causing large errors for more than 700 days after launch. For dates closer to launch, the same procedure can be followed, but then the actual number of days after launch has to be substituted in Equations (7) and (8).

In Table 10, as an example for one location in Tunisia (frame 192—036), the average tape DN s for a small area are converted using: (i) pre-flight data; (ii) preflight data, but an adequate E_{sun} ; and (iii) with a complete correction. With the aid of an atmospheric model from Verhoef⁶, with known diffuse/total ratios as input, ground reflectances for this area were predicted. Ground reflectance measurements for the same area measured with a Barnes MMR are presented for comparison. The agreement between the measured ground reflectance and that based on TM using this model is remarkable, the difference being less than 10% for all bands, despite the many inaccuracies that may exist. The most important are:

- (i) Solar exo-atmospheric irradiances given by different authors vary by up to 6 to 8% for TM bands 5 and 7. There is better agreement for TM bands 1 to 4.
- (ii) Inaccuracies in determining diffuse/total irradiance ratio and panel reflectance data.
- (iii) Limitations and assumptions of the atmospheric model.
- (iv) Deviations from Lambertian reflectance.

However, the data suggest that only after atmospheric correction can a good relation be found for this complete correction.

Table 8. Ratios of incompletely and completely corrected planetary TM reflectance data, to reflectance based on original pre-flight gain and solar irradiance for quadratic-moment band interval

	(a)	(b)	(c)
TM-1	1.06	1.19	1.26
TM-2	1.08	1.16	1.25
TM-3	1.14	1.20	1.38
TM-4	1.05	1.07	1.13
TM-5	1.04	1.01	1.05
TM-7	1.07	1.02	1.08

- (a) correction for bandwidth
 (b) correction for gain change
 (c) complete correction

Table 9. A_0 , A_1 and E_{sun} values which can be applied after 1000 days after launch for the Earthnet tapes, and E_{sun} values based on quadratic-moment method

	A_0	A_1	E_{sun}
TM-1	-0.06662	0.04979	129.2
TM-2	-0.15732	0.11958	150.0
TM-3	-0.11269	0.07827	104.3
TM-4	-0.23286	0.12564	134.0
TM-5	-0.08640	0.02750	47.59
TM-7	-0.05114	0.01734	18.78

Table 10. Planetary reflectance data based on incomplete and complete corrections for an area in Southern Tunisia, and a comparison with ground-reflectance measurements

	DN (a)	Refl. (1)	Refl. (2)	DN (b)	Refl. (3)	TM-based ground refl.	Measured ground refl.
TM-1	133	0.159	0.168	158	0.201	0.155	0.154
TM-2	78	0.192	0.208	90	0.241	0.235	0.235
TM-3	110	0.233	0.266	132	0.320	0.318	0.301
TM-4	99	0.319	0.334	106	0.358	0.353	0.343
TM-5	166	0.353	0.368	168	0.373	0.371	0.392
TM-7	92	0.297	0.316	93	0.320	0.319	0.322

- (a) = average DN of specific area
 (b) = average DN corrected by multiplying with $gain(m_s)/gain(m_e)$
 (1) = planetary reflectance using A_0 , A_1 and $E_{sun}^{(1)}$ of Table 2
 (2) = planetary reflectance using A_0 , A_1 and $E_{sun}^{(2)}$ of Table 2
 (3) = planetary reflectance using A_0 , A_1 and $E_{sun}^{(2)}$ of Table 2, but with DN multiplied by $gain(m_s)$ [column DN(b)] (solar zenith angle 37° and Earth-Sun distance 1.0015) or using figures of Table 8 and DN's of column (a).

The author is much indebted to: W. Verhoef of the National Aerospace Centre; M. Menenti of the Winand Staring Centre (Wageningen, NL); and to Earthnet in Frascati (I), especially Dr. Fusco and Dr. Gilles. The research reported is part of a project funded by the Netherlands Remote Sensing Board (BCRS, AO-4.2).

Acknowledgements

1. Barker J L & Wanchoo I 1988, Radiometric performance of calibrators on the Landsat Thematic Mappers, Proc. XXVII COSPAR Meeting, Espoo, Finland, Invited Paper A.3.1.1.
2. Markham B L & Barker J L 1987, Thematic Mapper bandpass solar exoatmospheric irradiances, *Int. J. Remote Sensing*, Vol. 8, No. 3, pp. 517-523.
3. Barker J L & Wanchoo L 1988, Radiometric performance of the Landsat Thematic Mappers, Proc. Landsat Final Results Workshop, 22-25 August 1988, Maryland.

References

4. Iqbal I 1983, *An Introduction to Solar Radiation*, Academic Press.
5. Gurney R J & Hall D K 1983, Satellite-derived surface energy balance estimates in the Alaskan Sub-Arctic, *J. Climate Appl. Meteorol.*, Vol. 22, pp. 115-125.
6. Verhoef W 1985, A scene radiation model based on four-stream radiative transfer theory, Proc. Third Int. Colloquium on Spectral Signatures of Objects in Remote Sensing, Les Arcs, France, 16-20 December 1985, ESA SP-247, pp. 143-150.

Manuscript received 5 December 1989.

CHAPTER 9

MAPPING SURFACE CHARACTERISTICS AND THEIR DYNAMICS IN A DESERT AREA IN SOUTHERN TUNISIA WITH LANDSAT THEMATIC MAPPER.

Submitted to Remote Sensing of Environment.

MAPPING SURFACE CHARACTERISTICS AND THEIR DYNAMICS IN A DESERT AREA IN SOUTHERN TUNISIA WITH LANDSAT THEMATIC MAPPER

G.F.Epema

*Wageningen Agricultural University, Department of Soil Science and Geology, P.O.Box 37
6700 AA Wageningen, The Netherlands*

ABSTRACT

Classification of TM products using information from field reflectance data was examined. First an unsupervised classification was applied to the TM data. After merging and deleting of classes, using field reflectance, a supervised minimum distance to mean classification was applied. It was possible to derive a number of useful classes for playas, footslopes and eolian material, having differences in origin and showing variation in gypsum, carbonate, halite, moisture content and surface type. The good fit between reflectance derived from field measurements and that derived from the satellite, which is vital in this approach was achieved by applying correct processing of the data and applying the Verhoef model including an estimate of water vapour of the atmosphere.

INTRODUCTION

In a desert area in Southern Tunisia in situ ground reflectance measurements with a Landsat Thematic Mapper (TM) compatible instrument (a Barnes Modular Multiband Radiometer; MMR) in combination with observations of surface characteristics in different seasons have been carried out (Epema subm.). In this way it was possible to determine the effect of different surface characteristics under natural conditions for TM and MMR bands. These field data will be used in the present research as an aid in interpretation of the TM data. This article is focused on the question: "to which extent is it possible to derive surface characteristics and their dynamics in a desert area from TM data?"

Landsat TM data of two different days will be used in this research: 18 December 1987 in the wet season and 8 April 1988 in the dry season. The information from TM will be evaluated with the results of field measurements in two periods of about 30 days: November/December 1987, just before satellite overpass day and April 1988, including satellite overpass. The selection of the field plots was based on a general knowledge of the main factors affecting reflectance and the variation in the area, observed on former satellite images and in the field.

For a comparison between field reflectance data and reflectance data derived from Landsat TM the following has to be evaluated:

- 1) accuracy of measurements and processing of field reflectance data
- 2) influence of solar zenith angle and atmosphere on field reflectance data
- 3) accuracy of processing and correction for atmosphere for Landsat TM
- 4) time difference between field data and TM data causing difference in surface characteristics like moisture content
- 5) difference in size of a TM ground observation elements (30 x 30 meters) and that of the used radiometer (a circle with a diameter of 40 centimetres).

6) the fact that TM covers a whole area, while ground observations cover only specific locations.

Epema (1991a) discussed possible errors regarding (1), Epema (1990a) and Epema (1992) evaluated respectively influence of solar zenith angle and atmosphere. Epema (1990b) evaluated corrections needed for transforming Landsat TM counts of Fucino tapes, which are used in Tunisia, to planetary reflectance. Epema 1992 showed that, for a homogeneous area and after atmospheric correction with the Verhoef model, a good fit existed between simultaneously determined ground reflectance derived from TM and from MMR data. In this article we will apply this model to both April and November/December data.

To solve problems mentioned under 4 - 6, it was decided to start the analysis with TM data and explain the structure with the aid of field reflectance data. The results of different steps, automatic clustering, functional labelling of classes and supervised classification with the minimum distance to means method are described.

STUDY AREA AND FACTORS AFFECTING GROUND REFLECTANCE

In figure 1 the location of the study areas is given. In plate 1 imagery is shown of these areas for both seasons. Extensive descriptions of (parts of) the region on various aspects are given by Coque (1962), Coque and Jauzein (1967), Meckelein (1977), Mitchell (1983), Ongaro (1986), Millington *et al.* (1987), Townshend *et al.* (1989), Millington *et al.* (1989) and Epema (1990a, submitted). The areas are situated at the margin of the Saharan Platform and the folded Atlas ranges. A large part of the zone of subsidence is occupied by entirely flat playas (locally known as chotts). The Chott el Djerid is the largest of them and has an elongated northeastern arm (Chott Fedjaj), which has been formed by faulting in the top of an anticlinal uplift (Coque 1962; Jones and Millington 1986). The cuesta ridge of the Djebel Tebaga, consisting mainly of dolomitic limestones is located in the southern part of this uplift. It is surrounded by footslopes. Sandsheets and dunes of various size and mineralogy cover parts of playa margins and footslopes.

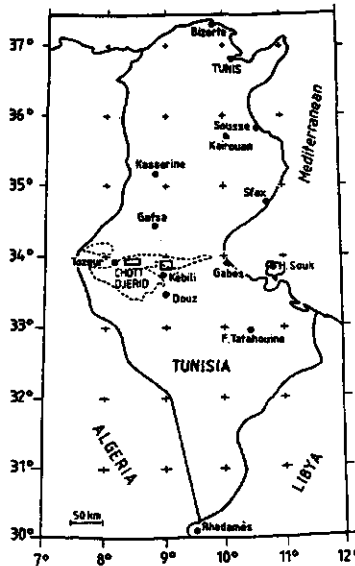


Figure 1 Location of the study areas

Rainfall in the study areas is less than 100 millimetres per year. Yet the ground water table in the playas is generally at less than 1 meter depth, due to artesian water inflow. Apart from some oases, vegetation cover exceeds 5% of the surface only in exceptional cases. The inner parts of the playa have no vegetation cover at all due to high salt content, except for some parts covered with small dune fields. The species are typically for this area adapted to low rainfall and high halite and gypsum content of the soil (Floret and Pontanier, 1982; Epema *et al.*, 1985; Ongaro, 1986).

The study areas comprise parts of the playas and the footslope areas with or without eolian cover. The western area is located in Chott Djerid, while the eastern area covers both the margin of Chott Fedjaj and footslopes of Djebel Tebaga.

No large differences in morphology, mineralogy and moisture condition exist between sand sheets on the footslopes and on the playa. Therefore in the following discussion playa areas and non-playa areas are treated separately.

The playa shows only minor height differences. The major zones are those dominated by deposition, those with thick salt crusts and zones with seepage points (aiouns). The location of the major zones and ephemeral channels has remained constant for several years (10 at least) as can be observed from satellite images.

A classification was made of the dominant surface types in a relatively dry season. In the wet season or after storms, the morphology of the surface types may change considerably depending on intensity and amount of rainfall. The following surface types have been distinguished (cf. also figure 2):

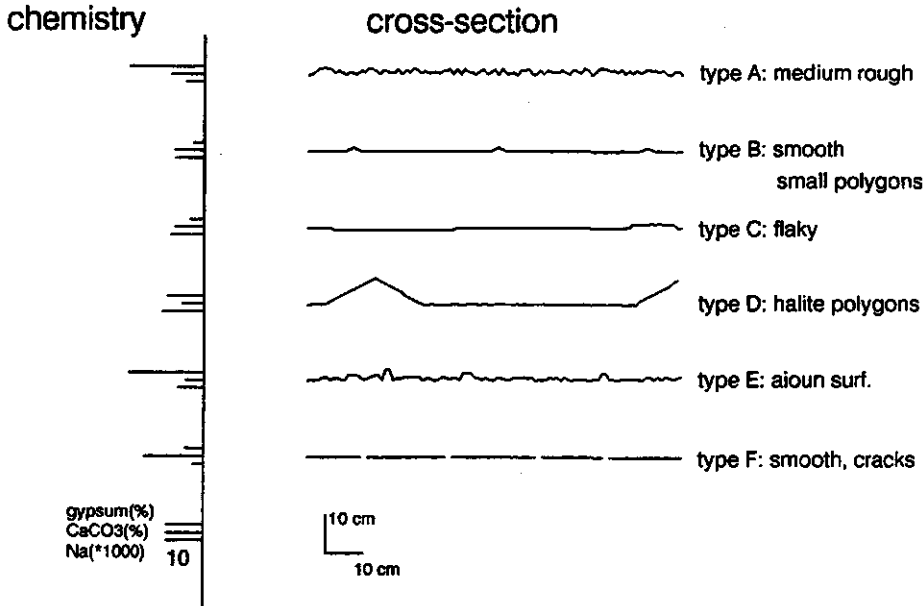


Figure 2 Simplified cross-sections of playa surface types and examples of gypsum, CaCO₃, and Na content

- **Type A** :dry porous brown crusts, with friable, rough surfaces (1 to 2 centimetres height difference). Small gypsum crystals are present.
 - **Type B** :very thin (0.1 centimetre) light brown crusts, with or without presence of polygons, due to salt (halite) growing, with a diameter of in general 30 to 60 centimetres and of height of polygon fringe of 0.5 centimetres and a polygon fringe diameter of 3 centimetres. The polygon fringes are not connected with the rest of the profile, and are therefore less moist and less dark than the area within the polygons. The surface is often covered with a thin transparent halite layer. Small salt cuboids with a diameter of 0.5 to 2 centimetres are scattered over the surface types A and B. Concentrations of these cuboids are sometimes so high that even on satellite images these patterns can be found.
 - **Type C** :dry, thin flaky crusts. These crusts occur mainly within polygon patterns with sides of 10 to 20 meters. Loose sand with gypsum crystals are present in parts where these crusts are blown away.
 - **Type D** :thick halite salt crusts generally exhibiting polygons. The diameter of the polygons is between 60 and 200 centimetres. The height of fringes increases with increasing polygon diameter and range from 5 to 30 centimetres.
 - **Type E** :aiouns, characterised by quasi-circular features, with diameters from 30 meters to 1000 meters. The centre (diameter less than 3 meter) is formed by a source, and rises somewhat above the surrounding area. The groundwater table is close to the surface. Periodically water comes to the surface and spreads out over the surroundings. Therefore circular features develop around the sources. These aiouns are also described by Jones and Millington (1986), Roberts and Mitchell (1987) and Millington *et al.* (1989).
 - **Type F** smooth, brown to greybrown crusts with polygonal cracks. These were observed in the Chott Djerid area only.
- Halite and moisture contents change considerably during the year.

A large range of factors affect reflectance in the playa area (Epema submitted). Only two characteristics of the playa affect the spectral curve shape by influencing some bands more than the others (Epema 1990c and subm.). An increase in moisture content gives an extra decrease in reflectance in MMR bands 6 and 7. These bands are comparable with TM bands 5 and 7 (table 1). Halite causes a relatively low 4/1 ratio (TM bands 1-4 are comparable with MMR bands 1-4). Variation in spectral signatures are more pronounced in the wet season, when large variation in moisture and halite content exist. Differences between surface types A - F can be partly derived from overall reflectance. Reflectance for all bands increases with decreasing roughness. For a further discrimination of types or subtypes 4/1 and 7/4 ratio may be of help. Even in April areas dominated by evaporation have more salt (a lower 4/1 ratio) and have in general a higher moisture content (a lower 7/4 ratio). Field measurements on plots showed that confusion between and within classes can exist due to gradual changes of characteristics.

Table 1 Bandpasses (-3dB) of Barnes MMR field radiometer (50% power bandpass limits) and Landsat Thematic Mapper (full-width at half-maximum method) of reflectance part of the spectrum.

	Barnes MMR		Landsat TM	
	nr. of band	wavelength limits	nr. of band	wavelength limits
Blue	1	0.458-0.525	1	0.4524-0.5178
Green	2	0.519-0.601	2	0.5280-0.6093
Red	3	0.637-0.687	3	0.6264-0.6923
Near IR	4	0.739-0.898	4	0.7764-0.9045
	5	1.174-1.334		
MIR 1	6	1.574-1.803	5	1.5675-1.7842
MIR 2	7	2.083-2.371	7	2.0972-2.3490

Footslopes in the area are mainly erosional features. The top layers are often sealed. Close to the mountain ridge footslopes are incised by gullies. Parts of the surface are covered with gravel and stones and eolian material. Locally degraded gypsum crusts form part of the surface (in general less than 20 %).

Eolian sand can be found as thin sheets on footslopes or in gullies, as sheets with dunes less than 1 meter, as scattered small dunes on gypsum crusts and footslopes, and as deposition behind hummocks. The appearance of the different sand types varies as a function of wind direction and also of sealing of the surface.

Like in the playa area many factors affect reflectance. Spectrally differences in mineralogy are most important. Dominant minerals are gypsum, calcite and quartz. Gypsum shows a low reflectance in MMR 7 and 6, calcite a low reflectance in MMR 7, while quartz has no specific absorption. On sealed footslopes these differences in spectral reflectance, although relatively small, were observed for areas dominated by gypsum, calcite and quartz respectively. Spectral differences between gypsum, calcite and quartz sand were very significant. With the exception of an area close to a quarry, calcite was hardly present in the eolian material. Natural eolian deposits show large differences between quartz and gypsum sand. Relations were found between gypsum content and the MMR 7 / MMR 4 ratio. Gypsum crusts show low MMR 7 and 6 values like gypsiferous sand. Most difficult to differentiate spectrally are: (1) gypsum crusts from gypsiferous sand and (2) footslopes from quartz sand.

COMPARISON OF GROUND REFLECTANCE DERIVED FROM LANDSAT TM AND MMR

In Epema (1991) the model of Verhoef (1985, 1990) applied to April data has been described. The relation between planetary reflectance ($\rho_p(\lambda)$) and ground reflectance ($\rho_o(\lambda)$) is described by a simplified equation, after Verhoef (1990):

$$\rho p(\lambda) = R_{so}(\lambda) + \frac{T_1(\lambda) T_2(\lambda)}{1 - R_{ad}(\lambda) \rho o(\lambda)} * \rho o(\lambda) \quad (1)$$

where $R_{so}(\lambda)$ = atmospheric reflectance

$T_1(\lambda) T_2(\lambda)$ = two way transmittance

$R_{ad}(\lambda)$ = spherical albedo of the atmosphere

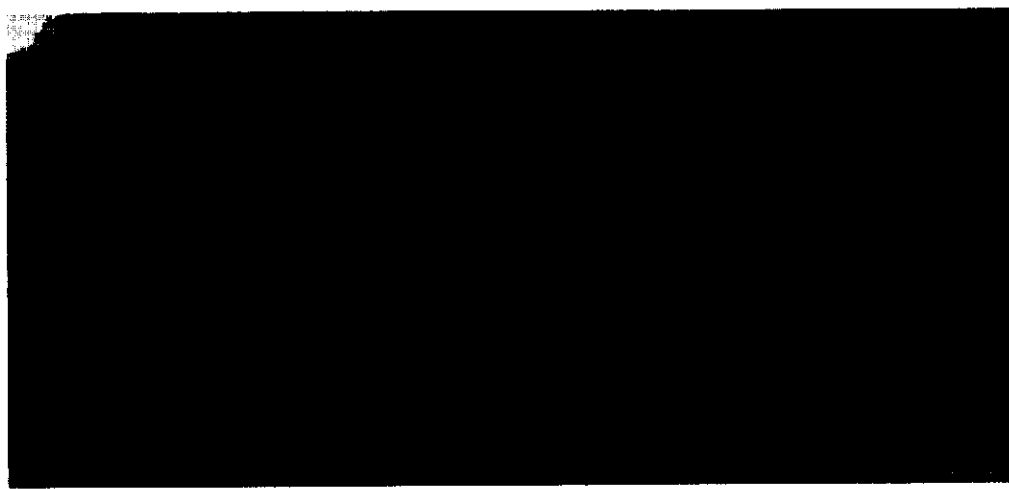
For the April image atmospheric factors in (1) were derived from the measured ratio diffuse to total irradiance. Application of the Verhoef model with measured ratios on different clear days showed a limited variation of atmospheric influence on reflectance. Relations between ground reflectance derived from field measurements and derived from TM fitted quite well for the April data (Epema, 1992). However relations for the December data were not evaluated.

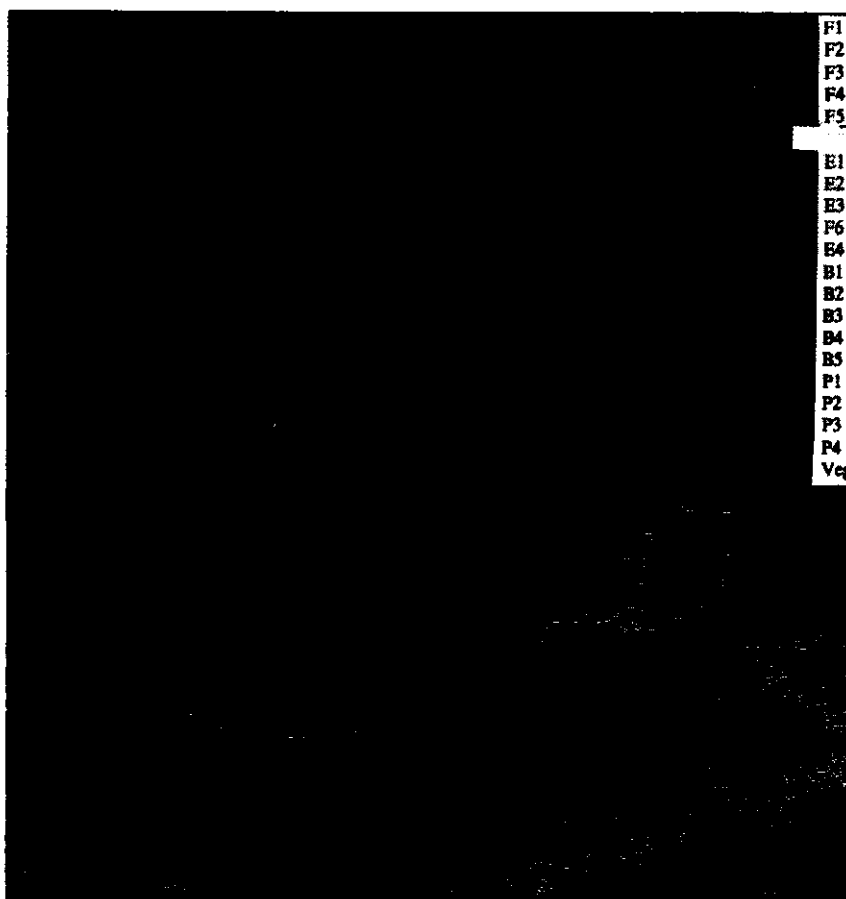
Applying the Verhoef model to the December data, a considerably less good fit was found. Ground reflectances derived from TM bands 4 - 7 for December were consistently lower than the field measurements. The assumption in the model of Verhoef that absorption for water vapour in atmosphere is zero is likely to be the cause of this error. Absorption by water vapour plays a role in TM bands 4 - 7, as can be derived from tables by Iqbal (1983). The influence will be lower due to low water vapour concentrations in the April period. Based on these consideration absorption by water vapour was also incorporated in the model. Values of spectral absorption coefficients were derived from Iqbal (1983). New values for $T_1(\lambda) T_2(\lambda)$, corrected for water absorption, and the original $R_{so}(\lambda)$ and $R_{ad}(\lambda)$ values are presented in table 2. The assumption in all calculations was that atmospheric conditions in April and December are comparable with the exception of precipitable water vapour (April 0.5 and December 2.0 centimetre).

Table 2. Values of $R_{so}(\lambda)$, $T_1(\lambda) T_2(\lambda)$, $R_{ad}(\lambda)$ for December 1987 and April 1988

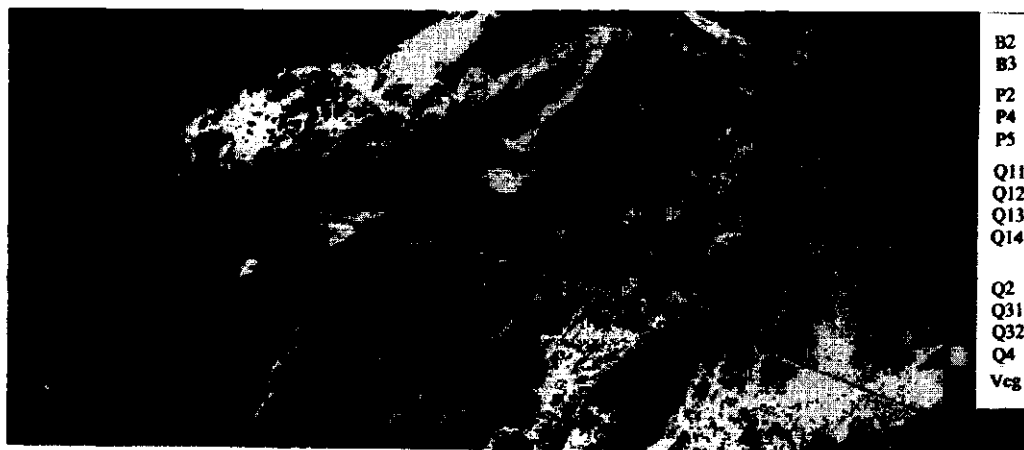
Band nr.	18 December 1987				8 April 1988			
	$R_{so}(\lambda)$	$T_1(\lambda)$	$T_2(\lambda)$	$R_{ad}(\lambda)$	$R_{so}(\lambda)$	$T_1(\lambda)$	$T_2(\lambda)$	$R_{ad}(\lambda)$
TM 1	.0870	.7387	.1586		.0737	.7928	.1586	
TM 2	.0501	.7664	.1018		.0432	.8196	.1018	
TM 3	.0315	.8747	.0622		.0267	.9047	.0621	
TM 4	.0164	.8788	.0324		.0141	.9246	.0330	
TM 5	.0052	.7970	.0104		.0039	.8691	.0107	
TM 7	.0044	.8048	.0087		.0031	.8872	.0091	

In figure 3a - 3c scatter plots of ground reflectance values derived from Landsat TM and field data are given. The field data are weighted sums of measurements of the elements with a solar zenith angle close to that during satellite overpass. No corrections are made for shadow effects, which will only be significant in the footslope areas with vegetation and for rough parts of the playa. Other bands show comparable relations as presented in figures 3a - 3c. The good fit between ground reflectance derived from satellite and field data implies that relations between surface characteristics and reflectance, which were found in the field (Epema subm.), can be applied in principle to the TM data.





F1
F2
F3
F4
F5
E1
E2
E3
F6
B4
B1
B2
B3
B4
B5
P1
P2
P3
F4
Veg

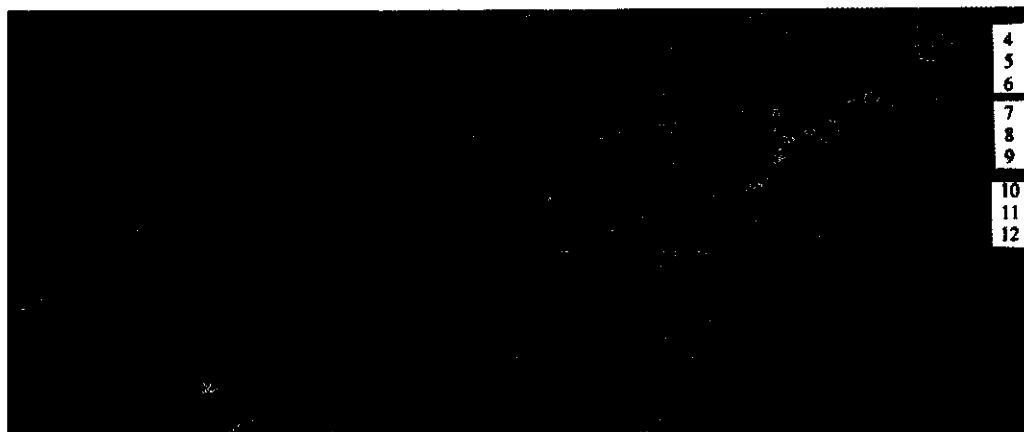


B2
B3
P2
P4
P5
Q11
Q12
Q13
Q14
Q2
Q31
Q32
Q4
Veg

Plate 3



1
2
3
4



4
5
6
7
8
9
10
11
12



PLATES 1 - 4

Scale



2 km eastern area (=upper part) Fedjaj



5 km western area (=lower part) Djerid



- Plate 1 Landsat TM 7,4,1 combination of December (respectively red, green and blue) for eastern area and western area
- Plate 2 Supervised classification of eastern and western area (explanation is given in Legend 1)
- Plate 3 Classified moisture and salt situation maps of December (explanation is given in Legend 2)
- Plate 4 Moisture differences in % between December and April for the Fedjaj playa.

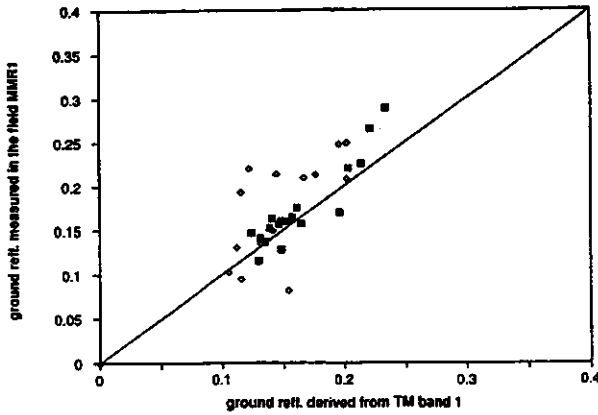


Figure 3a Scatter plots of ground reflectance values derived from Landsat TM and field data for band 1.

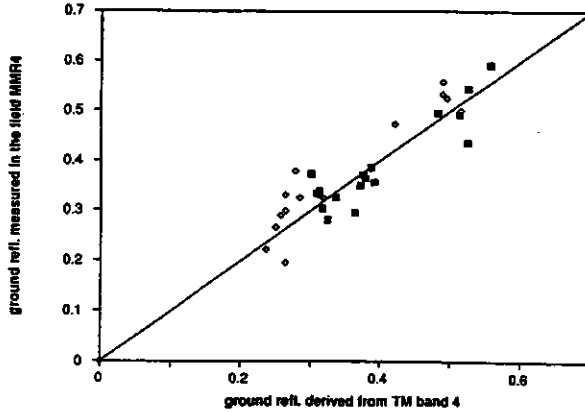


Figure 3b Scatter plots of ground reflectance values derived from Landsat TM and field data for band 4.

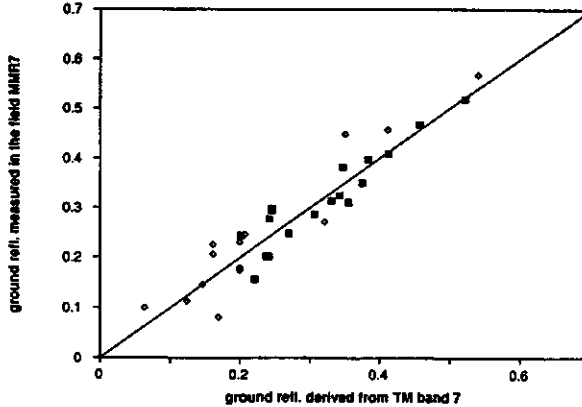


Figure 3c Scatter plots of ground reflectance values derived from Landsat TM and field data for band 7.

ANALYSIS OF TM DATA

The feature space of the TM data set will be different from the field set due to difference in size of ground observation elements, the non-complete coverage of the area by field measurements and time difference of observation. This time difference between field observation and satellite observation implies measurements at different moisture contents.

Since TM data cover the whole area at one moment, it was decided to statistically cluster the TM data first and then to explain the clusters with field measurements. Unsupervised clustering based on the k-mean algorithm (Tou and Gonzalez 1974) was applied. This unsupervised clustering was applied to TM data sets of both eastern and western area for both December and April. In every clustering 40 or 60 clusters were looked for. A comparison of this unsupervised classification with field reflectance measurements led to a reduction in the number of clusters and a functional labelling of the other classes.

In figure 4a and 4b as an example feature space plots of band 4 and 7 of April are given for both field and clustered TM data. In this example differences are obvious. Field measurements show both higher and lower reflectance values than TM based ground reflectance (respectively due to sun-exposed slopes and higher moisture content in the morning before satellite overpass time). TM data show clusters, which are a spectral mixture of sanddunes and playas (for instance clusters with reflectance factors in TM 4 and TM7 of respectively about 0.4 and 0.25).

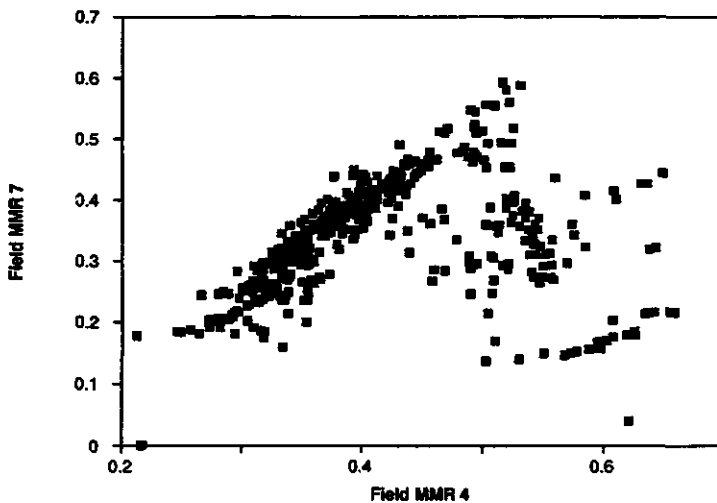


Figure 4a Feature space plots of band 4 and 7 of April for field data.

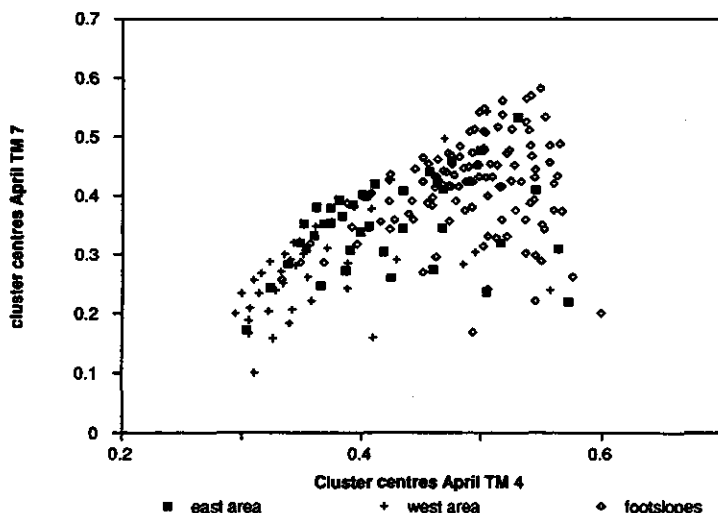


Figure 4b Feature space plots of band 4 and 7 of April for clustered TM data.

For a general classification on landscape and mineralogical units, April TM data were most suitable. Since the digital numbers are higher, the signal to noise ratio of April is superior to that of December, and moreover the shadow effect is limited. For the relatively unchanging non-playa area the choice for classification based on April data is therefore obvious. From a comparison with the field data it turned out that for the playa area, the more constant factors like surface roughness (surface type) could also be discriminated more easily in April. December data of the playa show a large spectral variation due to salt and moisture variation. December data were used to show spatial variation in salt and moisture for the playa area in the wet season, and dynamics of these factors.

April data

For the footslope area, covering only a part of the eastern area, the number of defined clusters (arbitrarily put on 40 for both playa and footslopes) turned out to be too low. Field data showed that a further discrimination was possible. Therefore two more clusterings, now looking for 60 clusters, were performed to two areas dominated by footslope samples. The original 160 (40+60+60) clusters of the eastern area, were reduced to 75 clusters, which actually represents 20 functional classes. This reduction in number of clusters and definition of 20 classes was done by: (1) comparing clusters with each other in the feature space, (2) comparing clusters with the field data and (3) examining the spatial distribution of the clusters of the unsupervised classification images. A supervised minimum distance to mean classification with the aid of these 75 clusters was applied. The image of the eastern area was coloured using the 20 functional classes (plate 2a).

The western area covering largely Chott Djerid was divided in 14 classes using 40 clusters of the unsupervised classification (plate 2b). In this area classes were limited to the playa itself and the playa partly covered with sand sheets.

The results of the supervised classification of the eastern and western area are given respectively in plate 2a and 2b. The legend of the supervised classification in plate 2a and 2b is given in Legend 1.

Legend 1 Units of April

Footslopes

- F1 Footslopes dominated by calcite, non-dissected
- F2 Footslopes dominated by quartz, non-dissected
- F3 Footslopes dominated by gypsum, non-dissected
- F4 Footslopes dominated by gypsum, gypsum crusts covering 5 - 20% of the surface, dissected by valleys filled with sand.
- F5 Valleys filled with gypsum sand
- F6 Footslope area covered with 20 - 80% of eolian sand sheets or dunes

Dunes and sand sheets

- E1 Dunes and sand sheets dominated by quartz sand (gypsum content < 20%)
- E2 Dunes and sand sheets dominated by quartz sand with some gypsum sand (gypsum content 20% - 40%)
- E3 Dunes and sand sheets of both quartz sand and gypsum sand (gypsum content 40% - 60%)
- E4 Dunes and sand sheets dominated by gypsum sand (gypsum content > 60%)

Playa covered with sand sheets and dunes

- B1 Playa area covered with 60 - 80% of eolian sand sheets or dunes
- B2 Playa area covered with 40 - 60% of eolian sand sheets or dunes
- B3 Playa area covered with 20 - 40% of eolian sand sheets or dunes
- B4 Playa area covered with 5 - 20% of eolian sand sheets or dunes

P Playa area not dominated by evaporation

	Roughness	Dominant surface type	Salt effl.	Moistur
P1	Playa area, smooth,	type B, only few polygons and salt bubbles	1	1
P2	Playa area, somewhat rough:	type C, flaky	1	1
P3	Playa area, somewhat rough,	type B, with small polygons and some salt bubbles	1	1
P4	Playa area, somewhat rough,	type A	1	1
P5	Playa area, smooth,	type F	1	1

Q Playa area dominated by evaporation

	Roughness	Dominant surface type	Salt effl.	Moistur
Q11	Playa area, smooth,	type B	2	1
Q12	Playa area, smooth,	type B	3	2
Q13	Playa area, smooth,	type B	2	3
Q2	Playa area, somewhat rough,	type B, polygons and/or bubbles	2	1
Q31	Playa area, rough,	type D, small salt polygons	2	1-2
Q32	Playa area, very rough,	type D, large salt polygons	2	2
Q4	Playa area, rough,	type E, rough due to halite and gypsum bubbles	2	2

Veg More than 20% vegetation cover (oases)

Explanation: (1) very low; (2) low; (3) moderate; (4) high; (5) very high

In the following a description of the April Legend Units of the classification is given.

F Footslopes and valleys

Footslopes in this area are mainly erosional features, with a variation in drainage pattern. Most parts of the footslopes have a coverage of stones less than 10%. Coverage with small eolian dunes varies in general from 0-5%. The non-dissected parts (F1 - F3) were discriminated based on respectively dominance of calcite, quartz and gypsum. The dissected parts of the footslopes show a range of clusters. The clusters could be ascribed with the aid of field measurements to gypsum crust dominated surfaces, gypsiferous sand (in general covering the valleys) and gypsum dominated footslopes. At the used scale it is decided to combine these classes to one class (F4). Valleys in footslopes covered with sand are classified in a separate class (F5).

Footslopes with a eolian sand coverage between 20 and 80% are classified as (F6), while parts with more than 80% coverage are classified as eolian deposits (E).

E Eolian material

Areas with more than 80% eolian cover are grouped in 4 classes E1 - E4, based on their gypsum and quartz content. More than 95% of the eolian sand consists of quartz and gypsum. A further subdivision of the eolian classes is difficult due to:

- a non-linear relation between gypsum content and MMR 7 / MMR 4 ratio. This may cause confusion between areas consisting of small dunes and sand sheets having different gypsum contents and areas with a rather homogeneous coverage with a mixture gypsum and quartz.
- dependence of MMR 7 / MMR 4 ratio for a specific gypsum content on grainsize.

An assumption of dominant grainsize and knowledge of presence of dunes may lead to more detailed maps. The accuracy of these maps are limited as long as not more observations are performed.

B Playas covered with sand dunes or sheets.

Four classes are discriminated based on difference in coverage by sand, with a gypsum content above 40%. One more is defined in which the coverage is mainly by quartz sands. In general coverage by quartz sand is in the form of sand sheets, while gypsum sand is often dominant in small dunes.

In the eastern area quite large areas along the playa border belong to these classes. The actual coverage with sand dunes and sandsheets was estimated from position in the feature space plots (a linear mixture of sand and playa) corroborated by field observations. It has to be noted that especially these composed units formed clusters which were not present in the field reflectance data, due to a difference in aggregation scale.

- P Playa area dominated by deposition
- Q Playa area dominated by evaporation

The playa area is a depression without external drainage. In this legend areas with a coverage of sandsheets or dunes of more than 5% are considered as a part of the playa border zone (B units). The playa area could be subdivided in parts with dominance of deposition (P) and dominance of evaporation (Q). Dominance by deposition is found all over the studied area of Chott Fedjaj and in a relatively small part along the western edge of Chott Djerid. In the April data a spectral difference between P and Q was present. Areas with a dominance by deposition show a somewhat higher TM 4 / TM 1 ratio, indicating almost absence of salt on the surface. Despite the large coverage by dust over all playas in April, presence of halite in the areas dominated by evaporation (Q), is not completely obscured. Another spectral difference is the low average reflectance in TM bands 4 - 7 of the Djerid area in comparison with chott Fedjaj. This is caused both by presence of rough parts in chott Djerid, especially areas with surface type D and E, and the relatively high moisture content of the surface (aiouns or in evaporating halite). Due to these differences between the two playas almost no overlapping clusters exist. The only overlapping clusters in the playas are found for type F areas in chott Djerid (defined as P5) with P2-P4 present in Chott Fedjaj.

Based on field measurements in the chott Fedjaj 4 classes were discriminated. All classes show an absence of salt efflorescence at the surface and a low moisture content. The clusters (P1, P3 and P4) are mainly separated by amount of reflectance. An increasing reflectance correlates with decrease in roughness. A prudent labelling to classes is given in the legend. Cluster P2 has a somewhat higher 7 / 4 ratio indicating that this is probably a type C class.

The labelling in the Djerid area is based on a combination of roughness, moisture and halite content (see legend 1).

December data

Legend 2: Salt-moisture classification of playa in November

	Salt effl.	Moisture cont.
1	2-3	2
2	3	3
3	3	4
4	3-4	2
5	3	4
6	4	3
7	4	4
8	4	5
9	4-5	5
10	5	4
11	5	4-5
12	5	5

Explanation: (2) low; (3) moderate; (4) high; (5) very high

Due to large solar zenith angle, inducing a smaller signal to noise ratio and an increase in amount of shadow, December data are less favourable than April data for mapping non dynamic parts like the footslopes. The December data can be used effectively to gather more information on the playa.

In the wet season differences in spectral characteristics are dominated by moisture and halite content of the surfaces (Epema subm.). Therefore these data are used to make maps of moisture and salt situation (plate 3a and 3b, Legend 2). The mapping was performed in classes, since difference in roughness makes it impossible to apply one algorithm to map moisture content of the surface.

Dynamics

Moisture and halite content are the most important dynamic factors in the playa area. The dynamics can be derived by comparing imagery of different seasons or by combining this information. In plate 4 as an example moisture differences between April and December are shown for the Fedjaj area. It is assumed that a linear relation exist between MMR 4 and volumetric moisture content between dry and wet reflectance. Dry and wet reflectance values are derived from field experiments (Epema 1990). Different algorithms were applied to the classes P1-P4 of the eastern area.

EVALUATION OF RESULTS

This article focused on the question: "to which extent is it possible to derive surface characteristics and their dynamics in a desert area from TM data?" For an answer to this question we will evaluate:

- (1) the classes as presented in the plates and legends;
- (2) why a further discrimination than in the mentioned classes is impossible;
- (3) examples of applications of results of (1)
- (4) the possibility to extrapolate the results of this study to other areas;
- (5) the value of the methodology and the possibility to extrapolate it
- (6) role of extra information of TM in environmental mapping in arid areas.

1) It is possible to discriminate dominant landscape units, and within these units a variation in mineralogy and moisture content (Legend 1 and 2). Dominant landscapes in this area are: footslopes, dunes and sandsheets, playas partly covered by dunes or sandsheets, and playas dominated or not dominated by evaporation. In addition it is possible on footslopes, dunes and sandsheets to differentiate based on gypsum, carbonate and quartz content, while on the playa halite and moisture differences can be observed.

Largest problems in discriminating between classes are:

- quartz dominated footslopes and eolian quartz-rich sand. Spectrally these classes differ only slightly, while the overall reflectance is comparable. Although spectral curve shapes of gypsum-rich footslopes and quartz sand with some gypsum are also comparable as shown also in Epema (subm.) it is possible to separate these classes on overall reflectance for the field data set, but for the TM misclassifications may occur.

- differences between classes on playa not dominated by evaporation. If salt cuboids are present on smooth surfaces the spectral signatures will be comparable with more rough surface types.

2) For an evaluation of results we have to consider also why a further discrimination than in the mentioned classes is impossible:

- no further discrimination of footslopes is possible than based on dominant minerals. Bandwidth of TM bands makes an indication of amount of quartz, gypsum and carbonate impossible.

- a more detailed estimate of gypsum content of eolian material is impossible. This is caused by the dependency of absorption from grain size.

- a further discrimination in surface types of the playa is impossible. This is both by definition since classes are fuzzy and by the measuring techniques. The relation between roughness, halite and moisture content is complex and time dependent.

- a more precise estimate of moisture content is impossible as long as dry and wet reflectance are not known of all types and subtypes.

3) The possibility to discriminate landscape units, mineralogy and moisture content is vital in most landscape studies in arid areas. Some examples, where this information can be used are:

- different types of footslopes may indicate a diverse origin and a variation in soil types,

- differences in mineralogy of sand may give information on origin and processes which formed these deposits,

- calibrating absolutely TM data allows to follow changes of dune areas and sandsheets on playas and footslopes

- possibility to monitor spatial and temporal variation of moisture and halite condition give insight in main processes in the playas.

4) Extrapolation of these results to other arid areas is in principle possible. Major problems will only arise if other minerals dominate. In that case confusion may occur since it is very likely that also other OH bearing minerals give a decrease in reflectance in TM bands 7 and 5, while at the other hand minerals without OH or CO₃ will show no specific absorption like we now have for quartz. These problems would not occur if TM had a higher spectral resolution as is foreseen for the future generation earth observation satellites.

5) The proposed methodology, including field reflectance measurements, turned out to be very useful in this area. The direct information of reflectance in relation with natural or artificial surface characteristics is an aid in the final interpretation. If we evaluate the results of Epema in former publications a somewhat modified experimental set-up can be developed:

- number of field measurements on same plots under different solar zenith angles and atmospheric conditions may be decreased

- number of plots of observation and measurement should be increased. A general description with an estimate of gypsum and carbonate content, and for the playas a measurement of moisture content is recommended. It makes an estimate of accuracy more easy. With accuracy we mean the statistical probability that the class assigned to a location on the classification map is the class that would be found at that location in the field.

- experiments with wetting and drying should be performed in all major playa units.

Extrapolation of this methodology to other areas, including field reflectance measurements, seems very well possible. In that case relations with other minerals can be developed and applied to the whole area. If only field observations are performed it is possible that for non-dynamic areas the wrong surface characteristics are extrapolated, while for the more dynamic parts errors in explanation are even more likely.

6) If both aerial photographs and satellite images are present of an area, earth scientists will use satellite images for getting an overview over a large area and for extrapolating results. Aerial photographs, due to its stereoscopic viewing and its scale, will be used for delineation of the main units and for guiding the location of observation. The present study shows that in arid areas satellite TM imagery provides additional information, which is not visible on aerial photographs or on satellites like Landsat MSS and SPOT. This additional information relates to surface mineralogy and moisture content.

REFERENCES

- Coque, R., 1969. *La Tunisie Pre-Saharienne: Etude Geomorphologique*. Armand Colin, Paris.
- Coque, R. and Jauzein, A., 1967. The geomorphology and Quaternary geology of Tunisia. In: Martin, L. (ed.) *Guidebook to the Geology and History of Tunisia*. Society of Libyan Petroleum Geologists, Handbook 3: 227-257.
- Epema, G.F., Van Dijk, H., Elzinga, E. and Van den Hoek, A.I., 1985. Soil and vegetation mapping with the aid of Landsat Thematic Mapper Images near Kebili (Tunisia), Wageningen Agricultural University, department of Soil Science and geology.
- Epema, G.F., 1990a. Diurnal trends in reflectance of bare soil surfaces in southern Tunisia. *Geocarto International* Vol.5, No.4 33-39.
- Epema, G.F., 1990b. Determination of planetary reflectance for Landsat 5 Thematic Mapper tapes processed by Earthnet (ITALY). *ESA Journal*, 14, 101-108.
- Epema, G.F., 1990c. Effect of moisture content on spectral reflectance in a playa area in southern Tunisia. *Proceedings international symposium, Remote Sensing and Water Resources, Enschede, August 20-24 1990: 301-308.*
- Epema, G.F., 1991. Studies of errors in field measurements of the bidirectional reflectance factor. *Remote Sensing of Environment* 35, 37-49.
- Epema, G.F., 1992. Atmospheric condition and its influence on reflectance on bare soil surfaces in Southern Tunisia. *International Journal of Remote Sensing International Journal of Remotesensing* Vol.13, No.5: 853.
- Epema, G.F., Ground spectral reflectance in a desert area in southern Tunisia. Submitted to: *Remote Sensing of Environment*.
- Floret Ch. and Pontanier R., 1982, *l'Aridite en Tunisie Presaharienne*. Travaux et documents de l'ORSTOM no. 150, Paris 544p.
- Jones A.R. and Millington A., 1986. Spring mound and aïoun mapping from Landsat TM Imagery in south-central Tunisia. *Symposium on Remote sensing for Resources Development and Environmental Management, Enschede: 607-613.*
- Meckelein, W., 1977. *Zur Geomorfologie des chott Djerid*. *Stuttgarter geographische Studien* 91: 247-301.

- Millington, A.C., Jones, A.R., Quarmby, N., Townshend, J.R.G., 1987. Remote sensing of sediment transfer processes in playa basins. In: Frostick, L. & Reid, I. (eds), 1987, Desert sediments: Ancient and Modern, Geological Society Special Publication No.35: 369-381.
- Millington, A.C., Drake, N.A., Townshend, J.R.G., Quarmby, N., Settle J.J., Reading A. J., 1989. Monitoring salt playa dynamics using Thematic Mapper data, IEEE Transactions on geoscience and remote sensing, Vol. 27, No. 6: 754-761.
- Mitchell, C.W., 1983. The soils of the Sahara with special reference to the Maghreb, *Maghreb Review* 8: 29-37.
- Ongaro, L., 1986. Studio integrato delle risorse naturali del Nefzaoua (Tunisia): carte delle unita di terre dell'area Kebili-Douz. *Rivista di agricoltura Subtropicale e Tropicale, Trimestrale LXXX-n.2 Aprile-Giugno 1986.* 165-310.
- Roberts, C. and Mitchell, C.W. 1987. Spring mounds in southern Tunisia in *Desert sediments: Ancient and Modern*, L Frohstick and J. Reid, Eds Blackweell, U.K.: geological Society London, Spec. Publication no 35: 321-336.
- Tou, J.T. and Gonzalez R.C., 1974. *Pattern recognition principles*. Reading, Massachusetts: Addison-Wesley Publishing Company.
- Townshend, J.R.G., Quarmby, N.A., Millington, A.C., Drake, N.A., Reading A. J., White, K.H., 1989. Monitoring playa sediment transport systems using Thematic Mapper data, *Advanced Space Research: Vol. 9, No.1: (1)177-(1)183.*
- Verhoef, W., 1985. A scene radiation model based on four-stream radiative transfer theory. *Proceedings of the 3rd International Colloquium on spectral signatures of objects in Remote Sensing, Les Arcs, France, 16-20dec, 1985 ESA SP-247 (European Space Agency):* 143-150.
- Verhoef, W., 1990. *Informatie-extractie uit multispectrale beelden met behulp van stralingsinteractiemodellen*, NLR TP 90243 L, Amsterdam Nationaal lucht- en ruimtevaartlaboratorium, 48p.

CHAPTER 10

CONCLUSIONS

CONCLUSIONS

1. Reliable field reflectance measurements in TM-like bands can be gathered in deserts with a Barnes MMR radiometer, using a sprayed barium sulphate panel as reference. A prerequisite for processing of the data is that optical properties of the panel, especially solar zenith angle dependent reflectance for the different bands, are known. For large solar zenith angles, at short wavelengths and for panels deviating substantially from an ideal Lambertian behaviour, effect of diffuse irradiation cannot be neglected.

2. Solar zenith angle dependence of field reflectance is limited for solar zenith angles up to 65 degrees. For medium rough surfaces as present on the footslopes reflectance with a solar zenith angle of 28 degrees is about 10% higher than for a solar zenith angle of 63 degrees. Differences on the smooth playa parts are even less, if no other phenomena, like dew or drying out after rainfall occur. This implies that for establishing a field reference set all field measurements with a solar zenith angle less than 65 degrees can be used. Assuming a field plot representative for a pixel of 30 x 30 meters and assuming that no temporal change occurs, Landsat TM of 8 April will observe a 10 % higher field reflectance than Landsat TM on 18 December.

3. Influence of atmosphere on field reflectance is limited. Atmospheric variation, as can be checked visually or with a solarimeter, only affects the accuracy of the measurements. It is possible to correct reflectance values if simultaneously solarimeter values are known. Having many good days accuracy can be increased using only measurements under stable atmospheric conditions for the field reference set.

4. An increase in moisture content gives a decrease in reflectance of all bands, due to internal reflections in the waterfilm covering the particles. MMR bands 6 and 7 show a larger decrease in reflectance than the other bands with increasing moisture content. Water absorption bands affect MMR bands 6 and 7. Linear relations can be applied to predict from reflectance in MMR bands the volumetric moisture content, if porosity, and wet and dry reflectance are known. Due to field experiments for a considerable part of the playa area reliable estimates of moisture content can be made. For the footslopes and sand-dunes establishing relation between reflectance and moisture content is not relevant, since shortly after storms the moisture content of the toplayer is very low again. Occurrence of halite on the surface in the playa area is spectrally detectable from a high MMR 1 / MMR 4 ratio. Halite is a complication in estimates of moisture content from reflectance.

5. Considerable differences in spectral behaviour exist between dominant surface minerals of the footslopes and dunes: gypsum, quartz and carbonate. Due to a specific position of the OH groups in gypsum a range of absorption bands between 1.0 and 2.4 μm are present. The CO_3^{2-} ion in carbonate gives a strong absorption band at 2.34 μm . Pure quartz has no specific absorption bands. Laboratory and field experiments with (almost pure) eolian samples of the area showed that gypsum, carbonate and quartz can be discriminated since gypsum has a low reflectance in MMR bands 6 and 7, carbonate has a low reflectance in MMR 7, while for quartz no low reflectance in MMR bands 6 and 7 can be observed.

6. Analysis of field signatures of the footslopes and the dunes and sand-sheets can best be performed in the following groups: (1) eolian material, (2) footslopes with sealed crusts (3) footslopes with gypsum crusts.

(1) Due to relatively low amount of carbonate, amounts of gypsum and quartz are important in determining reflectance for eolian material. Non-linear, grainsize dependent, significant relations between MMR 7 /MMR 4 ratio and gypsum content for laboratory conditions were found.

(2) For the plots on the footslopes 3 types of sealed surfaces can be discriminated based on spectral signature dominated by gypsum, quartz and carbonate respectively. Remarkable are the high values in MMR bands 6 and 7 for both gypsum and carbonate dominated footslopes.

(3) Gypsum crusts have low reflectance in MMR bands 6 and 7. For pure plots they can be discriminated from gypsiferous sand due to extra low reflectance in band 6.

7. Spectral variation for field data of the playa showed statistically to be much higher in the wet season than in the dry season. Larger variation in moisture content and halite on the surface in the wet season are the main causes for this difference. Six surface types have been discriminated based mainly on surface roughness. The dry season data were most useful for identification of the surface types.

8. Calibration coefficients given for Landsat TM tapes processed in Fucino (the ground station covering both Europe and Northern Africa) are based on preflight data and turned out to be obviously wrong. It was possible to correct these data in such a way that reliable planetary reflectance data could be achieved.

9. Use of atmospheric model of Verhoef with as input the ratio of measured diffuse to total irradiance and assuming a certain water vapour absorption leads to highly accurate values. Ground reflectance derived from Landsat TM deviates only slightly from that measured directly in the field.

10. Clustering of Landsat TM data with an unsupervised classification leads to a number of clusters, which could be compared with the field reference set. After merging and deleting of classes, using field reflectance, supervised minimum distance to mean classifications were applied. It was possible to derive from Landsat TM a number of useful classes for playas, footslopes and eolian material, having differences in origin and showing variation in surface mineralogy, moisture content and playa surface type. With Landsat TM it is possible to monitor dynamics of a factor like moisture content.

11. The followed methodology, including field measurements, is very useful for an understanding of different factors affecting Landsat TM data. Application of this method in comparable areas should be possible. Knowing main factors influencing the signal, number of measurements throughout the day can be reduced, so that measurements on more locations become possible. Direct application of results to comparable areas, without measurements and field observations may induce errors if other minerals are present.

12. Landsat Thematic Mapper is a very useful instrument for monitoring arid areas with no or sparse vegetation cover. Spatial and spectral resolution is sufficient for most applications. Spectrally TM is superior to other satellites operating in the optical region. The bands in the middle infrared give possibilities to identify the dominant minerals of arid areas, gypsum, carbonate and indirectly quartz, while also moisture condition of the very top layer could be detected. The blue band makes identification of halite possible.

13. In most geological and soil research studies aerial photographs in combination with fieldwork are used. Satellite information is generally only used for getting overview over large areas and extrapolation of results. The present study shows that Landsat TM not only makes this overview possible but that new additional information for arid areas can be derived from its imagery.

11. SAMENVATTING

Satellieten geven een overzicht van de verschijnselen op het aardoppervlak. Satellieten die in het optische deel van het spectrum werken hebben echter als nadeel dat waarnemingen onmogelijk worden zodra er wolken zijn. Daarom zijn woestijngebieden beter geschikt om observaties te doen met zulke satellieten dan de gematigde streken en de natte tropen. De kwetsbaarheid vooral aan de randen van de woestijngebieden en de moeilijke bereikbaarheid maken gebruik van optische remote sensing zeer zinvol.

De Landsat Thematic Mapper (TM) satelliet heeft een betere spectrale resolutie dan de andere satellieten, terwijl de ruimtelijke en temporele resolutie redelijk zijn. Dit onderzoek was derhalve gericht op de spectrale mogelijkheden van de Landsat Thematic Mapper voor het bepalen van eigenschappen aan het aardoppervlak en hun dynamiek in woestijngebieden. In verschillende seizoenen zijn veldreflectiemetingen uitgevoerd om het effect op reflectie van de verschillende factoren en hun dynamiek vast te stellen. De veldreflectiemeter (MMR) meet in een golflengtebereik vergelijkbaar met Landsat TM. Het geselecteerde gebied in zuid Tunesië vertoont een grote variatie in landschappen: voethellingen, duinen en dynamische zoutvlaktes. In alle gebieden was de vegetatiebedekking gering. De mineralogie, een grote variatie in het voorkomen van gips, kalk, kwarts en zout, is representatief voor vele droge gebieden.

Om de resultaten van de veldmetingen te vergelijken met de gegevens die de Landsat Thematic Mapper levert is een goede bewerking van de gegevens noodzakelijk. De algemeen geaccepteerde aanname dat referentiepanelen ideale reflectoren zijn moest worden verworpen. De paneel reflectie is afhankelijk van golflengte en zonnehoogte. Het bleek dat bij lage zonnestanden ook gecorrigeerd moest worden voor de hoeveelheid diffuse straling (Hoofdstuk 2).

Als we de calibratiefactoren voor Landsat Thematic Mapper gegevens die in Fucino worden voorbereid zouden gebruiken treden grote fouten op in het berekenen van reflectie. Het bleek dat de gegeven factoren niet gecorrigeerd waren voor het verlies in gevoeligheid van de sensoren in de loop van de tijd en dat de factoren bovendien bepaald waren op grond van het verwisselen van twee definities van bandbreedte. Om de juiste waarden te berekenen is er voor deze fouten gecorrigeerd (Hoofdstuk 8).

De factoren die reflectie bepalen kan men onderverdelen in externe en interne. Van de externe factoren werd de invloed van zonnehoek en atmosfeer onderzocht (Hoofdstuk 3 en 4). De invloed van zonnehoogte bleek gering in dit gebied als alleen metingen gedaan werden met een zonnehoek groter dan 25 graden met de horizon. In het voorjaar bleken de reflecties rond het middaguur ongeveer 10% hoger dan als de zonnehoek 25 graden was. Aangezien de satellieten op deze breedtegraad waarnemingen doen met een zonnehoek tussen 62 en 27 graden is het zinvol om metingen niet met kleinere hoeken dan ongeveer 25 graden te doen.

De atmosferische invloed op veldreflectie is gering vooral als de zon niet erg laag staat. Gebaseerd op een evaluatie van de externe factoren werd geconstateerd dat alle metingen met een zonnehoek groter dan 25 graden en stabiele en heldere omstandigheden geschikt zijn om een dataset van veldreflectiemetingen op te stellen.

Veldmetingen toonden aan dat Landsat TM banden zeer geschikt zijn om oppervlakte-eigenschappen (interne factoren) in dit gebied waar te nemen (Hoofdstukken 5 tot 7).

Gips vertoont absorptiebanden in beide middeninfrarode banden (vergelijkbaar met TM band 5 en 7), en kalk in TM band 7. Aangezien op de voethellingen en in de duinen kwarts het derde mineraal is dat veel voorkomt, wijst in dit gebied een hoge reflectie in de middeninfrarode banden op aanwezigheid van kwarts. De veldreflectiemetingen vertonen verschillende spectrale signaturen voor voethellingen die gedomineerd werden door één van deze drie mineralen. De verschillen in de eolische afzettingen waren nog duidelijker: het was mogelijk om verbanden tussen gipsgehalte en spectrale reflectie af te leiden.

Halietzout op de zoutvlaktes gaf een hoge reflectie in het hele zichtbare deel van het spectrum, in het bijzonder in de blauwe band. Experimenten op veldplots toonden aan dat een toename in vochtgehalte van de bovengrond een verlaging van reflectie geeft. Deze verlaging in reflectie is in de middeninfrarode banden extra hoog. Er werden lineaire verbanden tussen vochtgehalte en reflectie gevonden.

De zoutvlaktes bleken de meest dynamische delen van het veldwerkgebied. Na regenbuien veranderde het vochtgehalte en het zoutgehalte voor langere tijd. Ondanks bedekking met stof bleven verschillen lang merkbaar. Ook in de duingebieden veranderde de reflectie op de verschillende plots vooral onder invloed van de wind. De dynamiek op de voetvlaktes was het kleinst. Variatie in vegetatie was relatief gering, terwijl het effect van regenbuien al na enkele dagen niet meer zichtbaar was.

De resultaten van de veldreflectiemetingen bleken extrapoleerbaar naar de Landsat TM gegevens. Het was mogelijk om met Landsat TM een aantal nuttige klassen te onderscheiden zowel in de zoutvlaktes, als op de voethellingen en in de duinen. Deze klassen vertonen een variatie in oppervlaktermineralogie (gips, kwarts, kalk en zoutgehalte) en een variatie in oppervlaktype (ruwheid). De zout en vochtdynamiek kon worden afgeleid uit de vergelijking van Landsat TM beelden van verschillende tijdstippen.

De in dit proefschrift gepresenteerde methodiek, het uitgebreid doen van reflectiemetingen in het veld, geeft inzicht in de mogelijkheden van Landsat TM onder verschillende omstandigheden. Er is aangetoond dat voor operationeel gebruik in droge gebieden de Landsat TM een belangrijke aanvullende bron van informatie is op andere vormen van remote sensing, zoals de luchtfoto's.

CURRICULUM VITAE

Gerrit Frans Eperna werd geboren op 9 augustus 1955 in Heerenveen. In 1973 behaalde hij het Gymnasium diploma aan het Gemeentelijk Lyceum te Dordrecht. In datzelfde jaar begon hij de studie fysische geografie aan de Rijksuniversiteit Utrecht. Hij studeerde af in januari 1980 in de fysisch geografische proceskunde met als bijvakken bodemnatuurkunde en bodemscheikunde in Wageningen en fysisch geografische landschapskunde. Na het behalen van een lesbevoegdheid in de aardrijkskunde, kwam hij in datzelfde jaar in dienst van de Rijksuniversiteit Utrecht. Tot eind december 1981 verrichtte hij onderzoek op het gebied van splash erosie. In januari 1982 werd hij aangesteld aan de Landbouwhogeschool Wageningen bij de vakgroep Bodemkunde en Geologie. Hij verrichtte hierbij naast een kleine onderwijstaak onderzoek op het gebied van remote sensing en bodemkunde. In 1987 werd het in dit proefschrift resulterende, door de BCRS gefinancierde, onderzoek aangevangen. Sinds 1990 nam de onderwijstaak sterk toe. Momenteel is hij bij de vakgroep Bodemkunde en Geologie werkzaam als universitair docent op het gebied van de GIS en remote sensing . Hij verricht hierbij onderzoek naar imaging spectroscopy in semiaride gebieden. In 1980 trouwde hij met Tineke Scherer. Zij hebben drie dochters: Meike, Anniek en Sietske.